Field Theories à la Gravity: From Navier-Stokes to Superconductivity.

by

Nikhil Monga

A Dissertation Presented in Partial Fulfillment
of the Requirements for the Degree
Doctor of Philosophy

Approved October 2020 by the
Graduate Supervisory Committee:

Cynthia Keeler, Chair
Onur Erten
Matthew Baumgart
Richard Lebed

ARIZONA STATE UNIVERSITY

December 2020

ABSTRACT

Recent developments inspired by string theoretic considerations provide multiple maps between gravitational and non-gravitational degrees of freedom. In this dissertation I discuss aspects of three such dualities, the gauge/gravity duality and how it applies to condensed matter systems, the fluid-gravity duality, and the color-kinematics duality.

The first of these, colloquially referred to as holography, in its simplest form posits a mapping of d-dimensional conformal field theory (boundary) partition functions onto d+1 dimensional gravitational(bulk) partition functions, where the space-time carries a negative cosmological constant. In this dissertation I discuss the results of our calculations examining the emergence of Fermi-surface like structures in the bulk spacetime despite the absence of explicit Fermions in the theory.Specifically the 4+1 dimensional Einstein-Maxwell-Chern-Simons theory with scalar degrees of freedom, with and without symmetry breaking is considered. These theories are gravity duals to spatially modulated gauge theories. The results of calculations presented here indicate the existence of a rich phase space, most prominently Fermi shells are seen.

The second set of dualities considered are the color-kinematic duality, also known as the double-copy paradigm and the fluid-gravity duality. The color-kinematic duality involves identifying spin-2 amplitudes as squares of spin-1 gauge amplitudes. This double copy picture is utilized to construct "single copy" representations for spacetimes where Einstein's equations reduce to incompressible Navier-Stokes equations. In this dissertation I show how spacetimes that characterize irrotational fluids and constant vorticity fluids each map to distinct algebraically special spacetimes. The Maxwell fields obtained via the double-copy picture for such spacetimes further pro-

vide interesting parallels, for instance, the vorticity of the fluid is proportional to the magnetic field of the associated gauge field.

DEDICATION

To everyone who helped me get here, my friends, family, mentors and most of all my partner in crime, science and everything inbetween, Anusha ...

... and mass spectrometers.

ACKNOWLEDGMENTS

My path to physics has been rather non-linear. Along my short mean free path, I've had multiple scattering events as a consequence of which I've had the good fortune of learning and experiencing a broad spectrum of science, of which I shall always remain humbly in awe. I have also met several wonderful people without whom this journey would not have been possible.

I would like to thank my advisor Cynthia Keeler for her unwavering support through my thesis and for all the physics that I have had the fortune of learning with her, Victoria Martin for guiding me in my research when I needed it the most, this dissertation would not have been possible without your help, my committee members, Richard Lebed, Matthew Baumgart and Onur Erten for all the conversations on physics that I got to have with them, my former advisors while I was at SESE, Steve Desch, John Shumway and Ariel Anbar for teaching me the scientific method and for egging me on to learn more physics, Stephen Romaniello for teaching me that "perfection is the enemy of getting things done". My academic path would not have been possible without guidance from Subir Sabharwal whose willingness to support and guide me has always left me in awe.

Without the freedom I have had to explore my interests I would not be where I am today, this would not have been possible anywhere else and for that I shall forever be grateful.

I would also like to thank my fellow officemates and friends, Logan M. Thomas (and Sophia Schinske), Ayush Saurabh, Panagiotis Christeas, Tucker Manton, Carlos Cardona, Dipankar Dutta and Manoj Venkat for all of the support they have given

to me over the years, for all conversations we had and for lending me a patient set of ears to drone onto.

I am also grateful for the support from my parents, my younger brother Rahul and my wife Anusha's parents and her sister Pavithra. Lastly I am grateful to my wife Anusha for her companionship and unfettered presence and patience through thick and thin.

TABLE OF CONTENTS

CHAPTER Page

CHAPTER Page

LIST OF FIGURES

Chapter 1

OVERVIEW: DUALITIES IN PHYSICS

Mathematical dualities allow the reformulation of otherwise difficult problems into relatively more manageable forms. In this dissertation we leverage three such mathematical dualities that have been illuminated recently. Each of these dualities allows one to look at various classical and quantum field theoretic quantities under a geometric lens.

The dualities we consider include the gauge/gravity duality which relates partition functions in gravitational theories to gauge theories, the double-copy picture which relates amplitudes in gravitational theories to gauge theories and finally the fluid-graviy duality wherein the long wavelength limits of Einstein's equations are related to the Navier-Stokes equations in various forms.

We will discuss each of these dualities as well as their various formulations in more detail in chapter 2 and chapter 4. However, before delving into the details of these dualities, we first set the stage by discussing a more well known duality - the electric-magnetic duality. We will see various flavors of this duality from its simpler constructions to its non-Abelian extensions. In this process we will, albeit briefly, see the computational benefits that arise from such mappings as well as the physical

insights that emerge from them.

1.1 Why Study Dualities? The Electric-Magnetic Duality and its Uses.

In this section the motivations for studying dualities are provided by considering the electric-magnetic duality. The first manifestation of a duality that a physics student comes across is the electric-magnetic duality. The simplest form of this duality is apparent when considering source free Maxwell equations, $dF = 0$ and $d^*F = 0$, the transformation $F \leftrightarrow {}^*F$, or equivalently $\vec{E} \to \vec{B}$ and $\vec{B} \to -\vec{E}$ allows for Maxwell's equations to remain satisfied by the transformed fields.

This mapping breaks down when sources are present, unless one introduces a magnetic charge that behaves just as an electric charge does. Such magnetic charges are magnetic monopoles. Similar to its electric counterpart, the magnetic field for a magnetic charge m is,

$$\vec{B} = \frac{m\hat{r}}{4\pi r^2}. \tag{1.1}$$

For the wave function of a particle carrying a magnetic charge to be quantum-mechanically sensible one needs to impose an additional constraints on the magnetic charge above, this is known as Dirac's quantization condition for magnetic monopoles[1],

$$em = 2n\pi\hbar. \tag{1.2}$$

It is worth noting here that a small electric coupling e will amount to a large magnetic coupling m and vice-versa. Extensions of this concept prove useful when considering non-Abelian gauge theories where monopoles arise more naturally and are

[1]This concept can be further generalized to dyons - which point particles that carry both a magnetic charge and an electric charge.

topological objects ['t Hooft (1974); Polyakov (1974)]. The extension of the electric-magnetic duality that thus arises when considering non-Abelian fields is known as the Montonen-Olive duality, first proposed by [Montonen and Olive (1977)].

Witten and Olive (1978) further generalized this duality by considering the effect of the degeneracy of vacua in non-Abelian gauge theories. This generalization was made possible by including an additional term in the action known as the θ term. They considered an action of the form,

$$\begin{aligned}\mathcal{L} &= \mathcal{L}_{YM} + \mathcal{L}_{Higgs} + \mathcal{L}_{\theta} \\ &= -\frac{1}{4g^2} F^a_{\mu\nu} F^{a\,\mu\nu} + \theta \frac{g^2}{32\pi^2} F^a_{\mu\nu} \tilde{F}^{a\,\mu\nu} + \frac{1}{2} D_\mu \phi^a D^\mu \phi^a - V(\phi^a),\end{aligned} \tag{1.3}$$

where in the above action, $\tilde{F}^a_{\mu\nu} \equiv \frac{i}{2}\epsilon_{\mu\nu\rho\sigma} F^{a\,\rho\sigma}$, or equivalently, $\tilde{F} \equiv {}^*F$. If we make the following identification,

$$G^a_{\mu\nu} = F^a_{\mu\nu} + i\tilde{F}^a_{\mu\nu}, \tag{1.4}$$

then the action eq. (1.3) can then be packaged into a compact form as,

$$\mathcal{L} = -\frac{1}{32\pi} \mathrm{Im}\left(\tau G^a_{\mu\nu} G^{a\,\mu\nu}\right) + \frac{1}{2} D_\mu \phi^a D^\mu \phi^a - V(\phi^a), \tag{1.5}$$

where, the complex coupling τ is is given by:

$$\tau = \frac{4\pi i}{g^2} + \frac{\theta}{2\pi}. \tag{1.6}$$

Witten and Olive (1978) observed that the mass of the lowest energy stationary monopole solutions (or Bogomol'nyiPrasadSommerfield or BPS states, [Bogomolny (1976); Prasad and Sommerfield (1975)]) is invariant under the following transformation of the coupling constant,

$$\tau \to \frac{a\tau + b}{c\tau + d} \quad \text{where} \quad \begin{pmatrix} a & b \\ c & d \end{pmatrix} \in SL(2, \mathbb{Z}). \tag{1.7}$$

It is precisely this symmetry of the coupling constant in leaving the monopole-mass invariant that was identified as the Montonen-Olive SL(2,$\mathbb{Z}$) duality.

The biggest computational benefit that comes from the Montonen-Olive duality is that a topological object–the magnetic monopole–can be identified as a perturbation[2] [Montonen and Olive (1977); Witten and Olive (1978)]. Historically however, we see that the electric-magnetic duality and its generalizations lead us down a trajectory of realizing that objects such as monopoles should be expected as fundamental ingredients of gauge theories.

Lastly we point out the supersymmetric extensions of the electric-magnetic duality, this duality is also known as the S-duality [Seiberg (1995)][3]. In its original form the S-duality treats quarks and gluons of one supersymmetric non-Abelian theory as solitons in another. Like the previous iterations of the electric-magnetic duality, the S-duality also related strong coupling computations to weak coupling computations. The applications of the S-duality are numerous and span various aspects of string theory (for a pedagogical review see Alvarez-Gaume and Hassan (1997))[4]. We shall see that such reformulations where the physics of strongly interacting systems can be described by "dual" weakly coupled theories are a frequent and often useful feature of dualities in physics. In the next section we provide a quick overview of the dualities considered in this thesis.

[2]First shown in Montonen and Olive (1977), appropriately titled "Monopoles as Gauge Particles".

[3]Seiberg (1995) aptly titled his work - "Electric-magnetic duality in supersymmetric non-Abelian gauge theories".

[4]See Rajaraman (1982) and Figueroa-OFarrill (1998) for reviews on topological objects and the electric-magnetic duality respectively, the latter of which is also aptly titled - "Electromagnetic Duality for Children".

1.2 An Overview of Dualities Considered.

The previous section illustrates the usefulness of considering dualities. Having discussed a more familiar setup in the electric-magnetic duality, we now provide an overview of the dualities used in this dissertation. The first of these dualities that we discuss is the gauge-gravity duality, the most concrete examples of which involve the Anti-de Sitter Space/Conformal Field Theory correspondence [Maldacena (1999); Alday *et al.* (2010); Aharony *et al.* (2008)]. Using this family of dualities it is possible to perform computations in weak(strong) coupling supergravity in place of strong(weak) coupling "dual" gauge theories in one lesser dimension.

Taking this approach further, one then asks the question: what would gravitational duals for real world field theories, such as various condensed matter systems, look like? The work presented in this dissertation on the gauge/gravity duality focuses on aspects of this question.

The second duality that forms a center piece of the research presented here involves what is referred to as the double-copy picture. Stated briefly, the double-copy picture implies that gravitational amplitudes $\sim$ (gauge amplitudes)^2. Of interest to us in this dissertation is the form of this duality based on the Weyl tensor[Luna *et al.* (2019)]. The third duality we will use in this dissertation involves a mapping between Einstein's equations and Navier-Stokes equations, referred to as the fluid-gravity duality[Bredberg *et al.* (2011, 2012)]. We will use the double-copy picture to further dissect the fluid-gravity duality.

The structure of this dissertation is as follows: we provide a more detailed overview of the gauge/gravity duality, particularly in the context of condensed matter physics in chapter 2. In chapter 3[5] we discuss our results pertaining to a specific holographic condensed matter physics model - the Einstein-Maxwell-Chern-Simons-Dilaton theory with and without symmetry breaking. In chapter 4 we provide a detailed overview of the fluid-gravity duality. In chapter 5[6] we provide discuss our findings of applying the double-copy paradigm to a specific set of metrics we refer to as fluid metrics. Finally in chapter 6 we provide concluding remarks and discuss future directions.

[5]Chapter 3 is based on the published paper titled "Spectral weight in Chern-Simons theory with symmetry breaking" by V.L Martin and the author..

[6]Chapter 5 is based on the published paper titled "From Navier-Stokes to Maxwell, via Einstein" by C. Keeler, T. Manton and the author. Note that the *Journal of High Energy Physics* uses alphebatized authorship. These works are reproduced here with permission from the co-authors.

Chapter 2

HOLOGRAPHIC CONDENSED MATTER PHYSICS: FOLLOWING THE SYMMETRIES

Holography allows the computation of field theory correlators by computing gravitation partition functions in one higher dimension, most successfully for spacetimes with negative cosmological constants. The strongest evidence for this conjecture exists for the duality between $\mathcal{N} = 4\,SYM$ and type IIB string theory on $AdS_5 \times S^5$ [Maldacena (1999)].

The need to study holographic theories was motivated, among other reasons, by the need to understand strongly interacting systems. Calculations from IR QCD to several strongly correlated condensed matter systems have presented several technical challenges when adopting perturbative methods. For QCD amplitudes, one finds an unwieldy factorial growth of the number of Feynman diagrams. For several condensed matter systems such as high temperature superconductors, usual approaches such as Landau's Fermi liquid theory are not enough because they lack a quasiparticle description of excitations. Thus mean-field approximations for theories such as what is done in BCS do not work for these systems.

The reason for the usefulness of holography as a tool here follows from how it relates strong coupling field theory partition functions to weak coupling gravitational partition functions in one higher dimension. In the next section we will see how by following the symmetries of the physical system in question gauge theory quantities

are mapped onto their dual gravitational counterparts.

2.1 Following the symmetries: à la Holography.

The Holographic conjecture can be briefly summarized as the following relation between field theory partition functions and gravity partition functions in one higher dimension [Gubser *et al.* (1998)]:

$$\begin{aligned} Z_{QFT}^{d+1} &= Z_{AdS}^{d+2} \\ \langle e^{i\int dx\, h_i(x)\,\mathcal{O}_i(x)} \rangle &= \int^{\phi_i \to h_i} \prod_i (\mathcal{D}\phi_i)\, e^{iS[\phi_i]}, \end{aligned} \tag{2.1}$$

where the set of fields h_i correspond to the boundary values of bulk fields ϕ_i. Note that bulk here refers to anti-de Sitter spacetimes, where we study the gravitational theory. We see from the (2.1) that the boundary values h_i of bulk fields ϕ_i source operators on the boundary theory.

In constructing this map from bulk fields to boundary operators we seek to establish a dictionary. At this point it is pertinent to discuss "top-down" vs "bottom-up" constructions in holography. For "top-down" constructions of the gauge-gravity duality such a dictionary can be obtained by performing compactifications of higher dimensional string theory actions (see for eg. the GPKW dictionary Gubser *et al.* (1998)).

On the other hand, in bottom up constructions of holography the objective is to construct gravity duals relevant for phenomenology. Such duals are however not well defined - i.e. we do not know the precise form of the field theory dual. Nevertheless one attempts to recreate as many phenomenologically pertinent features as possible.

The construction of such phenomenologically meaningful gravitational models is made possible by adding matter content to the gravitational action. This matter field content in bulk (in AdS) has similar symmetries and symmetry breaking behavior as

the dual boundary operators of the associated gauge theory. It is in this way by "following the symmetries" that we attempt to create holographic models of superconductors. Some mappings that typically manifest in the gauge-gravity duality are given in table 2.1,

Bulk Field	**Dual Field Theory Operator**
Gauge fields A_a	Conserved currents J_μ
Metric Tensor g_{ab}	Boundary Stress Tensor $T_{\mu\nu}$
Surface gravity κ	Temperature

Table 2.1: Examples of bulk-boundary maps in the gauge/gravity Duality.

As an example of this map, we now study how gauge symmetry in the bulk relates to symmetries of the associated current on the boundary. Consider a gauge field A_n in d+2 dimensions whose boundary value i.e. $A_a \to A_\mu$ sources the boundary current J_μ in d+1 dimensions. Often the additional coordinate in the bulk spacetime (i.e. AdS spacetime) is referred to as the radial coordinate[1]. We shall see below in eq. (2.2), how a conserved U(1) gauge symmetry in the bulk theory corresponds to a globally conserved current on the boundary gauge theory:

$$\begin{aligned} Z_{QFT}[A_a(r,x) \to A_\mu(x)] &= \int d^{d+1}x\sqrt{-\gamma}\ A_\mu J^\mu \\ &= \int d^{d+1}x\sqrt{-\gamma}\ (A_\mu + \partial_\mu\chi)J^\mu \\ &= \int d^{d+1}x\sqrt{-\gamma}\ A_\mu J^\mu - \chi\,\nabla_\mu J^\mu, \end{aligned} \tag{2.2}$$

[1]It is worth pointing out that scaling of the bulk partition function with this radial coordinate rather neatly corresponds to renormalization of the boundary field theory. Appropriately the study of renormalization group flow associated with the radial coordinate is a field of research by itself, oft referred to as holographic renormalization (see Bianchi *et al.* (2002); Skenderis (2002); de Boer *et al.* (2000); Hartnoll *et al.* (2016) for a review).

here γ refers to the determinant of the boundary metric, $\gamma_{\mu\nu}$. The above quantity is invariant if the current is conserved, i.e. $\nabla_\mu J^\mu = 0$.

The AdS/CFT correspondence is most precisely understood in the context of the duality between $\mathcal{N} = 4$ SYM and type II-B string theory. Observing this one might ask the extent to which such constructions for condensed matter systems are meaningful given that in bottom-up constructions one does not know the precise form of the associated field theory dual. However, it is useful here to recall that the Ginzburg-Landau theory was constructed by following the symmetries of the charge carriers. *In Holography as in Ginzburg-Landau, the key detail which makes such calculations possible is universality in second order phase transitions.*

2.2 Holographic Superconductors: A Brief Overview

Superconductivity requires the condensation of charge carriers which results in an infinite DC conductivity. This can be seen as a symmetry breaking process in the field theory, such that the current operator picks up a non-vanishing vacuum expectation value.

Holographic gravity-duals to such superconductors realize these symmetry breaking processes via the formation of condensates of relevant matter fields outside of black-hole horizons [Gubser (2008); Hartnoll *et al.* (2008); Hartnoll and Shaghoulian (2012)]. The first hint that the AdS/CFT correspondence could be used to study superconductors was provided by Gubser (2008). The action used is of the form,

$$\mathcal{S} \sim \int d^4x\sqrt{-g}\left(R - \frac{6}{l^2_{AdS_5}} - \frac{1}{4}F_{\mu\nu}F^{\mu\nu} - |\partial_\mu\psi - iqA_\mu\psi|^2 - m^2|\psi|^2\right). \tag{2.3}$$

For a charged Reissner-Nordstrom AdS black-hole background and with a background electric field, Gubser (2008) showed that it is possible for large enough masses and charge of the scalar field for condensates to form outside the Horizon. This is

a consequence of the shift in the Breitenlohner-Friedman bound which allows one to have "hairs" outside of the horizon in addition to mass, charge and angular momentum.

The first complete picture of a holographic superconductor emerged in Hartnoll *et al.* (2008). The authors then observed that scalar hair shows up at low temperatures below a critical temperature & not above it. This was interpreted as a strongly interacting S-wave superconductor as the condensate did not carry angular momentum. The bulk action considered here has the form,

$$\mathcal{S} \sim \int d^4x\sqrt{-g}\left(-\frac{1}{4}F_{\mu\nu}F^{\mu\nu} - |\partial\psi - iA\psi|^2 + \frac{2}{L^2}|\psi|^2\right). \tag{2.4}$$

The background metric that was utilized for this work was the planar Schwarzschild AdS black hole,

$$\begin{aligned} ds^2 &= -f(r)dt^2 + \frac{dr^2}{f(r)} + r^2(dx^2 + dy^2), \\ f(r) &= \frac{r^2}{L^2} - \frac{M}{r}, \end{aligned} \tag{2.5}$$

where the temperature relates to the mass of the black hole and size of the AdS radius as $T = 3M^{1/3}/4\pi L^{4/3}$. In addition, the authors interpreted excitations on the background as quasi-particle/hole pairs. Although this is interpreted as an S-wave superconductor and the existance of quasi-particle excitations makes it tempting to think of this as a BCS superconductor, however this is not the case. The reason is that the gap in the excitation spectrum obtained here is significantly larger than what is predicted by BCS theory. Further, owing to the strong-weak nature of the AdS/CFT correspondence the associated field theory dual of a weak coupling Einstein gravity calculation would be a strongly coupled field theory, this fact is consistant with the former stated observation of the larger gap.

The first sets of holographic p-wave superconductors were constructed by promoting on an AdS-Schwarzchild background where the gauge field was promoted to an

SU(2) field [Gubser and Pufu (2008); Roberts and Hartnoll (2008)]. A holographic superconductor consisting of a d-wave condensate was constructed by Benini *et al.* (2010). In all, holographic superconductors constructed thus far encompass (but are not limited to) s-wave, p-wave and d-wave order parameters [Ammon *et al.* (2010a,b); Benini *et al.* (2011); Chen *et al.* (2011)].

2.3 Mathematical Tools

We now provide an overview of two of the most important mathematical tools that we use in chapter 3. The first of these pertains to calculations of Green's functions in the context of the gauge/gravity duality, while the second deals with the spectral weight. The spectral weight can be related to the counting of the degrees of freedom for our system. This quantity will be our diagnostic for evaluating the presence or absence of Fermi-surface like structures. We begin first by discussing Green's functions below.

2.3.1 Computing Green's Functions Holographically

We will now look at a simple model to illustrate how holography can be used for computing Greens functions (for a review see Hartnoll *et al.* (2016)). Consider a massive scalar on an AdS_{d+2} background,

$$ds^2 = \frac{L^2}{r^2}(-dt^2 + dr^2 + d\vec{x}_d^2), \tag{2.6}$$

while the action is specified by,

$$\mathcal{S} = -\int d^{d+1}x\sqrt{-g}\left(\frac{1}{2}(\partial\phi)^2 + \frac{m^2\phi^2}{2}\right). \tag{2.7}$$

If we consider modes of the form $\phi(r,t,\vec{x}) = \phi(r)e^{i\vec{k}.\vec{x}-i\omega t}$, the equation of motion then can be rewritten as,

$$\phi'' - \frac{d}{r}\phi' + \left(\omega^2 - k^2 - \frac{(mL)^2}{r^2}\right)\phi = 0. \tag{2.8}$$

Solving this expression as a series expansion near $r \to 0$, the boundary of the AdS_{d+2} spacetime we get,

$$\phi_{Boundary} = \phi^{(0)} r^{d+1-\Delta} + ... + \phi^{(1)}\, r^{\Delta} + ... \tag{2.9}$$

where the quantity Δ, is essentially representing the scaling dimension of the field theory operator. Δ is related to the bare mass of the scalar field via the following relation,

$$\Delta(\Delta - d - 1) = m^2 L^2 \tag{2.10}$$

The coefficient $\phi^{(0)}$ plays the role of the boundary value of the field h, which as we saw earlier sourced the field theory operator. Now using linear response theory for boundary operators $\mathcal{O}$ dual to the field ϕ, we have,

$$\mathcal{G}^R_{\mathcal{O}\mathcal{O}}(\omega,k) = \frac{\langle\mathcal{O}\rangle}{h} = \frac{\phi^{(0)}}{\phi^{(1)}}. \tag{2.11}$$

The retarded Greens function so computed has a simplification in the near horizon limit,

$$G^R_{\mathcal{O}\mathcal{O}} \sim \omega^{2\nu}. \tag{2.12}$$

Above ν is an exponent that linearly depends on the scaling dimension of the field theory operator. We shall use such exponents used extensively and their computation will be central to our work as we shall see in chapter 3.

2.3.2 Spectral Weight: A Fermi Surface Diagnostic.

The quantity that is of most interest to us here is known as the low energy spectral weight. This quantity counts the charged degrees of freedom in a given field theory

and can thus provide a diagnostic for the Fermi surface. The low energy spectral weight is effectively the imaginary part of the retarded current-current correlator. Suppressing indices, we can describe it as,

$$\sigma(k) = \lim_{\omega \to 0} \mathrm{Im} \left[\frac{G_{JJ}(\omega, k)}{\omega} \right] \tag{2.13}$$

A spectral decomposition of the imaginary part of the Greens function shows how it counts the charged degrees of freedom of the system.

$$\mathrm{Im} G^R_{JJ}(\omega, k) = \sum_{m,n} e^{-\beta E_m} \left| \langle n(k^{'}) | J(k) | m(k^{''}) \rangle \right|^2 \delta(\omega - E_m + E_n). \tag{2.14}$$

Following the previous section, we can see that the holographic computation of the IR Greens function is made simple via the near horizon limit of bulk correlators, (Gubser *et al.* (1998); Gubser (2008); Hartnoll *et al.* (2008) see Hartnoll *et al.* (2016) for a review). Under this limit one finds that the spectral weight takes the form (with suppressed indices),

$$\sigma_k = \lim_{\omega \to 0} \frac{\mathrm{Im}[\mathrm{G^R_{JJ}}(\omega, \mathrm{k})]}{\omega} \sim \lim_{\omega \to 0} \omega^{2\nu_k - 1} \quad \& \quad \mathrm{G^{IR}_{bulk}} \sim \frac{\delta \mathrm{A}^{(1)}}{\delta \mathrm{A}^{(0)}} \tag{2.15}$$

From (2.15) above we see that in the zero frequency limit a critical value of the exponent ν_k emerges. For values of this exponent $\nu_k > 1/2$ no spectral weight exists while for values of the exponent $\nu_k < 1/2$ one finds that charged degrees of freedom exist,

$$\sigma_k \sim \lim_{\omega \to 0} \omega^{2\nu_k - 1} = \begin{cases} \infty & \text{if } \nu_k < 1/2. \\ 0 & \text{if } \nu_k > 1/2. \end{cases} \tag{2.16}$$

As we shall see in detail, the exponent ν_k explicitly depends on the perturbed momentum as well as the geometry of the spacetime in consideration. This observation suggests that we can identify a momentum K^* below which most charged degrees of freedom exist, and above which no charged degrees of freedom are there.

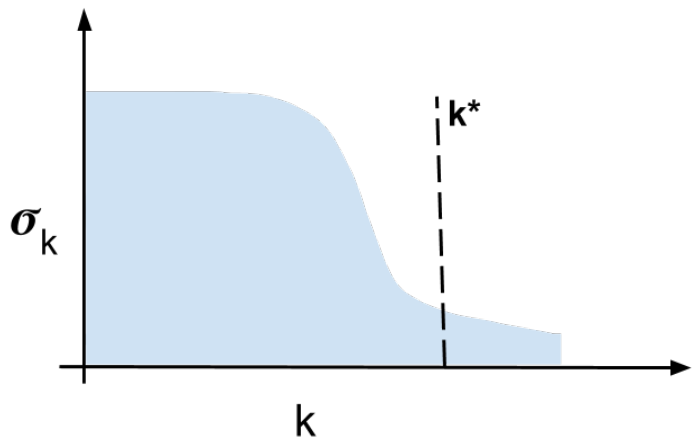

Figure 2.1: Schematic showing the spectral weight indicating the existance of charged degrees of freedom below some critical momentum k^*.

2.4 Unexpected Spectral Weight: Gouteraux et. al. 2016

While it is interesting to note these structures in the bulk and what they imply for boundary theories, some aspects of the spectral weight remain to be understood. In particular this work was motivated by the results of Goutéraux and Martin (2017) where a spectral weight was seen simultaneously with the existence of a charged condensate (they studied a 4 dimensional Einstein-Maxwell-Dilaton theory with massive gauge fields). The authors postulated that the true underlying ground state of the system studied could be a spatially modulated phase. This property has in fact been suggested as a general feature of holographic superconductors.

Following these hints we conjectured that a possible ground state for the system studied in Goutéraux and Martin (2017) could be identified by a 5-dimensional Einstein-Maxwell-Dilaton + Chern-Simons theory with massive gauge fields.

In the paper we present in chapter 3, we computed the spectral weight for various theories, finally building up to the Einstein-Maxwell-Dilaton with a massive vector

and Chern-Simons action. We limit our considerations to backgrounds that contain only electric fields.

2.5 Spatially Modulated Phases in Condensed Matter Physics

Before turning our attention to spatially modulated phases in holography, we will first discuss these in condensed matter systems. Phenomena such as spin density waves and charge density waves exhibit a breaking of spatial isotropy of their ground states. Thus a spatially modulated phase can be defined as a state which has a ground state which breaks spatial isotropy, breaking either translation invariance, rotation invariance or a combination of both in the ground state. This spatial anisotropy can be identified by a non-zero wave-vector $\mathbf{k}$, which is indicative of the direction in which the ground state breaks spatial isotropy. Not only does the ground state of such a system pick up a vacuum expectation value, but given that spatial isotropy is broken one also finds a gradient associated with the ground state. For instance, for charge density waves in a 2 dimensional ordered condensed matter phase one would find for eg. one finds, $\langle Q \rangle \sim Q_0 Cos(kx)$.

Here we will briefly discuss the quantum Lifshitz model (QLM) its renormalization group evolution thereby giving a concrete example of spatial modulation. The QLM model can be thought of as a continuum description for quantum dimer models. Quantum dimer models exhibit a phase transition where the ground state changes from a columnar state to a spatially modulated phase(see fig. 2.2 below).

It is useful to introduce the effective Hamiltonian for the dimer model first in eq. (2.17) below before we turn to its field theory formulation, the QLM in eq. (2.18),

$$\mathcal{H} = -\sum_{plaquettes} J[|H_{i,j}\rangle\langle V_{i,j}| + |V_{i,j}\rangle\langle H_{i,j}|] + V[|H_{i,j}\rangle\langle H_{i,j}| + |V_{i,j}\rangle\langle V_{i,j}] \qquad (2.17)$$

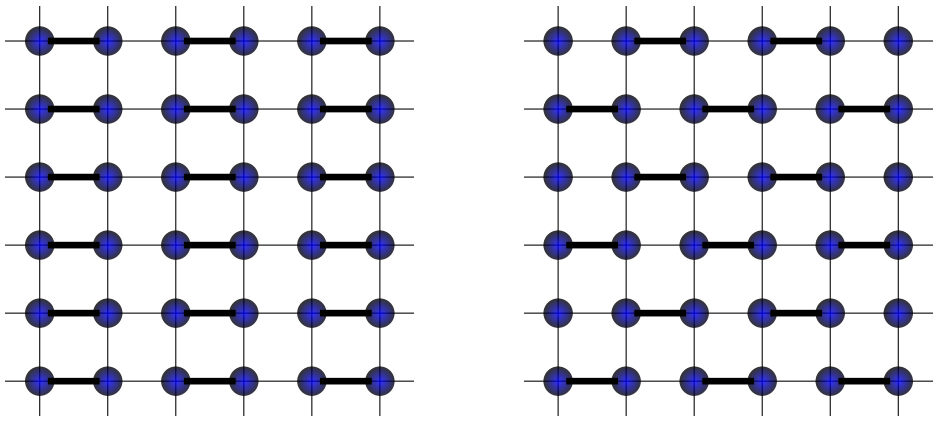

(a) Columnar states at RK fixed point (b) Tilted states

Figure 2.2: Ground states of the dimer model (c.f. ch. 8, 9 Fradkin (2013)).

The state $|H_{i,j}\rangle$ above referes to a pair of horizontal dimers in a single plaquette [2], while $|V_{i,j}\rangle$ refers to two vertical dimers in a plaquette. It is easy to see from the form of the Hamiltonian that the first operator shifts one type of plaquette to another while the other counts the total number of plaquettes of each type.

Quantum dimer models in $2+1$ dimensions exhibit what are known as Rokhsar Kivelson fixed points. At the RK point phonons have relativistic dispersion relations, i.e. $E \sim P$, where as at deviations away from this RG fixed point, the dispersion relations go as $E \sim P^2$. The RK fixed point corresponds to $J/V = -1$ in the above Hamiltonian (2.17), and represents the columnar states above.

Having provided a brief but necessary context above, we now turn to the quantum Lifshitz model and briefly touch upon its RG flow. The last step will allow us to explicitly derive the spatial modulation of the ground state and its associated wave vector. The Euclidean action for the Quantum Lifshitz model is:

$$S_E = -\frac{1}{2}\int d^2x\, d\tau \left((\partial_\tau \phi)^2 + \tilde{\kappa}(\nabla^2\phi)^2)\right) \tag{2.18}$$

[2]Plaquette here refers to the repeating structure of the lattice, in this case we consider square plaquettes.

This action is non-relativistic, in the sense that the dispersion relation goes as $E \sim P^2$, or it exhibits Lifshitz symmetry (i.e. the mass dimensions are [L]=-1 and [T]=-2). Here the field ϕ is related to the height of the columnar set of dimers that one finds in these sorts of models.

We now discuss various deformations of this model and see how these deformations will allow us to describe the "tilted states" mentioned above. We now consider the introduction of deformations of the form, $\rho(\vec{\nabla}\phi)^2$ to the action (2.18); we will be particularly interested in cases where $\rho < 0$. We emphasize the choice $\rho < 0$ as that choice leads to a spatially modulated ground state with non-zero "wave-vector". To fully construct the action for the tilted phase (fig. b above) one must also include additional deformation terms of the form, $g_4(\nabla\phi)^4$ [c.f. ch. 9 Fradkin (2013)]. The full action in $(+,-,-)$ signature then reads,

$$S = \frac{1}{2}\int d^2x\, dt \left((\partial_t\phi)^2 - \rho(\vec{\nabla}\phi)^2 - g_4(\vec{\nabla}\phi)^4 - \tilde{\kappa}(\nabla^2\phi)^2)\right) \tag{2.19}$$

Note that the above description of the RG flow of the Lifshitz model describes a shift in the dispersion relations. This also entails a shift in the mass dimensions of the effective field. For instance the scalar ϕ, which is representative of the height of the columnar states changes its mass dimension from $[\phi] = 0$ with $\rho = 0$ to $[\phi] = 1/2$. A direct consequence of this change in mass dimensions is that $\tilde{\kappa}$ becomes marginally irrelevant and can be ignored. We now write the effective action for the QLM as (once again in a $(+,-,-)$),

$$S_{eff} = \frac{1}{2}\int d^2x\, dt \left((\partial_t\phi)^2 - g_4\left((\vec{\nabla}\phi)^2 + \frac{\rho}{2g_4}\right)^2 + \frac{\rho^2}{4g_4^2}\right). \tag{2.20}$$

The observation that the ground state is spatially modulated can best be seen from the Hamiltonian, which is:

$$\mathcal{H}_{eff} = \frac{1}{2}\int d^2x \left(\Pi(\phi)^2 + g_4\left((\vec{\nabla}\phi)^2 + \frac{\rho}{2g_4}\right)^2 - \frac{\rho^2}{4g_4^2}\right) \tag{2.21}$$

Now we consider time invariant or static solutions for this Hamiltonian, one sees that for $\rho > 0$ the solution is a state with $\vec{\nabla}\phi = 0$ and the ground state is a state with E = 0. However for $\rho < 0$ we will notice that something more interesting is observed, let $\rho = -A$ where $A > 0$. We now have,

$$\mathcal{H}_{eff} = \frac{1}{2}\int d^2x \left(\Pi(\phi)^2 + g_4\left((\vec{\nabla}\phi)^2 - \frac{A}{2g_4}\right)^2 - \frac{\rho^2}{4g_4^2}\right), \tag{2.22}$$

for this Hamiltonian, as before for a static solution it is clear that the ground state is a state where $\vec{\nabla}\phi \neq 0$. This can be interpreted as the ground state acquiring a VEV for the gradient term, $\langle\vec{\nabla}\phi\rangle \neq 0$ This is the state with the lowest energy, whereas any state with vanishing $\vec{\nabla}\phi = 0$ are no longer the lowest energy states.

$$\begin{aligned}(\vec{\nabla}\phi)^2 &= \frac{A}{2g_4} \\ \Rightarrow \phi &\sim \vec{Q}.\vec{x},\end{aligned} \tag{2.23}$$

here if the vector **Q** is non-zero it represents the tilt of the spatially modulated phase (fig. 2.2b above). However if instead **Q**=0, one obtains a columnar state (fig. 2.2a above).

2.6 Spatial Modulation In Holography

Having discussed what a spatially modulated phase is, we now turn to gravitational descriptions of spatially modulated phases. As with any consideration in holographic systems, symmetries of field theory states are mapped onto symmetries of the bulk field content, matter and gravitational. For holographic fields spatial modulation can show up in multiple different ways, for instance one can find "striped" black-branes [Rozali *et al.* (2013a,b)].

Of interest to us in this dissertation will be work by Nakamura *et al.* (2010) where the spatial modulation is primarily mapped onto the spin-1 matter content

in the bulk. We begin by looking at the Einstein-Maxwell-Chern-Simons theory, as considered by Nakamura *et al.* (2010),

$$\mathcal{S} = \int d^5x\sqrt{-g}\ \left[R - \frac{12}{L^2} - \frac{1}{4}F_{mn}F^{mn} + \frac{\alpha}{3!}\frac{\epsilon^{abcde}}{\sqrt{-g}}A_aF_{bc}F_{de}\right], \tag{2.24}$$

here we set the AdS radius to 1. α corresponds to the Chern-Simons coupling. In our paper, chapter 3, we only consider backgrounds that carry electric fields[3]. This action admits the AdS-Reissner-Nordström black hole (AdS-RN) as a solution. The near horizon geometry of this metric is $\mathrm{AdS}_2 \times \mathbb{R}^3$.

$$ds^2 = \frac{-dt^2 + dr^2}{r^2} + dx^2 + dy^2 + dz^2 \quad A_m = (A_t(r), 0, 0, 0, 0) \quad A_t(r) = E_0\, r^{-1}. \tag{2.25}$$

Perturbations of the gauge field can be decomposed into transverse and longitudinal modes. We shall see for the transverse channel, for sufficiently large Chern-Simons coupling α, this background is unstable Nakamura *et al.* (2010),i.e. in the presence of a background E field one can obtain tachyonic modes. On the other hand, in the presence of a background B field alone, the modes will not be tachyonic[4].

As we note below, these tachyonic modes which can be obtained with background electric fields can in fact violate the Brietenlohner-Freedman(BF) bound. Recall, as we discussed in section 2.2, the violation in the BF bound is associated with the violation of no-hair theorems for black holes. This violation of the BF bound characterizes the instability of the black hole solution and is found to be associated with a helical

[3]In similar but not identical actions, turning on a background magnetic field has been shown to be related to holographic realizations of Weyl semi-metalsJimenez-Alba *et al.* (2015); Landsteiner and Liu (2016).

[4]Since our interest is in studying phase transitions of the holographic system, and since background magnetic fields do not appear to result in unstable modes, we will not consider background magnetic fields here.

current at the boundary. It is the helicity of this current that corresponds to spatial modulation, in particular since we break translational invariance.

We now provide context to our work by demonstrating this instability. In order to do so, first consider Maxwell's equations for this system,

$$\partial_b(\sqrt{-g}F^{ba}) + \frac{\alpha}{2}\epsilon^{abcde}F_{bc}F_{de}. \tag{2.26}$$

Following arguments by Nakamura *et al.* (2010), we first see how the tachyonic modes can arise in 5 dimensional flat space, further we decompose our modes such that $\mathbb{R}_{1,4} \cong \mathbb{R}_{1,1} \times \mathbb{R}_3$. Linearizing the equation above as $F_{mn} = F^{(0)}_{mn} + f_{mn}$, where the background has a constant E field, specifically for $\mu = 0, 1$ we have $F^{(0)}_{\mu\nu} = \epsilon_{\mu\nu}E$ and zero otherwise. The equation of motion for the gauge field is thus linearized and has the form,

$$\partial^\mu f_{\mu i} + \partial^j f_{ji} - 2\alpha E\epsilon_{ijk}f_{jk} = 0. \tag{2.27}$$

Further simplifications can be performed to the above expression using Bianchi identities $\epsilon_{ijk}\partial_i f_{jk} = 0$ and making the identification that $f_i = \frac{1}{2}\epsilon_{ijk}f_{jk}$. Thus we reduce the above linearized expression to,

$$(\partial^\mu\partial_\mu + \partial^j\partial_j)f_i - 4\alpha E\epsilon_{ijk}\partial_j f_k = 0.$$

Next we take the Fourier transform of the above modes while keeping track of the decomposition of the associated momentum vectors in the full spacetime $\mathbb{R}^5$ to $\mathbb{R}_{1,1} \times \mathbb{R}_3$, i.e. with $e^{ip_\mu x^\mu + ik_i y^i}$, where $\mu = 0, 1$ and $i = 1, 2, 3$.

Modes f_i that solve eq. (2.27) are circularly polarized, we thus work with the ansatz, $f_i \sim \vec{u}\, e^{ik_i y^i}$. Here the $\vec{u}$ is circularly polarized, i.e. $\vec{k} \times \vec{u} = \pm i|k|\vec{u}$. Substituting this ansatz for f_i into eq. (2.27) yields the following dispersion relation,

$$(p_0)^2 - (p_1)^2 = (|k| \pm 2\alpha E)^2 - 4\alpha^2 E^2. \tag{2.28}$$

It is evident from eq. (2.28) above that these modes can be tachyonic, the lowest value of m^2 is $-4\alpha^2 E^2$[5]. For the electric field background case, one than finds the values of momentum k (along y_i) that will appear violate the BF bound. The behavior of m^2 is similar for the $AdS_2 \times \mathbb{R}_3$ case. Nakamura *et al.* (2010) show that the range of momenta for which one observes an instability in the gravitational theory (which is asymptotically AdS) is,

$$2|\alpha E|\left(1-\sqrt{1-\frac{1}{16\alpha^2 E^2 l^2_{AdS_2}}}\right) < k < 2|\alpha E|\left(1+\sqrt{1-\frac{1}{16\alpha^2 E^2 l^2_{AdS_2}}}\right). \quad (2.29)$$

It is important to note here that in eq. (2.29) unless the Chern-Simons coupling is turned off, the instability occurs only at finite momenta. Nakamura *et al.* (2010) argue that observation of helical boundary currents as well as the presence of instabilities at finite momenta are indicative of spatially modulated phases. They further state that the two aforementioned features provide a gravitational theory whose behavior is similar to what one observes in the cholestic/chiral-nematic liquid crystals, thereby constructing a gravity dual to spatially modulated phases.

In the next chapter in which the results of our paper Martin and Monga (2019) are presented. We study the spectral weight associated with a set of theories that reduce to (and including), the action in eq. (3.8). We will first reproduce the instability of eq. (2.29) by computing the spectral weight instead. We then consider multiple models to evaluate their spectral weight so as to diagnose their Fermi-surface structure. Our approach closely follows Goutéraux (2014); Goutéraux and Martin (2017). As we shall see, one finds a rich phase space structure with several geometry dependent

[5]On the other hand, with a background B field one obtains the dispersion relation $(p_0)^2-(p_1)^2-(k_2)^2=\left(\sqrt{(k_3)^2+(k_4)^2+4\alpha^2B^2}+2|\alpha B|\right)^2$, which is not going to be tachyonic.

properties. Most notably we observe for the presence of Fermi shell like behavior for a subset of models that we consider.

Chapter 3

SPATIALLY MODULATED PHASES IN HOLOGRAPHY WITH SYMMETRY BREAKING

This chapter is a reproduction of the paper Martin and Monga (2019), titled "Spectral weight in Chern-Simons theory with symmetry breaking" published in the *Journal of High Energy Physics*[1]. It has been appropriately formatted for inclusion in this document.

3.1 Introduction

Harnessing the AdS/CFT correspondence Maldacena (1999) to explore the space of potential phenomena occurring in strongly interacting quantum matter is now a well-established research enterprise (see Hartnoll *et al.* (2016) and references therein). One phenomenon of interest is the role of Pauli exclusion in strongly interacting quantum field theories, where a quasi-particle description is absent. We know from experimental techniques like ARPES (angle-resolved photoemission spectroscopy) that Fermi surfaces can form in such strongly coupled materials (see for example Damascelli *et al.* (2003); Gonda *et al.* (1995)). A famous example of this occurs in the normal state of certain high-T_c cuprate superconductors, known as a "strange metal" phase due to the anomalous linear scaling of quantities like resistivity and specific heat with temperature Varma *et al.* (1989). The superconducting phase transition occurs due to competition between the free energies of the normal and superconducting states, and thus characterizing the strange metal phase is a prerequisite for understanding

[1]Note that the *Journal of High Energy Physics* uses alphebatized authorship. This work is reproduced here with permission from the co-authors.

the mechanism for the high-T_c transition. Understanding Pauli exclusion and the formation of Fermi surfaces at strong coupling is one aspect of this characterization.

In studying Pauli exclusion in strongly interacting quantum field theories via the AdS/CFT correspondence, a natural question arises: in which contexts do Fermi surfaces appear in holography? To address this question, one can employ an exploratory method known as bottom-up holography[2]. In this method, one chooses by hand a sensible classical bulk theory exhibiting the symmetries and field content of interest, and then uses perturbation theory to extract information about the dual quantum field theory (such as correlation functions) via the holographic dictionary. The field theory quantity of interest to us that diagnoses the presence of a Fermi surface is called the low energy spectral weight:

$$\sigma(k) = \lim_{\omega \to 0} \frac{\mathrm{Im} G^R_{\mathcal{O}\mathcal{O}}(k)}{\omega}. \tag{3.1}$$

The object $\mathrm{Im} G^R_{\mathcal{O}\mathcal{O}}$ is called the spectral function, and $\mathcal{O}$ is a field theory operator. We will see now that the spectral weight (3.1) identifies Pauli exclusion in two distinct ways, both of which have been studied holographically in several bottom-up constructions.

The first (and most traditional) diagnostic for a Fermi surface is a pole in the spectral function $\mathrm{Im} G^R_{\mathcal{O}\mathcal{O}}$ near the Fermi momentum $k = k_F$. For example, for free fermions, when $\mathcal{O} = \psi$ and

$$G^R_{\psi\psi} = \frac{1}{\omega - v_F(k - k_F) + i\epsilon} \tag{3.2}$$

is the fermion propagator, a Fermi surface is defined by a pole in $\mathrm{Im} G^R_{\psi\psi}$ at $k = k_F$. This is the sense in which ARPES detects the presence of a Fermi surface: it measures

[2]Bottom-up holography can be contrasted with top-down constructions, which involve consistent Kaluza-Klein reductions of relevant string theories. In practice, one does not necessarily know the UV completion of a particular bottom-up model, but nevertheless many features of our bottom-up constructions are motivated by top-down ones (cf equation (3.20)).

a pole in the spectral function. Diagnosing the presence of such a pole in strongly coupled theories using holography requires knowledge of the full spacetime, including UV data. For example, one can consider a bulk theory with an explicit fermion ψ, solve the Dirac equation over the full asymptotically AdS background (often using numerical techniques), and extract the UV spectral function $\mathrm{Im}G^R(\omega, k)$ associated with this fermion. This was the approach taken in Lee (2009); Liu *et al.* (2011); Cubrovic *et al.* (2009); Cremonini *et al.* (2018).

There is a second, distinct way in which the spectral weight informs us of the presence of Pauli exclusion. Furthermore, in contrast to the pole discussed in the previous paragraph, this diagnostic only requires knowledge of the near-horizon IR geometry, rather than the full UV theory. Indeed, to leading order in $\omega \to 0$ (see for example Hartnoll *et al.* (2016); Iqbal *et al.* (2011)),

$$\mathrm{Im}G^R_{\mathcal{O}\mathcal{O}}(\omega, k) \propto \mathrm{Im}\mathcal{G}^R_{\mathcal{O}\mathcal{O}}(\omega, k). \tag{3.3}$$

As is standard in the literature, we reserve the symbol $G^R_{\mathcal{O}\mathcal{O}}$ for the UV Green's function and $\mathcal{G}^R_{\mathcal{O}\mathcal{O}}$ denotes the IR Green's function. The UV data are stored in the proportionality constant of (3.3), and in throwing that away we are denying ourselves access to any potential poles discussed in the previous paragraph. *Nevertheless*, (3.3) still carries physically relevant information. To see this, consider the spectral decomposition:

$$\mathrm{Im}G^R_{JJ}(\omega, k) = \sum_{m,n} e^{-\beta E_m} \left|\langle n(k^{'})|J(k)|m(k^{''})\rangle\right|^2 \delta(\omega - E_m + E_n). \tag{3.4}$$

From (3.4), we can see that the spectral weight directly counts *charged* degrees of freedom at a given frequency and momentum[3]. Thus we take nonzero low energy spectral weight at finite momentum to be an indication that a Pauli exclusion-like

[3]We refer the reader to Hartnoll *et al.* (2016) for a more elaborate discussion regarding this spectral decomposition.

phenomenon is taking place. One can study this effect holographically by considering a bulk theory even *without* explicit fermions. Much like before, one must solve the bulk equations of motion, but this time only using the IR near horizon geometry. One then obtains the ω scaling of $\mathrm{Im}G^R(\omega, k)$ at low energies. If this spectral function is nonzero for finite momenta, it signals the presence of charged degrees of freedom with a nontrivial momentum space structure. This is a signature of Pauli exclusion, occurring without explicit fermions in the theory. This approach was taken in Hartnoll and Shaghoulian (2012); Anantua *et al.* (2013); Goutéraux and Martin (2017), and it is the approach that we will use in this work.

Low energy spectral weight has been calculated in a variety of theories and background geometries. The authors of Hartnoll and Shaghoulian (2012) argued that low energy spectral weight should be exponentially suppressed in hyperscaling violating geometries (labeled by exponents z and θ), and then showed this explicitly for the Einstein-Maxwell-dilaton theory. They (and Anantua *et al.* (2013)) also showed that in the limit $z \to \infty$ with the quantity $\eta = -\theta/z$ fixed, the spectral weight is no longer exponentially suppressed. This indicated that these so-called semi-local theories Iqbal *et al.* (2011) are perhaps more fermionic in nature, and deserve further study. The authors of Goutéraux and Martin (2017) studied the low energy spectral weight again in near horizon η geometries, but this time in the case of the holographic superconductor Hartnoll *et al.* (2008). For the holographic superconductor, the bulk charge density manifestly forms a condensate, and so nonzero low energy spectral weight at finite momenta was not expected to be observed. Interestingly, however, Goutéraux and Martin (2017) did report the presence of low energy spectral weight over a range of momenta, as well as a finite k instability in the longitudinal channel. Such an instability coincides with a violation of the Breitenlohner-Freedman bound

Breitenlohner and Freedman (1982a,b), since for the theories we consider[4]

$$\mathrm{Im}\mathcal{G}^R_{JJ}(\omega,k) \sim \omega^{2\nu_k}, \tag{3.5}$$

where the ν_k is related to the conformal dimension of the dual field theory operator (see Iqbal *et al.* (2011) for more details on this). In particular, the authors of Anantua *et al.* (2013); Goutéraux and Martin (2017) reported finding a "smeared" Fermi surface, which they define as the low-energy spectral weight $\sigma(k)$ vanishing only above a particular momentum k_*:

$$\sigma(k) = \lim_{\omega\to 0} \frac{\mathrm{Im}G^R_{JJ}(\omega,k)}{\omega} = \left\{ \begin{array}{ll} \infty & k < k_* \\ & \\ 0 & k > k_* \end{array} \right\}. \tag{3.6}$$

Further, Goutéraux and Martin (2017) found a Fermi shell in a region of parameter space, which they define as $\sigma(k)$ existing between two nonzero momenta k_- and k_+:

$$\sigma(k) = \lim_{\omega\to 0} \frac{\mathrm{Im}G^R_{JJ}(\omega,k)}{\omega} = \left\{ \begin{array}{ll} \infty & k_- < k < k_+ \\ & \\ 0 & \text{otherwise} \end{array} \right\}. \tag{3.7}$$

In this work when we refer to a smeared[5] Fermi surface or a Fermi shell, we will mean spectral weight of the form (3.6) and (3.7), respectively.

These results regarding the above momentum space structure and the regions of instability led to questions such as 1) What are the bulk degrees of freedom that are contributing to this nonzero spectral weight? and 2) In some range of parameter space, the instability suggests that our model is not the true ground state. Could the true ground state be a spatially modulated phase? Indeed, experimentally the superconducting phase of certain high T_c cuprate superconductors is seen to coexist

[4]In equation (3.5) the JJ subscript is schematic. It will become $J_\perp J_\perp$ in the transverse channel and $J_\parallel J_\parallel$ in the longitudinal channel, as explained in a later section.

[5]Sometimes we will drop the word "smeared", but by Fermi surface we will always mean spectral weight of the form (3.6).

with (or perhaps compete with) charge density wave (CDW) and spin density wave (SDW) order (see for example Chang *et al.* (2012) and references therein). Question 1) motivates us to study the low energy spectral weight of these η geometries in the presence of other interesting interaction terms, so that we might determine how robust this anomalous spectral weight is. Question 2) urges us to consider theories with broken translation invariance, so that we might better model the charge density wave order.

In this work we study the effect of introducing a Chern-Simons term on the results obtained in Goutéraux and Martin (2017). The addition of a Chern-Simons term is motivated by Nakamura *et al.* (2010), which studies a Chern-Simons theory in an AdS Reissner-Nordström background geometry. For large enough values of the Chern-Simons coupling, and in the presence of a constant background electric field, they too find an instability at finite momentum, and conjecture that the true ground state is a spatially modulated phase. The purpose of this paper is to study a theory with both a Chern-Simons coupling and a massive vector (this gives a broken $U(1)$ symmetry that is the hallmark of the holographic superfluid), so that we might learn how the presence of the low energy spectral weight and the presence of an instability changes as we very both the Chern-Simons coupling and the condensate charge.

In Section 3.2 we review the set-up of Nakamura *et al.* (2010) as a warm-up, and compute the spectral weight for transverse and longitudinal channels for the Einstein-Maxwell-Chern-Simons action in an $\mathrm{AdS}_2 \times \mathbb{R}^3$ background, which is the near horizon geometry of the extremal AdS Reissner-Nordström black hole. We reproduce the finite k instability obtained in Nakamura *et al.* (2010), this time in the language of spectral weight. In Section 3.3 we include a dilaton field (we call this theory Einstein-Maxwell-dilaton-Chern-Simons theory, or EMDCS for short) and discuss the implications on the spectral weight and the smeared Fermi surface momentum space structure that

the spectral weight suggests. In Section 3.4 we break the $U(1)$ symmetry of EMDCS by adding a massive vector. This model is a holographic superfluid with an added Chern-Simons term. We calculate the spectral weight to learn about how the Chern-Simons term affects the instability region and the smeared Fermi surface structure reported in Goutéraux and Martin (2017). In Section 3.5 we discuss our results.

3.2 Einstein-Maxwell-Chern-Simons

We begin our analysis by discussing the Einstein-Maxwell-Chern-Simons theory in $d = 5$ spacetime dimensions described by the action

$$\mathcal{S} = \int d^5x\sqrt{-g}\ \left[R - V_0 - \frac{1}{4}F_{mn}F^{mn} + \frac{\alpha}{3!}\frac{\epsilon^{abcde}}{\sqrt{-g}}A_aF_{bc}F_{de}\right]. \tag{3.8}$$

In equation (3.8) we set the AdS radius equal to 1, and α corresponds to the Chern-Simons coupling. Note that ϵ^{abcde} is the Levi-Civita symbol, and the Chern-Simons piece is metric independent.

This action was considered by Nakamura *et al.* (2010) in the near horizon geometry of the AdS-Reissner-Nordström black hole (AdS-RN), namely $\mathrm{AdS}_2 \times \mathbb{R}^3$, and in the presence of an electric field

$$ds^2 = \frac{-dt^2 + dr^2}{r^2} + dx^2 + dy^2 + dz^2 \quad A_m = (A_t(r), 0, 0, 0, 0) \quad A_t(r) = E_0\, r^{-1}. \tag{3.9}$$

The authors of Nakamura *et al.* (2010) observed that at sufficiently large Chern-Simons coupling α, this background is unstable against metric fluctuations. Further, they note that this instability occurs at non-zero momentum. This suggests that the instability signals a phase transition toward a spatially modulated phase.

We can reproduce this instability by computing the spectral weight, and further diagnose whether or not a smeared Fermi surface structure is present, in the spirit of Anantua *et al.* (2013). Our approach closely follows Goutéraux (2014);

Goutéraux and Martin (2017), and we consider perturbations of both the background gauge field and the metric. All perturbations $X \to X + \delta X$ are of plane wave form $\delta X = \delta X(r) e^{i(kx - \omega t)}$, where we choose the perturbations to propagate purely in the x direction. Then, as in electrodynamics, the perturbed equations of motion decouple into two channels. Those perturbations that are odd under the transformation $y \to -y$ comprise the so-called transverse channel (labeled by $\perp$), and those even under $y \to -y$ make up the longitudinal channel (labeled by $\parallel$). We now examine each of these channels in turn.

3.2.1 Transverse Channels

The Chern-Simons term allows some of the perturbations to combine into circularly polarized modes, as discussed in Nakamura *et al.* (2010); Hartnoll *et al.* (2016). This permits us to make the following identification for gauge and metric perturbations:

$$\delta A_{\pm}(r) e^{i(kx-\omega t)} \equiv \delta A_y \pm i \delta A_z \qquad \delta g_{t\pm}(r) e^{i(kx-\omega t)} \equiv \delta g_{ty} \pm i \delta g_{tz}, \tag{3.10}$$

The choice of polarization (+ or -) corresponds to choosing $\alpha E_0 > 0$ or $\alpha E_0 < 0$, respectively. This can be seen from the low energy limit ($\omega \to 0$) of the linearized equations of motion, presented below in (3.11). A brief examination of (3.11) reveals that $\alpha \to -\alpha$ corresponds to interchanging gauge field polarizations, i.e. $\delta A_+ \to -\delta A_-$

$$\begin{aligned} 2\delta A_{\pm}''(r) - 4\sqrt{6}\,\delta g_{t\pm}'(r) - k(k \mp 8\sqrt{6}\alpha)\frac{\delta A_{\pm}(r)}{6r^2} = 0 \\ 6r^2\,\delta g_{t\pm}''(r) + 12r\delta g_{t\pm}(r) - \sqrt{6}\delta A_{\pm}'(r) - \frac{1}{2}k^2 \delta g_{t\pm}(r) = 0. \end{aligned} \tag{3.11}$$

The transverse channel can thus be split into two subchannels, one for each polarization.

We look for solutions to the linearized equations of motion that have a simple radial scaling:

$$\delta A_{\pm}(r) = a_{\pm} r^{\lambda_{\pm}} \qquad \delta g_{t\pm}(r) = g_{t\pm} r^{\gamma_{\pm}}. \tag{3.12}$$

The equations of motion allow us to determine the scaling exponents $\lambda_{\pm}$ and $\gamma_{\pm}$ as a function of momentum k and Chern-Simons coupling α. As described in detail in Goutéraux and Martin (2017), these exponents are directly related to the scaling exponent ν_k of the low energy spectral weight, introduced in (3.5). Thus the problem of calculating low energy spectral weight is reduced to the problem of determining these exponents and coefficients, to obtain

$$\sigma_k^{\perp} = \lim_{\omega \to 0} \frac{\mathrm{Im} G^R_{J_\perp J_\perp}(\omega, k)}{\omega} \sim \lim_{\omega \to 0} \omega^{2\nu_k^{\perp} - 1} \tag{3.13}$$

We now proceed to look at the results of this computation. Solving for the exponents in (3.12), we find that

$$\sigma_k^{\perp} = \lim_{\omega \to 0} \frac{\mathrm{Im} G^R_{J_\perp J_\perp}(\omega, k)}{\omega} = \left\{ \begin{array}{cc} \infty & \nu_k^{\perp} < \frac{1}{2} \\ 0 & \nu_k^{\perp} > \frac{1}{2} \end{array} \right\} \tag{3.14}$$

with

$$\nu_k^{\perp} = \frac{\sqrt{k^2 + 4\sqrt{6}\alpha k + 15 - 2\sqrt{6}\sqrt{k\left(4\alpha^2 k + 4\sqrt{6}\alpha + k\right) + 6}}}{2\sqrt{3}} \tag{3.15}$$

As discussed in Anantua *et al.* (2013), the infinity in (3.14) is because we are at zero temperature. Turning on a small nonzero black hole temperature endows this with a finite value. The important part for us is that, for each α, the condition $\nu_k^{\perp} = \frac{1}{2}$ picks out a special momentum $k = k_\star$, below which we have low energy spectral weight at finite momentum. As we explained in the introduction, this is an indication that the Pauli exclusion principle is at work, and our system is exhibiting a smeared Fermi surface momentum space structure at low energies. The critical value $k_\star(\alpha)$ is shown in Figure 3.1 as the line separating the regions $\nu_k^{\perp} < \frac{1}{2}$ and $\nu_k^{\perp} > \frac{1}{2}$.

From (3.15) we can also see that there is a certain critical $\alpha = \alpha_{\text{crit}}$ above which $\nu_k^{\perp}$ can become imaginary. Because $\nu_k^{\perp}$ is related to the conformal dimension of the dual field theory operator via $\Delta_k^{\perp} = \nu_k^{\perp} + \frac{1}{2}$, we see that imaginary $\nu_k^{\perp}$ signals an instability. The results for the transverse channel are depicted in Figure 3.1. The α_{crit} that we report is the same value reported in Nakamura *et al.* (2010).

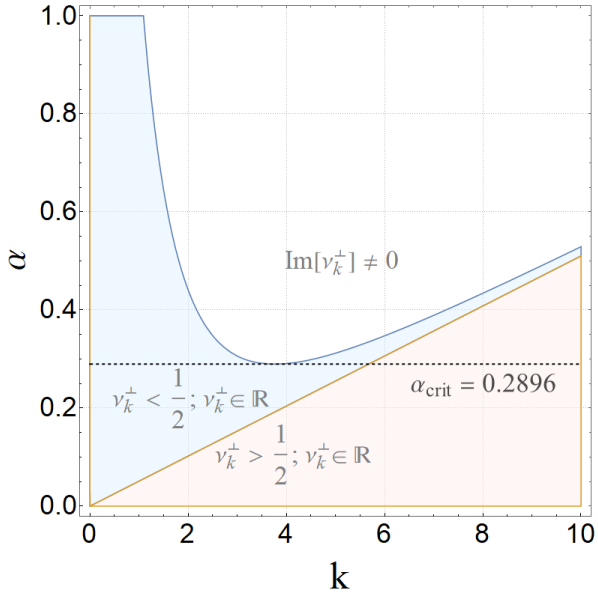

Figure 3.1: Transverse Channel. This is a region plot of the exponent $\nu_k^{\perp}$, occurring in $\sigma_k = \lim_{\omega \to 0} \omega^{2\nu_k^{\perp}-1}$. The upper shaded region, labeled $\text{Im}[\sigma_k^{\perp}] \neq 0$, represents the parameter space where an instability occurs. The α_{crit} reproduces the result of Nakamura *et al.* (2010). In the blue region there is low energy spectral weight at nonzero momentum, and in the red region there is not.

To make clearer the parallel between our approach and that followed by Nakamura *et al.* (2010), note that the general form of the exponent ν_k in $\text{AdS}_2 \times \mathbb{R}^{\text{d}}$ with fields charged under the relevant gauge group in consideration is given by Hartnoll *et al.* (2016)

$$\nu_k = \sqrt{\frac{1}{4} + m^2\, l_{AdS_2}^2 - \mathcal{Q}(\{\phi_i\}, l_{AdS_2})} \tag{3.16}$$

The quantity $\mathcal{Q}$ depends on the matter content in question. For the Einstein-Maxwell-Chern-Simons theory any charge present is carried only by the AdS-RN black-hole and thus this quantity is not present. One can quickly verify that plugging the ν_k found in (3.15) into the expression (3.16) we reproduce the quantity m^2 obtained by Nakamura et. al. (with a consistent choice of parameters, cf. eq. 3.11 in Nakamura *et al.* (2010)).

3.2.2 Longitudinal Channel

A significant simplification arises in the longitudinal channel. Because our background Maxwell field only has an electric component, the Chern-Simons term does not contribute to the perturbed equations of motion in this channel. Thus we are effectively looking at Einstein-Maxwell theory. For modes in the longitudinal channel we find no instability. However, we do again observe Pauli exclusion, where for $k < k_*$ we have non-zero low energy spectral weight at finite momentum. Explicitly, the exponent $\nu_k^{\parallel}$ is

$$\nu_k^{\parallel} = \frac{\sqrt{k^2 + 15 - 4\sqrt{2k^2 + 9}}}{2\sqrt{3}}, \tag{3.17}$$

from which we see that $k_* = 2\sqrt{2}$. This low energy spectral weight is shown in Figure 3.2.

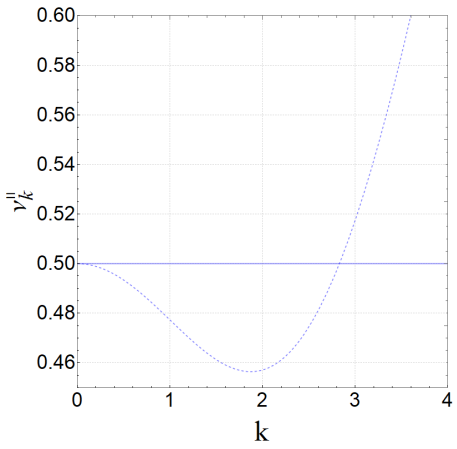

Figure 3.2: Plot shows longitudinal channel exponent $\nu_k^{\parallel}$. Note that below $\nu_k^{\parallel} = 1/2$ spectral weight exists, i.e. $\lim_{\omega\to 0}\ \omega^{2\nu_k^{\parallel}-1} \neq 0$.

3.3 Einstein-Maxwell-Dilaton-Chern-Simons

We now turn to Einstein-Maxwell-dilaton-Chern-Simons (EMDCS) theories, characterized by the action

$$\mathcal{S} = \int d^5x\sqrt{-g}\left[R - \frac{1}{2}\partial_m\phi\partial^m\phi - \frac{1}{4}Z(\phi)F_{ab}F^{ab} - V(\phi) + \frac{\alpha}{3!}\frac{\epsilon^{abcde}}{\sqrt{-g}}A_aF_{ab}F_{cd}\right]. \tag{3.18}$$

EMDCS theories admit a generalized version of the near-horizon AdS-RN geometries as solutions. We call these solutions η geometries, and the metric is given by

$$ds^2 = r^{-\eta}\left(\frac{-dt^2+dr^2}{r^2} + dx^2 + dy^2 + dz^2\right). \tag{3.19}$$

The value $\eta = 0$ corresponds to near-horizon AdS-RN. These η geometries can also be obtained from hyperscaling violating geometries Huijse *et al.* (2012); Charmousis *et al.* (2010); Fisher (1986); Dong *et al.* (2012) by taking the dynamical critical exponent $z \to \infty$ while keeping a ratio of z and the hyperscaling violating exponent θ fixed: $\eta \equiv -\theta/z$. These more general η geometries were not viable solutions in the previous Einstein-Maxwell-Chern-Simons thoery, but the addition of a dilaton allows for them.

As before, we take the background gauge field to have only an electric field component. The scalar field runs logarithmically in the radial coordinate to provide scaling solutions. The forms on $Z(\phi)$ and $V(\phi)$ are motivated by top-down constructions (see for example Iizuka *et al.* (2013); Goutéraux (2014))

$$A_t = A_0 r^{\zeta-1} \qquad A_i = 0 \qquad \phi(r) = \phi_0 \log r \tag{3.20}$$
$$Z(\phi) = e^{\gamma\phi} \qquad V(\phi) = V_0 e^{-\delta\phi}.$$

The scaling ansatz (3.20) only pertains to the near-horizon geometry. Obtaining consistent solutions of the field equations further constrains the background parameters, i.e. the exponents γ, δ and ζ satisfy the following conditions:

$$\delta = -\frac{\eta}{\phi_0} \qquad \gamma = \frac{2\eta}{\phi_0} \qquad \zeta = -\frac{3\eta}{2}. \tag{3.21}$$

In addition, we also have the following conditions for the coefficients associated with the cosmological constant term V, the background electric field and the scalar field

$$V_0 = -\frac{1}{4}(2+3\eta)^2 \quad \phi_0 = -\sqrt{\frac{3\,\eta\,(\eta+2)}{2}} \quad A_0 = \frac{2}{\sqrt{2+3\eta}}. \tag{3.22}$$

These parameters are required to be real and are further constrained by the null energy condition. Consistency with the NEC implies that $\eta > 0$. It is also worth noting that as we approach $\eta \to 0$, the dilaton field vanishes and the result reduces to the one obtained for the Einstein-Maxwell-Chern-Simons theory in the previous section. As before, we decompose modes into the longitudinal and transverse channels, and these modes carry momentum along $\mathbb{R}^3$. That is, we have $g_{mn} \to g_{mn} + \delta g_{mn}(r) e^{i\mathbf{k}.\mathbf{x}}$, and similarly for the gauge field $A_m \to A_m + \delta A_m(r) e^{i\,\mathbf{k}.\mathbf{x}}$. To reiterate, we work in the radial gauge where $\delta g_{mr} = 0$ and $\delta A_r = 0$.

3.3.1 Transverse Channels

We now move to the computation of the exponent $\nu_k^\perp$ for the two transverse directions. Recall that, as was shown in the previous section, these can be packaged together into polarizations. Choosing either positive or negative values of the Chern-Simons coupling is equivalent to swapping polarizations. The functional form of the transverse channel scaling exponent is:

$$\nu_k^\perp = \frac{1}{4}\Bigg(3\eta(3\eta+4) + 16k\left(-2\alpha\sqrt{3\eta+2}+k\right) + 20 \\ - 8\sqrt{(3\eta+2)\left(3\eta+4k\left(-2\alpha\sqrt{3\eta+2}+4\alpha^2 k+k\right)+2\right)}\Bigg)^{1/2}. \tag{3.23}$$

The exponent $\nu_k^\perp$ only becomes complex for $\alpha > 0$, as was the case for the Einstein-Maxwell-Chern-Simons theory. Thus instabilities only exist for positive values of α. Just as in the discussion surrounding Figure 3.1, there is a critical value $\alpha = \alpha_{\text{crit}}$ above which the theory is unstable. However, now we see that α_{crit} depends upon the metric parameter η. This dependence is shown in Figure 3.3. Interestingly, $\eta = 2/3$ appears to be a special value for which no stable theories exist.

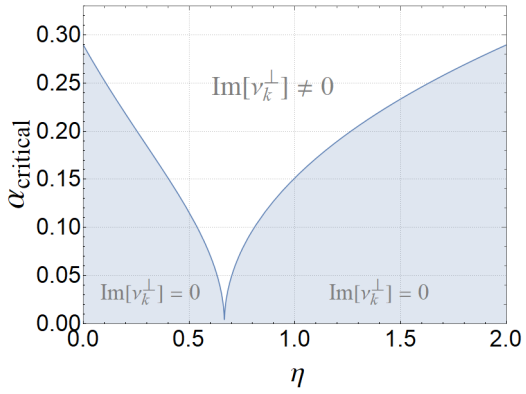

Figure 3.3: This figure shows the regions of stability and instability in the transverse channel for various values of η. The shaded region is stable, while the unshaded region where $\text{Im}[\nu_k^\perp] \neq 0$ indicates an instability.

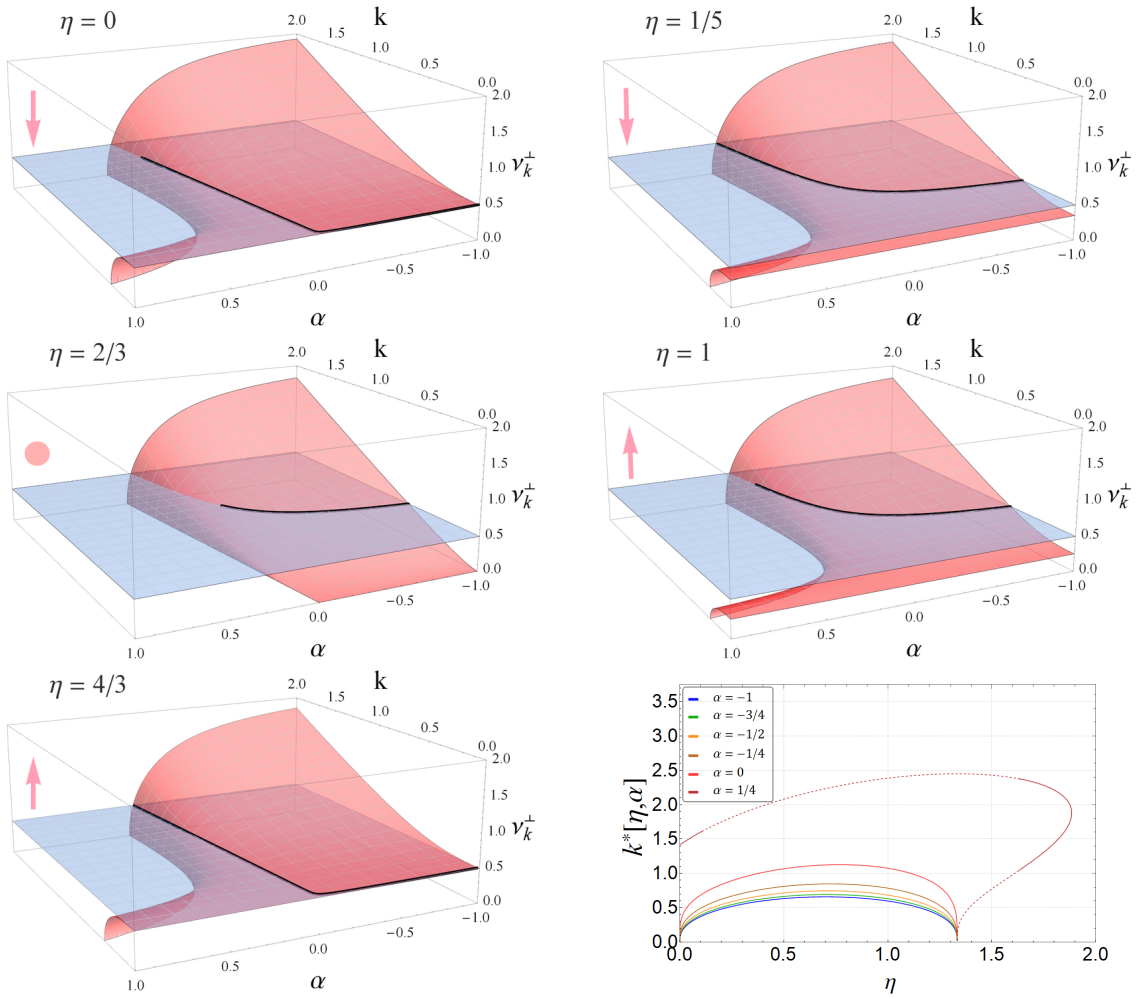

Figure 3.4: These figures elucidate the effect of the background metric parameter η and the Chern-Simons coupling on the exponent $\nu^\perp$. In the 3D plots, $\nu^\perp$ is plotted with the $\nu^\perp = 1/2$ plane, below which spectral weight exists (that is, $\sigma(k) \propto \omega^{2\nu_k^\perp - 1} \to \infty$). As η increases between $0 < \eta < 2/3$, the $\nu_k^\perp$ surface falls below the 1/2 plane. For $\eta > 2/3$ the $\nu_k^\perp$ surface rises again. For $\eta > 4/3$ no spectral weight exists. The bottom right plot shows how k^* changes for different values of α. We see that k^* increases for increasing α. For positive values of α the theory can become unstable, and these regions are indicated by dashed lines on the $\alpha = 1/4$ curve.

We can also see that this channel possesses low energy spectral weight at finite momentum for certain values of $\alpha < 0$[6] and for $\eta < 4/3$. For values of η greater than this value no smeared Fermi surface structure is present. The critical momentum $k^\star$ above which no spectral weight exists varies non-monotonically with increasing η. For $0 < \eta < 2/3$, $k^\star$ increases with increasing η, and then decreases for increasing η between $2/3 < \eta < 4/3$. This is displayed in Figure 3.4 above.

Further, it is worth noting that increasing the value of η never results in the formation of a Fermi shell (as opposed to a Fermi surface). That is, in Figure 3.5 the exponent $\nu_k^\perp$ intersects the $\nu_k^\perp = 1/2$ line only once. The critical value of the Chern-Simons coupling α above which the theory becomes unstable depends on the metric parameter η. Taking $\eta \to 0$ reduces to the condition for α_{crit} obtained by Nakamura *et al.* (2010).

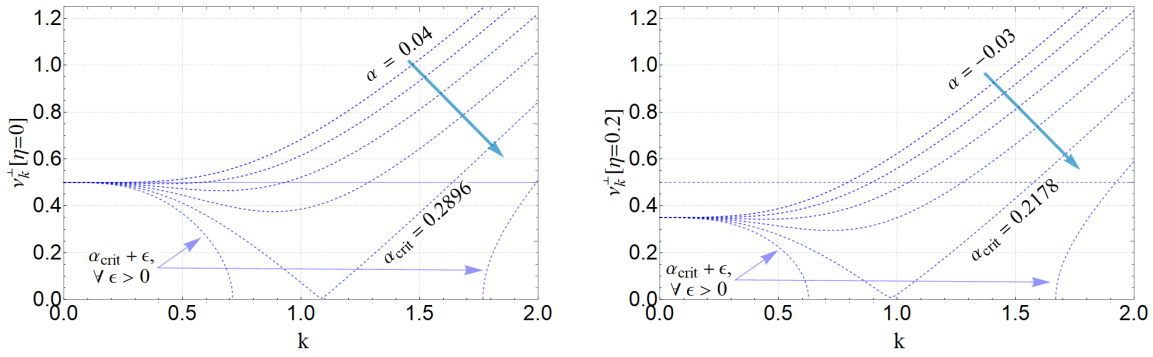

Figure 3.5: The exponent $\nu_k^\perp$ intersects the $\nu_k^\perp = 1/2$ line only once, indicating the presence of a smeared Fermi surface as opposed to a Fermi shell.

3.3.2 Longitudinal Channel: General Dimension

Since our background gauge field is purely electric, the Chern-Simons term does not contribute towards the longitudinal channel spectral weight at leading order.

[6]Taking $\alpha < 0$ ensures that we are well outside of the instability region.

Thus our EMDCS theory effectively reduces to the Einstein-Maxwell-dilaton theory in the longitudinal channel. The low energy spectral weight of the Einstein-Maxwell-dilaton theory was studied in Anantua *et al.* (2013). In this section we give a simple augmentation of that analysis by studying the low energy spectral weight of Einstein-Maxwell-dilaton theory in general dimensions. The general dimension ($d > 3$) longitudinal channel exponent is:

$$\nu_k^{\parallel}(d,\eta) = \frac{1}{2}\Bigg[\frac{4k^2(2+\eta)+\frac{1}{4}(10+\eta)(2+(d-2)\eta)^2}{2+\eta} - \frac{8}{2+\eta}\sqrt{\left(1+\frac{1}{2}(d-2)\eta\right)^4+\frac{(d-3)k^2(2+\eta)(2+(d-2)\eta)^2}{2(d-2)}}\Bigg]^{1/2}. \tag{3.24}$$

We have verified explicitly that (3.24) holds for $3 < d < 13$. We will discuss the large d behavior of this expression shortly. We also see from (3.24) that $\nu_k^{\parallel}(d,\eta)$ is real for all d and η, and thus no instability exists in this channel.

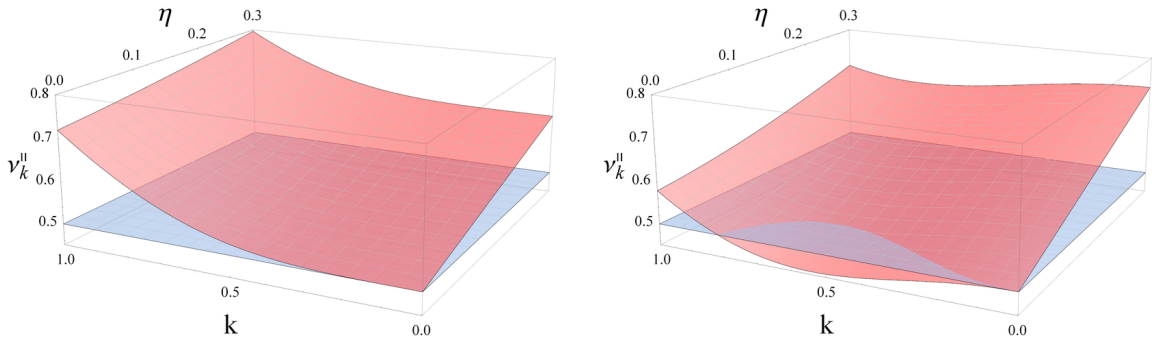

(a) (b)

Figure 3.6: Left: For 3+1 bulk dimensions, the longitudinal channel exponent $\nu_k^{\parallel}$ is plotted against the background metric parameter η and momentum k. Right: For 4+1 bulk dimensions the longitudinal channel exponent is shown. Note that the 3+1 dimensional case is the critical case where no spectral weight is observed, whereas in 4+1 dimensions (and higher) spectral weight exists.

We can now analyze the appearance of low energy spectral weight in the Einstein-Maxwell-dilaton theory for general dimension $d > 3$. The authors of Anantua *et al.* (2013) found that, for the geometry and matter content that we are considering in this subsection, the longitudinal low-energy spectral weight vanishes for all η in $d = 4$ dimensions. Interestingly, Figure 3.6 shows that this result is unique to $d = 4$ dimensions. Figure 3.6b shows that for $d = 5$ the $\nu_k^{\parallel}$ surface dips below the $\nu_k^{\parallel} = 1/2$ plane, which corresponds to a non-vanishing spectral weight. Furthermore, Figure 3.6b shows that when spectral weight is present it exists between two nonzero values k_+ and k_-. This signals the presence of a Fermi shell, and from Figure 3.6b we can see that the shell thickness $k_+ - k_-$ monotonically decreases as η increases. We will see that this behavior is distinct from what is observed upon making the gauge field massive, as in 3.12a, where $k_+ - k_-$ is not monotonically decreasing in η. At $\eta = 0$, $k_- = 0$ for all d. Thus for $\eta = 0$ only we have a smeared Fermi surface in the longitudinal channel, rather than a shell. This is shown in Figure 3.7.

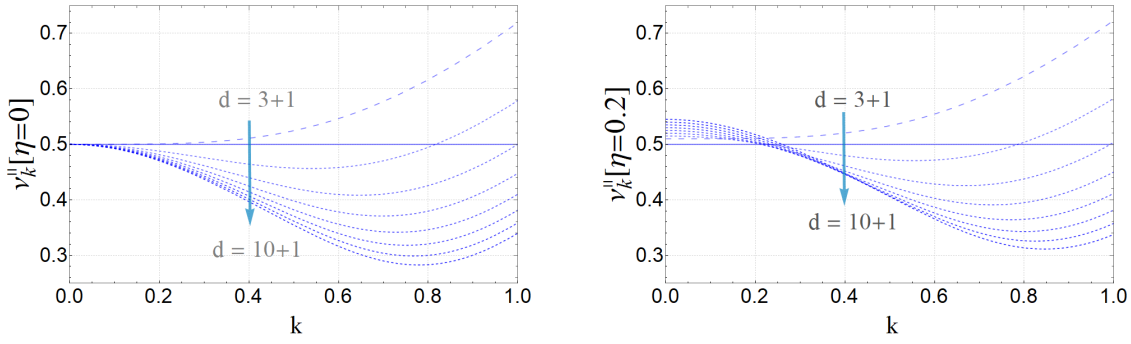

(a) (b)

Figure 3.7: Left: For $\eta = 0$ and $d > 4$ low energy spectral weight is present in the form of a smeared Fermi surface. For $d = 4$ there is no spectral weight. Right: Increasing η immediately lifts the smeared Fermi surface to a Fermi shell, as in Figure 3.6b above.

Another observation that we can make from Figure 3.6b is that, for each spacetime dimension d, there exists a critical value of η above which no spectral weight exists for any momenta. For $d = 4$ dimensions this critical value is $\eta = 0$.

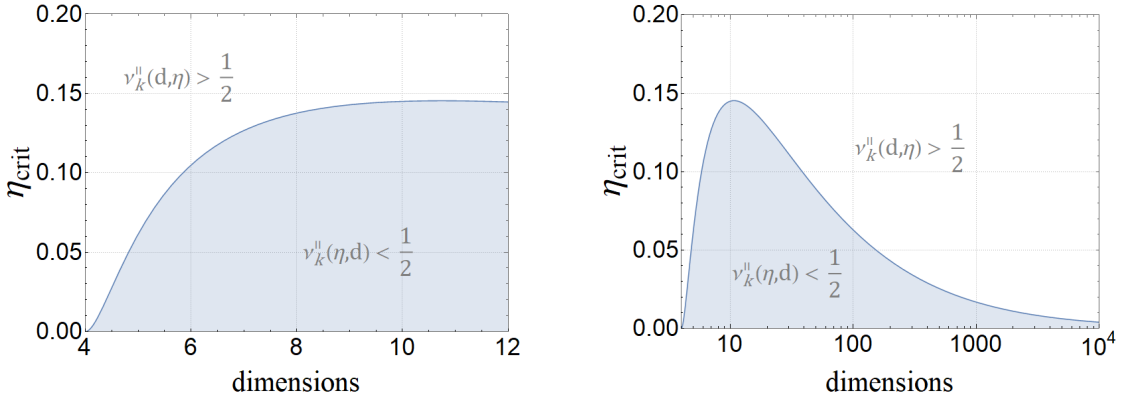

(a) (b)

Figure 3.8: The critical value of the metric parameter η (above which no spectral weight exists) is plotted as a function of dimension d. At $d = 11$, the η_{crit} reaches a maximum value. In the large d limit non-zero low energy spectral weight is suppressed.

However for higher dimensions η_{crit} increases with d, until it eventually reaches a maximum and begins to decrease. It is amusing to note that this maximum occurs at $d = 11$, the dimension of the conjectured M-theory and the associated low energy 11-dimensional supergravity. The quantity η_{crit} is plotted as a function of spacetime dimension in Figure 3.8 above.

3.4 Holographic Superfluid Plus Chern-Simons

We now examine the effect of a Chern-Simons term on the spectral weight of the holographic superfluid studied in Goutéraux and Martin (2017). The main technical difference between this section and Section 3.3 is that the massive vector lets us add another tunable parameter to the theory (namely the exponent ζ in Equation (3.27)).

The results of Section 3.3 are recovered when $\zeta = -3\eta/2$. As before, we work with η geometries with only an electric field present. We work with the background metric,

$$ds^2 = r^{-\eta}\left(\frac{-dt^2+dr^2}{r^2} + dx^2 + dy^2 + dz^2\right) \tag{3.25}$$

and action

$$\begin{aligned}\mathcal{S} = \int d^5x\sqrt{-g}\,\Big[R - \frac{1}{2}\partial_m\phi\partial^m\phi - \frac{1}{4}Z(\phi)F_{ab}F^{ab} - \frac{1}{2}W(\phi)\,A_m\,A^m - V(\phi) \\ + \frac{\alpha}{3!}\,\frac{\epsilon^{abcde}}{\sqrt{-g}}A_aF_{ab}F_{cd}\Big].\end{aligned} \tag{3.26}$$

We again ensure that we have a scaling solution by imposing the background conditions

$$\begin{aligned} A_t = A_0 r^{\zeta-1} \qquad A_i = 0 \qquad\qquad \phi(r) = \phi_0 \log r \\ Z(\phi) = e^{\gamma\phi} \qquad V(\phi) = V_0 e^{-\delta\phi} \qquad W(\phi) = W_0 e^{-\chi\phi}.\end{aligned} \tag{3.27}$$

The background equations of motion relate these background parameters in the following way:

$$\begin{aligned} V_0 &= \frac{1}{4}\left(4\zeta - 9\eta^2 - 6\eta - 4\right) \qquad & A_0 &= \sqrt{\frac{2}{1-\zeta}} \\ \phi_0 &= \sqrt{\frac{3\eta^2 - 4\zeta}{2}} & W_0 &= \frac{1}{2}(1-\zeta)(2\zeta+3\eta)\end{aligned} \tag{3.28}$$

Some of the parameters introduced above are further constrained when we require that we are in a physically relevant parameter space. For example, we require that the null energy condition is satisfied, that our "cosmological constant" term $V_0 < 0$, the reality of all theory parameters, and a consistent radial deformation analysis described in detail in Goutéraux and Martin (2017); Goutéraux (2014). This results in the following constraints on the parameter space.

$$\begin{gathered} 0 < \eta \leq \frac{\left(\sqrt{33}-3\right)}{6} \;\&\; -\frac{3\eta}{2} \leq \zeta < \frac{3\eta^2}{4} \\ \text{Or} \\ \eta > \frac{\left(\sqrt{33}-3\right)}{6} \;\&\; -\frac{3\eta}{2} \leq \zeta < \frac{(2-3\eta)}{4}\end{gathered} \tag{3.29}$$

The shaded region in Figure 3.9 provides the allowed region of parameter space that is consistent with all of these conditions. Note from (3.28) that the line $\zeta = -\frac{3\eta}{2}$ appearing in Figure 3.9 corresponds to the massless vector case, when $W_0 = 0$. We now proceed to discuss our results in detail for the two sets of transverse channels and the longitudinal channel.

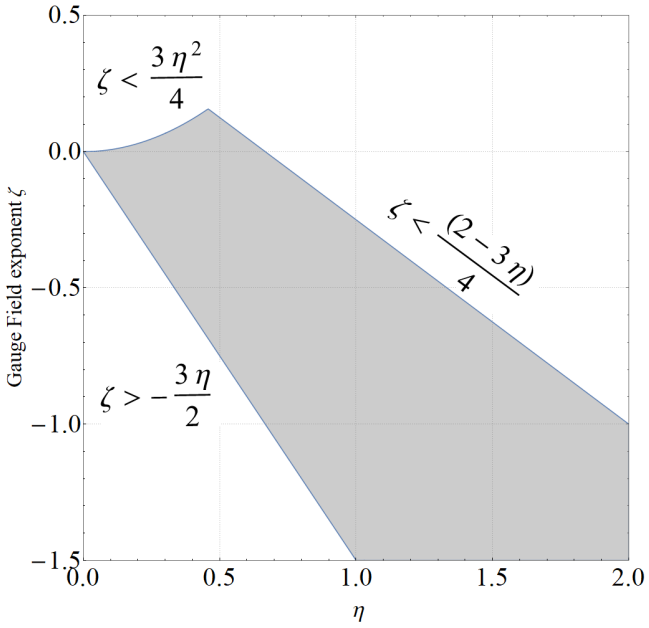

Figure 3.9: The shaded region represents the allowed values of the parameter ζ for different values of η. The Chern-Simons term does not constrain the parameter space, due to the simplicity of our electric field-only background.

3.4.1 Transverse Channel

In the transverse channel the spectral weight exponent ν is now a quantity which depends on ζ, η and α. The closed form expression for the transverse channel exponent here is,

$$\nu_k^{\perp} = \frac{1}{4}\Bigg(9\eta^2 + 12\eta + 16k^2 - 32\sqrt{2}\alpha k\sqrt{1-\zeta} + 20 \\ - 8\sqrt{(3\eta+2)^2 - 8\left(4\alpha^2+1\right)(1-\zeta)k^2 + 8\sqrt{2}\alpha k(3\eta+2)\sqrt{1-\zeta}}\Bigg)^{1/2}. \tag{3.30}$$

We can now investigate the combined effect of the massive vector and the Chern-Simons term on the region of instability and the low-energy spectral weight. The first thing that we can do is compare the instability plot from Section 3.3 (Figure 3.3) to the instability plot in Figure 3.10.

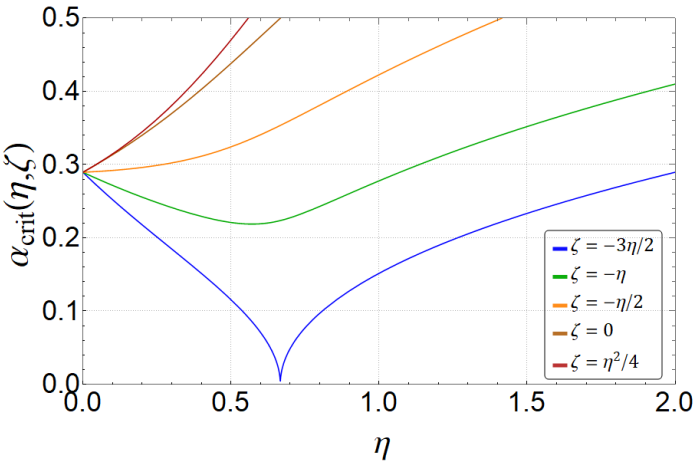

Figure 3.10: This plot demarcates the critical value of α above which the theory becomes unstable, as a function of η and for different values of ζ.

We can see from Figure 3.10 that $\eta = 2/3$ is no longer of special significance in the presence of a massive vector. The effect of increasing ζ is to lift the instability region, so that more stable theories are possible. However, one result of staying within our allowed parameter space is that the instability region never disappears completely.

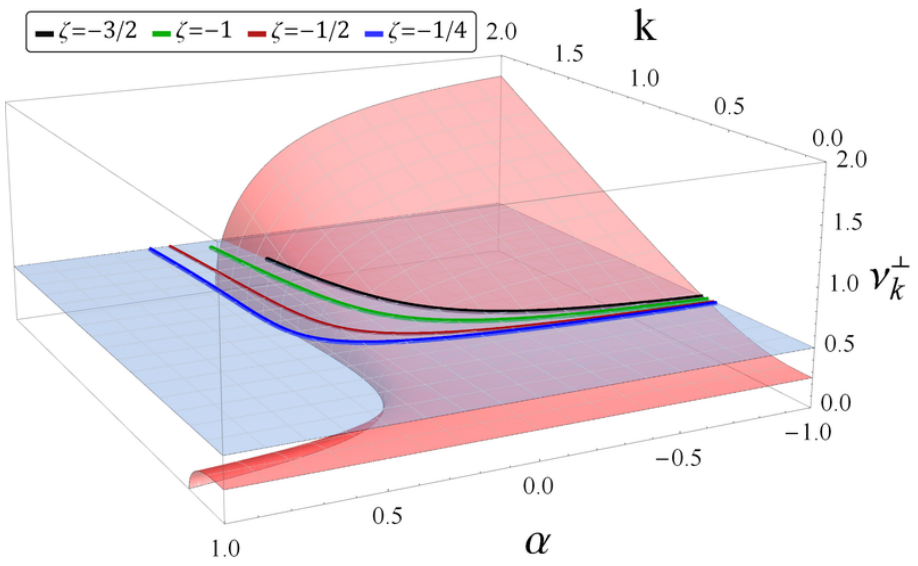

Figure 3.11: This plot illustrates the combined effect of the Chern-Simons coupling α and the massive vector (via the exponent ζ) on the exponent $\nu_k^\perp$. The 3D plot corresponds to $\eta = 1$. Above the $\nu_k^\perp = 1/2$ plane no spectral weight exists. The curves plotted in the $\nu_k^\perp = 1/2$ plane represent the critical momentum k_* for different values of ζ.

We now investigate the effect of the massive vector parameter ζ and the Chern-Simons coupling α on the low-energy spectral weight. Figure 3.11 illustrates that increasing either ζ or α decreases the critical momentum k_*, but only appreciably for $\alpha > 0$. Thus the Chern-Simons term and the massive vector both have similar effects on the spectral weight, though they break different symmetries (translation symmetry and $U(1)$ invariance, respectively).

3.4.2 Longitudinal Channel

Since the Chern-Simons term does not contribute to the spectral weight in the longitudinal channel, the theory effectively becomes a holographic superfluid. The spectral weight for the holographic superfluid was analyzed in Goutéraux and Martin

(2017), where they reported a finite k instability and a Fermi shell (that is, non-zero low energy spectral weight occurring between a k_+ and k_-) in the longitudinal channel. The only difference between our system and Goutéraux and Martin (2017) is that we work in five spacetime dimensions rather than four. Thus we will keep this section short and refer the reader to Goutéraux and Martin (2017) for more details (particularly regarding the finite k instability). We will, however, include plots regarding the Fermi shell structure of this theory that were absent in Goutéraux and Martin (2017) for completeness. We leave an analysis of this system in general dimension to future work.

One intriguing aspect of the Fermi shell in this channel is that the shell thickness $\Delta k \equiv k_+ - k_-$ does not change monotonically in η for a given ζ. Figure 3.12a shows that, for a particular value of ζ, Δk first decreases with increasing η until it vanishes completely, but then reappears for some larger η. This vanishing spectral weight for certain values of η does not occur for all ζ, however. This is shown in Figure 3.12b.

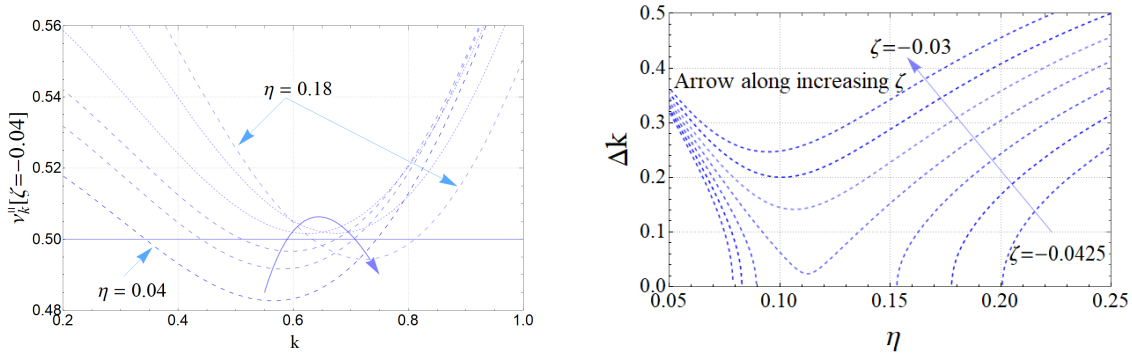

(a) (b)

Figure 3.12: Left: The longitudinal channel exponent $\nu_k^{\parallel}$ shows nonzero spectral weight between two nonzero values k_+ and k_-, both of which depend on η. We call this a Fermi shell. The shell thickness Δk varies non-monotonically with η. Right: For more negative values of ζ, the spectral weight can disappear entirely for a certain range of η.

3.5 Discussion

We have calculated the low energy spectral weight of a holographic superfluid model with an additional Chern-Simons term in a five-dimensional near-horizon η geometry and electric field-only background gauge field. One motivation for this was to compare the influence of the Chern-Simons term and the condensate charge on the spectral weight and the instability regions when they occur. In this section, we try to draw conclusions based on spectral weight calculations of the five theories that we have mentioned: 1) Einstein-Maxwell-dilaton (EMD) Anantua *et al.* (2013), 2) Einstein-Maxwell-Chern-Simons (EMCS) Nakamura *et al.* (2010), 3) Einstein-Maxwell-dilaton-Chern-Simons (EMDCS), 4) holographic superconductor (HS) Goutéraux and Martin (2017), and 5) holographic superconductor with Chern-Simons (HSCS).

There is something in common among all five theories that we've mentioned in this work: the transverse channels all possess low-energy spectral weight of the form (3.6), which we call a smeared Fermi surface. This underscores that it is really the geometry that is responsible for the presence of spectral weight, rather than any particular matter content. Furthermore, it shows that the η geometries in particular are robustly fermionic in nature. This fermionic quality is not present, for example, in the more general hyperscaling violating geometries Hartnoll and Shaghoulian (2012).

Another thing that all[7] of these theories have in common is that the longitudinal channel possesses low-energy spectral weight of the form (3.7), which we call a Fermi shell. This was a somewhat surprising result, given that Anantua *et al.* (2013) found that, for the EMD theory, low-energy spectral weight did not exist in the longitudinal

[7]Due to the simplicity of our electric field-only background gauge field, the Chern-Simons term does not effect any of the longitudinal channels. Therefore we can effectively only compare the EMD theory and the holographic superconductor in this channel.

channel. It turns out, though, that this result is unique to $d = 4$ spacetime dimensions. We found that for $d > 4$ the longitudinal channel supports low energy spectral weight in the form of a shell. This is another indication that the role of η is to determine the overall presence or absence of spectral weight. It is interesting to note that Fermi shells also appear in top-down constructions in $\mathcal{N} = 4$ supersymmetric Yang-Mills DeWolfe *et al.* (2012) and ABJM theory DeWolfe *et al.* (2015). In top-down constructions the matter content of the dual field theory is known, and it was seen explicitly that Fermi shells arise from a superposition of two Fermi surfaces (which result from two distinct fermions). In our bottom-up construction we don't have access to the dual field theory matter content, but perhaps the presence of the Fermi shell signals what sort of dual field theory we might expect. It is interesting and puzzling, however, that the presence of our Fermi shells seem to depend on the geometry rather than matter content. *However*, in a way the η geometry solutions *are* tied to matter content, in the sense that a dilaton is necessary for them to exist (Einstein-Maxwell theory is not enough, for example).

It appears that the role of both the Chern-Simons term (parameterized by α) and the massive vector (parameterized by ζ) is to dictate whether or not instabilities are present. Furthermore, we saw in Section 3.4.1 that both α and ζ act in the same way: increasing either one of them lifts the instability region so that more stable theories are possible. It appears, though, that the Chern-Simons coupling α more often controls transverse channel instabilities, whereas the vector mass parameter ζ tends to control the presence of an instability region in the longitudinal channel. This could be due to our choice of background gauge field. We leave the addition of a magnetic field for future work.

We generalized the result obtained in Nakamura *et al.* (2010) for the critical value of α above which the theory becomes unstable. For EMCS, Nakamura *et al.* (2010)

found that $\alpha_{\text{crit}} = .2896$, which we generalized to $\alpha_{\text{crit}}(\eta)$ for EMDCS and $\alpha_{\text{crit}}(\eta, \zeta)$ for HSCS. For the latter we found that $\eta = 2/3$ is a special value for which no stable theories exist. It might be the case that this is only true for $d = 5$ dimensions, and we leave checking that conjecture to future work. The authors of Nakamura *et al.* (2010) also commented that the value of α imposed by the UV complete superstring theory that they considered barely satisfied the stability bound $\alpha < \alpha_{\text{crit}}$. It would be interesting to identify a UV completion of the theories considered here and check whether or not the corresponding stability bound holds in our more general cases. We leave this for future work.

As we already mentioned, we extended the analysis of Anantua *et al.* (2013), which calculated the low-energy spectral weight of EMD in η geometries in $d = 4$, to general d. We found that the dimension $d = 4$ is in fact a special case that contains no spectral weight: for $d > 4$ low-energy spectral weight is always present (Figure 3.7). Furthermore, in Figure 3.8 we plotted the critical η above which the spectral weight vanishes as a function of dimension. It is amusing to note that this $\eta_{\text{crit}}(d)$ plot peaks at the value $d = 11$, the dimensionality of the conjectured M-theory and associated 11d supergravity. Beyond $d = 11$ spectral weight decreases, and then is suppressed for large d.

Chapter 4

FROM EINSTEIN TO NAVIER-STOKES: THE FLUID GRAVITY DUALITY

In this chapter we provide an introduction to the fluid-gravity duality in its various forms and set the stage for our calculations, the results of which are presented in chapter 5. We expound on select works in the field to provide a chronological context for our research. This includes early work by Damour (1978, 1979), to work on the membrane paradigm by Thorne *et al.* (1986); Price and Thorne (1986), finally to modern day formulations of the fluid-gravity duality by Policastro *et al.* (2001); Kovtun *et al.* (2003); Son and Starinets (2007); Bhattacharyya *et al.* (2009a); Bredberg *et al.* (2011, 2012); Bredberg and Strominger (2012).

We will elucidate various aspects of the tools and methodologies utilized. This includes the framework for classifying space-times based on Weyl tensors, also known as the Petrov classification Stephani *et al.* (2003), our chosen methodology for these computations following Cocke (1989), specifics on the form of the fluid-gravity duality we follow: Bredberg *et al.* (2012); Bredberg and Strominger (2012) and lastly we briefly touch upon the double copy paradigm we adopt Luna *et al.* (2019). A further discussion of the double copy approach can be found in chapter 5.

4.1 Historical Overview

Discussions of the fluid-gravity duality inevitably begin with the work of Damour [Damour (1978, 1979)]. Motivated by work on the emergence of black-hole thermodynamics, as had been discussed by [Hartle (1973, 1974); Hawking and Hartle (1972)] and others, Damour (1982) set out to study "mechanical properties" associated with

null hypersurfaces of black-holes, their horizons. Damour, attempting to compute a local conservation of momentum for these null hyper-surfaces, obtained a Navier-Stokes like expression in the process. He thereby demonstrated that horizons locally behave similar to surfaces of viscous fluid bubbles carrying negative surface tensions with pressure being proportional to the surface gravity κ and viscosity $\eta = (16\pi G_N)^{-1}$ [1]. This expression can be stated as,

$$\mathcal{L}_l \pi_A = -\nabla_A \frac{\kappa}{8\pi} + \frac{1}{8\pi}\nabla_B \sigma_A{}^B - \frac{1}{16\pi}\nabla_A \theta - l^\mu T_{\mu A} \tag{4.1}$$

where the vector l^μ is null and normal to the horizon. The quantity π^A is Damour's definition of the surface momentum density associated with black-hole horizons, κ refers to the surface gravity of the black-hole. In addition, based on the extrinsic curvature K_{AB} with respect to the horizon induced metric γ_{AB}, we have the following defintions,

$$\sigma_{AB} = -\gamma_{AC}\kappa^C{}_B + \frac{1}{2}\gamma_{AB}\theta \qquad \theta = -K^A{}_A. \tag{4.2}$$

Expression eq. (4.1) is very similar to a Navier-Stokes equation where the time derivative of velocity term (here identified by the Lie derivative of π^A) relates to the spatial derivative of a pressure term (identified by surface gravity κ) with shear viscosity $\eta = 1/16\pi$ and bulk viscosity $\zeta = -1/16\pi$ and lastly an external driving force provided by the stress tensor contraction, $f_A = -l^\mu T_{\mu A}$. This Navier-Stokes like expression is also known as the Damour-Navier-Stokes equation. If the black-hole in question is charged than one can similarly ascribe a resistivity to this fluid surface.

These developments lead us to the membrane paradigm of black-hole mechanics, whereby the dynamics of horizons, and thus its associated microstates are modeled as membranes whose thermodynamic, mechanical and electrical properties are known [Thorne *et al.* (1986); Price and Thorne (1986)].

[1] For the remainder of this chapter $G_N \to 1$.

There are multiple formulations of the fluid-gravity correspondence. For instance, in the context of the AdS/CFT correspondence [Rangamani (2009)] one obtains a map between black-hole solutions in the bulk of the spacetime which describe hydrodynamics for fluid flows associated with the boundary field theory. Notable successes of this approach include [Policastro *et al.* (2001, 2002a,b)], where hydrodynamics for $\mathcal{N} = 4$ Super Yang-Mills were linked to quasinormal modes for AdS black branes. Specifically [Policastro *et al.* (2001, 2002a)] found the existence of a lower bound on viscosity for arbitrary fluids *that are not superfluids* and have non-vanishing entropy density, specifying that the viscosity cannot be arbitrarily small,

$$\frac{\eta}{s} \geq \frac{\hbar}{4\pi}. \tag{4.3}$$

The ratio of shear viscosity to entropy for quark gluon plasmas has proven to be tantalizingly close to this number and consistent with the bound [Teaney (2003); Shuryak (2004)].

Lastly we turn our attention to the form of the fluid-gravity duality that we adopt in this paper. This is largely based on the work by [Bredberg *et al.* (2012); Bredberg and Strominger (2012); Lysov and Strominger (2011)]. In comparison to the previous approaches, the techniques adopted in these papers provides for an exact realization of the Navier-Stokes equations if the vacuum Einstein equations are satisfied. In the following section we discuss these developments in detail.

4.2 The Cutoff Surface/Wilsonian Approach to the Fluid-Gravity Duality.

The cutoff surface approach of [Bredberg *et al.* (2011, 2012)] attempts to construct a more explicit formulation of the fluid-gravity duality wherein Einstein's equations exactly give the incompressible Navier-Stokes equations. This approach involves introducing a cutoff surface Σ_c at some cutoff radius $r_c > r_h$, the horizon radius. Then

by imposing infalling boundary conditions on the horizon and considering graviton modes that originate from this cutoff surface. Bredberg *et al.* (2011) showed that the dispersion relations of these modes correspond to that of linearized limit of the Navier-Stokes equations, and finally Bredberg *et al.* (2012) extended this approach to include non-linear portions of the incompressible Navier-Stokes equation as well.

Damour's approach involves explicit constructions on horizons, the approach adopted by [Policastro *et al.* (2001)] involves considering timelike hypersurfaces at spatial infinity in AdS backgrounds. The work by Bredberg *et al.* (2011, 2012) in someways allows for a connection between the two prior approaches. Given that in holography changing scaling the radial coordinate from the horizon to infinity is associated with a holographic formulation of the renormalization group flows [Bianchi *et al.* (2001, 2002); Skenderis (2002)], the authors of Bredberg *et al.* (2011) identified their approach to the fluid-gravity duality as a Wilsonian approach.

It should be pointed out that the approach adopted in this work is perturbative, however versions of the fluid-gravity duality that extend to all orders have been found, eg. [Compere *et al.* (2011)]. Further details of the calculation and additional discussions are presented in chapter 5.

4.3 Methodology

We now describe the methodology adopted by us in Keeler *et al.* (2020), the results of which are expounded in the following chapter. We describe properties of the Weyl tensor that allow us to classify spacetimes, known as the Petrov classification. These classifications will prove to be important for us in finally implementing the double-copy picture proposed by Luna *et al.* (2019) for fluid spacetimes. We will conclude

with explanations of our implementations of the Newman-Penrose formalism using the methodology of Cocke (1989).

4.3.1 The Petrov Classification and Algebraic Speciality

Spacetimes in 4 dimensions[2] can be classified on the basis of the eigenbivectors of their associated Weyl tensors. For the Weyl tensor $C_{\mu\nu\rho\sigma}$ we have,

$$\frac{1}{2}C_{\mu\nu\rho\sigma}X^{\rho\sigma} = \lambda X^{\mu\nu} \tag{4.4}$$

A complex conjugate for these expressions can be defined, assuming real eigenvalues we have,

$$\frac{1}{2}C^{*}_{\mu\nu\rho\sigma}X^{*\,\rho\sigma} = \lambda X^{*\,\mu\nu} \tag{4.5}$$

Consider a timeline unit vector u^{μ} with $u^2 = -1$. Contracting both sides of the above expression by u_{μ} and using $u^2 = -1$, we obtain a rank 2 tensor Q obtained from the Weyl tensor, $Q_{\mu\nu} = -C^{*}_{\mu\nu\rho\sigma}u^{\rho}u^{\sigma}$.

These identifications allow us to recast the eigenbivector problem of the Weyl tensor eq. (4.4) as an eigenvector proble, we are now in a position to discuss the Petrov classification in more detail.

$$Q_{\mu\nu}X^{\nu} = \lambda X_{\mu} \tag{4.6}$$

[2]Classifications in higher dimensions using a similar methodology are possible, see for instance Lysov and Strominger (2011). However the complexity and associated labels change. For the purpose of keeping our discussion pertinent and to avoid unnecessary complexity we will restrict ourselves to 4 dimensions.

The eigenvalues of this matrix Q, identify for us the Petrov classification (c.f. table 4.1 Stephani *et al.* (2003)), we have,

$$\begin{aligned}
\text{Petrov type I} &: (Q-\lambda_1\mathbb{I})(Q-\lambda_2\mathbb{I})(Q-\lambda_2\mathbb{I})=0\\
\text{Petrov type D} &: (Q+\frac{1}{2}\lambda\mathbb{I})(Q-\lambda\mathbb{I})=0\\
\text{Petrov type II} &: (Q+\frac{1}{2}\lambda\mathbb{I})^2(Q-\lambda\mathbb{I})=0\\
\text{Petrov type N} &: Q^2=0.\\
\text{Petrov type III} &: Q^3=0.\\
\text{Petrov type O} &: Q=0.
\end{aligned} \tag{4.7}$$

In our work we perform this classification of spacetimes by computing invariants I,J,K, L and N [c.f. appendices A and B as well as the following subsection].

4.3.2 Spin Coefficients and Weyl Scalars.

As was alluded to above, instead of direct computations of the eigenbivectors of the Weyl tensor $W_{\mu\nu\rho\sigma}$ we reformulate our computations using SL(2,C) spinor representations of various geometric quantities thus computing the Weyl spinor C_{ABCD} instead. The Weyl spinor can be obtained from the tensor by using the appropriate curved space Pauli matrices(appendix A),

$$C_{ABCD}=\frac{1}{2}W_{\mu\nu\rho\sigma}\sigma^{\mu\nu}_{AB}\sigma^{\rho\sigma}_{CD} \tag{4.8}$$

This approach is known as the Newman-Penrose formalism. In this section we will discuss the methodology we follow in implementing this formalism which ultimately will give us a handle on the Petrov classification for spacetimes as we use them, details of this are compactly stated in appendices A and B.

The first step in implementing the Newman-Penrose (NP) formalism is the identification of a tetrad set consisting of 2 real and 2 complex vectors whose outer product

produces the metric,

$$g_{\mu\nu} = -l_{(\mu}n_{\nu)} + m_{(\mu}\overline{m}_{\nu)} \tag{4.9}$$

The tetrad components are null and obey the following conditions,

$$l^2 = n^2 = m^2 = 0, \quad \overline{m} \equiv m^*, \quad l.n = -1, \quad l.m = n.m = 0, \quad m.\overline{m} = 1. \tag{4.10}$$

Scalar products of the tetrad components and various directional derivatives above allow us to define spin coefficients and eventually a set of scalars that identify geometric properties of the space-time. The directional derivatives based on our tetrad set are,

$$D = l^\mu \nabla_\mu, \qquad \Delta = n^\mu \nabla_\mu, \qquad \delta = m^\mu \nabla_\mu, \qquad \bar{\delta} = \bar{m}^\mu \nabla_\mu. \tag{4.11}$$

Note that the approach we adopt here for the computation of these coefficients is based on Cocke (1989), see table 4.1 below. We adopt this approach over the original approach [Cocke (1989); Stephani *et al.* (2003)] for computing spin-coefficients since it is computationally quicker and easier. The reason is that in the [Cocke (1989)] approach several covariant derivatives are replaced by partial derivatives since the curl of the tetrad components are instead used for the calculation.

Spin Coefficient	$f(l^\mu, n^\mu, m^\mu, \overline{m}^\mu)$
κ	$2l_{[\mu,\nu]}m^\mu l^\nu$
ϵ	$l_{[\mu,\nu]}n^\mu l^\nu + \frac{1}{2}(l_{[\mu,\nu]}m^\mu\overline{m}^\nu + \overline{m}_{[\mu,\nu]}m^\mu l^\nu + m_{[\mu,\nu]}l^\mu\overline{m}^\nu)$
π	$l_{[\mu,\nu]}n^\mu m^\nu + \overline{m}_{[\mu,\nu]}n^\mu l^\nu + n_{[\mu,\nu]}l^\mu\overline{m}^\nu$
σ	$2\,m_{[\mu,\nu]}m^\mu l^\nu$
β	$m_{[\mu,\nu]}m^\mu\overline{m}^\nu + \frac{1}{2}(m_{[\mu,\nu]}n^\mu l^\nu + n_{[\mu,\nu]}m^\mu l^\nu + l_{[\mu,\nu]}n^\mu m^\nu)$
μ	$n_{[\mu,\nu]}m^\mu\overline{m}^\nu + m_{[\mu,\nu]}n^\mu\overline{m}^\nu + \overline{m}_{[\mu,\nu]}n^\mu m^\nu$
ρ	$\overline{m}_{[\mu,\nu]}m^\mu l^\nu + m_{[\mu,\nu]}\overline{m}^\mu l^\nu + l_{[\mu,\nu]}m^\mu\overline{m}^\nu$
α	$\overline{m}_{[\mu,\nu]}m^\mu\overline{m}^\nu + \frac{1}{2}(\overline{m}_{[\mu,\nu]}n^\mu l^\nu + n_{[\mu,\nu]}\overline{m}^\mu l^\nu + l_{[\mu,\nu]}n^\mu\overline{m}^\nu)$
λ	$2\overline{m}_{[\mu,\nu]}n^\mu\overline{m}^\nu$
τ	$n_{[\mu,\nu]}m^\mu l^\nu + l_{[\mu,\nu]}m^\mu n^\nu + m_{[\mu,\nu]}n^\mu l^\nu$
γ	$n_{[\mu,\nu]}n^\mu l^\nu + \frac{1}{2}(n_{[\mu,\nu]}m^\mu\overline{m}^\nu + \overline{m}_{[\mu,\nu]}m^\mu n^\nu + m_{[\mu,\nu]}n^\mu\overline{m}^\nu)$
ν	$2n_{[\mu,\nu]}n^\mu\overline{m}^\nu$

Table 4.1: Table of spin coefficients based on [Cocke (1989), c.f. Table 1], note that $l_{[\mu,\nu]} \equiv \partial_\mu l - \partial_\nu l$, similar definitions follow for n,m and $\overline{m}$.

Using the above spin coefficients and directional derivatives as well as the Ricci scalar for the spacetime we compute the Weyl scalars $\{\Psi_0, \Psi_1, \Psi_2, \Psi_3, \Psi_4, \}$.

$$\begin{aligned}
\Psi_0 &= D\sigma - \delta\kappa - (\rho + \bar{\rho} + 3\varepsilon + \bar{\varepsilon})\sigma + (\tau - \bar{\pi} + \bar{\alpha} + 3\beta)\kappa \\
\Psi_1 &= D\beta - \delta\varepsilon - (\alpha + \pi)\sigma - (\bar{\rho} - \bar{\varepsilon})\beta + (\mu + \gamma)\kappa + (\bar{\alpha} - \bar{\pi})\varepsilon \\
\Psi_2 &= D\mu - \delta\pi + (\varepsilon + \bar{\varepsilon} - \bar{\rho})\mu + (\bar{\alpha} - \beta - \bar{\pi})\pi + \nu\kappa - \sigma\lambda - R/12 \\
\Psi_3 &= \bar{\delta}\gamma - \Delta\alpha + (\rho + \varepsilon)\nu - (\tau + \beta)\lambda + (\bar{\gamma} - \bar{\mu})\alpha + (\bar{\beta} - \bar{\tau})\gamma \\
\Psi_4 &= \bar{\delta}\nu - \Delta\lambda - (\mu + \bar{\mu} + 3\gamma - \bar{\gamma})\lambda + (3\alpha + \bar{\beta} + \pi - \bar{\tau})\nu,
\end{aligned} \tag{4.12}$$

The Weyl scalars, as noted above, will be required for computing the Weyl spinor C_{ABCD}. It is important to note that the Weyl scalars are not independent of the tetrad

choice. The transformations of Weyl scalars under tetrad rotations are summarized [c.f. ch.3 Stephani *et al.* (2003)].

Finally having assembled all of the necessary pieces for the computation, we can use the Weyl scalars and thus rewrite the Weyl Spinor.

$$C_{ABCD} = \Psi_0 \iota_A \iota_B \iota_C \iota_D - 4\Psi_1 o_{(A} \iota_B \iota_C \iota_{D)} + 6\Psi_2 o_{(A} o_B \iota_C \iota_{D)} - 4\Psi_3 o_{(A} o_B o_C \iota_{D)} + \Psi_4 o_A o_B o_C o_D, \tag{4.13}$$

where the spinors ι^A, o^A are also known as principal null flag-poles and are such that $o^2 = 0$ and $o^A \iota_A = -1$. In order implement the Petrov classification (as was done in eq. (4.7)) of the spacetime we compute a set of invariant scalars that are independent of the tetrad choice one makes. These invariants care obtained from the Weyl spinors by,

$$\begin{aligned} I &\equiv \Psi_0 \Psi_4 - 4\Psi_1 \Psi_3 + 3\Psi_2^2, \\ J &\equiv \begin{vmatrix} \Psi_4 & \Psi_3 & \Psi_2 \\ \Psi_3 & \Psi_2 & \Psi_1 \\ Ka\Psi_2 & \Psi_1 & \Psi_0 \end{vmatrix}, \\ K &\equiv \Psi_1 \Psi_4^2 - 3\Psi_4 \Psi_3 \Psi_2 + 2\Psi_3^3, \\ L &\equiv \Psi_2 \Psi_4 - \Psi_3^2, \\ N &\equiv 12L^2 - \Psi_4^2 I. \end{aligned} \tag{4.14}$$

Depending on these invariants we can now compute the Petrov classification and as promised we have done so without the direct computation of the Weyl tensor or its eigenvalues eq. (4.7),

Petrov Type	Condition
Type I	$I^3 \neq 27J^2$, K,L and N carry no additional constrains.
Type II	$I^3 = 27J^2$, $I \neq J$ and $K \neq N$ and L carries no additional constrains.
Type D	$I^3 = 27J^2$, $I \neq J$, $K = N = 0$ and L carries no additional constrains.
Type III	$I^3 = 27J^2$, $I = J = 0$, $K \neq L$ and N carries no additional constrains.
Type N	$I^3 = 27J^2$, $I = J = 0$, $K = L = 0$ and $N \neq 0$

Table 4.2: Petrov Classification Based on Scalar Invariants Of The Spacetime

A succinct flow chart associated with this classification can be found in [Stephani *et al.* (2003), c.f. Fig. 9.1]. For flat space each of these invariants vanishes.

In our work the metric is perturbatively known only upto some finite order. A consequence of this as we shall see is that that the above statements on the Petrov classification can be sensibly made upto a finite order in the chosen expansion parameter. A detailed discussion of this is presented in the appendix D.

4.4 The Weyl Double-Copy

The third duality which is a topic of this thesis is the Weyl double-copy picture of Luna *et al.* (2019). The Weyl double copy states that for a Weyl spinor C_{ABCD} we have,

$$C_{ABCD} = \frac{1}{S} f_{AB} f_{CD} \tag{4.15}$$

The spinor f_{AB} above can be inverted to obtain a tensor $F_{\mu\nu}$ by using appropriate curved space vierbiens and Pauli matrices [see appendix A]. The Weyl double-copy picture then states that for certain algebraically special space-times a consistent background choice, $g^{(0)}_{\mu\nu}$ exists such that the tensor $F_{\mu\nu}$ satisfies vacuum Maxwell's equa-

tions, $dF = 0$ and $d^*F = 0$ and the scalar S above satisfies the wave equation on this background.

Lastly, it is worth making a note that the first hints towards the existence of such a map trace back to Walker and Penrose (1970) where the authors showed that for type-D space-times the Weyl tensor could be decomposed in the following manner,

$$C_{ABCD} = [\chi]^{-5}\chi_{(AB}\chi_{CD)} \qquad [\chi]^2 = \chi_{AB}\chi^{AB}. \tag{4.16}$$

For type-D spacetimes the spinor χ can be suitably inverted to obtain a tensor which satisfies Maxwell's equations and similarly one can identify a scalar, $S = [\chi]^{-1}$. However while this approach works for type-D spacetimes, for type-N space-times this approach runs into issues, the reason has to do with the spinor structure of χ for type-N space-times. As well see in the next chapter, for type-N spacetimes, $\chi \sim o_A o_B$, a consequence of this structure is that the inner product $[\chi] \to 0$, thus a scalar identified this way would diverge. In our work this issue does not arise since we make a different choice for the scalar S, that infact trivially satisfies the wave equation. However it would be an interesting exercise to elucidate the full relationship between the decomposition of the Weyl spinor in Walker and Penrose (1970) and Luna *et al.* (2019).

In the next chapter we will see how we apply this formalism to fluid-metrics whose Einstein's equations explicitly reduce to the incompressible Navier-Stokes equations and discuss our findings.

Chapter 5

FROM NAVIER-STOKES TO MAXWELL, VIA EINSTEIN

This chapter, including appendices A to C, is a reproduction of the paper Keeler *et al.* (2020) of the same title as published in the *Journal of High Energy Physics*[1]. It has been appropriately formatted for inclusion in this document.

5.1 Introduction

The fluctuations of spacetime near a horizon can be described by a fluid equation, as first found almost forty years ago Damour (1978, 1979). Further development of this idea led to the membrane paradigm Thorne *et al.* (1986); Parikh and Wilczek (1998); Eling and Oz (2010); Eling *et al.* (2009); Gourgoulhon and Jaramillo (2006); Gourgoulhon (2005); Gourgoulhon and Jaramillo (2008), in which the fluid lives on a stretched horizon. The advent of AdS-CFT duality twenty years ago allowed for a version of fluid-gravity duality where the dual fluid arises from the gauge theory living on the AdS boundary Policastro *et al.* (2001, 2002a); Kovtun *et al.* (2003, 2005); Son and Starinets (2007); Bhattacharyya *et al.* (2009b); Iqbal and Liu (2009); Oz and Rabinovich (2011); Faulkner *et al.* (2011); Eling and Oz (2013); for reviews see Son and Starinets (2007); Damour and Lilley (2008); Rangamani (2009); Padmanabhan (2010); Hubeny *et al.* (2012).

More recently, the cutoff surface approach to fluid-gravity duality, pioneered in Bredberg *et al.* (2011, 2012) and extended in Brattan *et al.* (2011); Compere *et al.* (2011, 2012); Taylor (2018); Bredberg *et al.* (2012); Lysov and Strominger (2011);

[1]Note that the *Journal of High Energy Physics* uses alphebatized authorship. This work is reproduced here with permission from the co-authors.

Pinzani-Fokeeva and Taylor (2015); De *et al.* (2019); Dey *et al.* (2020), built a precise version of the membrane paradigm which defines the fluid via the extrinsic curvature of an intrinsically flat hyperbolic 'cutoff' surface held outside the horizon. In the formulation of cutoff surface fluid-gravity we follow in this paper, Bredberg *et al.* (2012), the Einstein constraint equations on the hyperbolic cutoff surface become the nonlinear incompressible Navier-Stokes equations, while solving the remaining Einstein equations defines the rest of the spacetime. We will work mostly with the low order terms in the long-wavelength or hydrodynamic limit, which amounts to a gradient expansion; as shown in Compere *et al.* (2011), this procedure does allow a full perturbative expansion.

The classical double copy as first presented in Monteiro *et al.* (2014) builds a map between classical gravity solutions and classical Yang-Mills solutions, based on the color-kinematics duality valid at the amplitude level (see Bern *et al.* (2019a) for a comprehensive review). Since the metric of the gravitational solution is built out of two copies of the classical Yang-Mills solution, the Yang-Mills solution is referred to as the 'single copy' of the corresponding metric, and there is also a corresponding Klein-Gordon scalar solution termed the 'zeroth copy'. As an example, the single copy of the Schwarzschild black hole metric is the field arrangement due to a color charge at the origin, when the dilaton expectation value is tuned to zero Luna *et al.* (2020). Many other examples of the classical double copy have been built Luna *et al.* (2015, 2017); Monteiro *et al.* (2019); Alfonsi *et al.* (2020); Ridgway and Wise (2016); Adamo *et al.* (2018); Bahjat-Abbas *et al.* (2017); Carrillo-González *et al.* (2018); Ilderton (2018); Gurses and Tekin (2018); Carrillo González *et al.* (2019); Lee (2018); Bah *et al.* (2020); Andrzejewski and Prencel (2019); Goldberger and Li (2020); Kim *et al.* (2020); Bahjat-Abbas *et al.* (2020), including to some broad classes of spacetime Luna *et al.* (2019). Furthermore Goldberger *et al.* (2017); Luna *et al.* (2018); Goldberger

and Ridgway (2018); Shen (2018); Cheung *et al.* (2018); Kosower *et al.* (2019); Bern *et al.* (2019c); Antonelli *et al.* (2019); Bern *et al.* (2019b); Kälin and Porto (2020) have used this classical mapping to improve the perturbative series used in analytic calculations of black hole collisions.

We build herein the single copy gauge fields which map to fluid-dual metrics, for two different classes of Navier-Stokes solutions. We are able to accomplish this map by relying on the algebraic specialty of these fluid-dual metrics. A spacetime is algebraically special if its Weyl tensor exhibits extra symmetry; specifically, if two or more of its principal null vectors coincide. In four dimensions, spacetimes of Petrov type D have two pairs of coinciding principle null vectors, while spacetimes of type N have all four principal null vectors coincident. Using the constrained form of the Weyl tensor for algebraically special spacetimes, Luna *et al.* (2019) exhibited a single copy gauge field (and zeroth copy scalar field) valid for every type D vacuum solution to general relativity.

As Bredberg *et al.* (2012); Lysov and Strominger (2011) note, the spacetime corresponding to the fluid metric is algebraically special; for four dimensions, the spacetime has Petrov type II. As we will show, further restricting the fluid results in higher algebraic specialty. We focus on two special fluid classes: constant vorticity fluids and potential flows. Constant vorticity fluids are dual to spacetime metrics with Petrov type D, while potential flow fluids are dual to metrics with Petrov type N. Such fluids have also been studied in the context of holography, for instance for flows with vorticity Leigh *et al.* (2012b,a). Consequently, using the Weyl double copy proposed in Luna *et al.* (2019), we are able to exhibit the single copy gauge fields whose double copy metric is then dual to either a constant vorticity fluid or a potential flow fluid. Since these these gauge fields are in the U(1) sector of the Yang-Mills theory, we have thus mapped two classes of Navier-Stokes solutions to Maxwell solutions.

The gauge field corresponding to the constant vorticity fluid matches the constant axial field within a large solenoid, while the zeroth copy is a constant. For the potential flow fluids, the gauge field is the same for every potential flow; it corresponds to a static Maxwell field with Poynting vector pointing towards the horizon. We find the scalar flow potential maps to the zeroth copy scalar field. Thus, just as the nontrivial details of the constant vorticity fluid map to the single copy field, the nontrivial details of the potential flow fluid map instead on to the zeroth copy scalar potential.

In section 5.2 we begin by reviewing the cutoff approach to fluid-gravity duality from Bredberg *et al.* (2012). In section 5.3, we briefly review the classical double copy story, focusing on the Weyl double copy as developed in Luna *et al.* (2019). In section 5.4 we show that constant vorticity fluids map to type D vacuum metrics, while potential flow fluids map to type N metrics. In sections 5.5 and 5.6 we build the single copy for the gauge fields associated with these metrics. In section 5.7 we discuss the physical implications of our results and speculate on the viability of a classical double copy picture for generic fluid-dual spacetimes.

5.2 The Hydrodynamic Limit and Near-Horizon Expansion

In this section we review the cutoff surface formulation of fluid-gravity duality and reiterate the equivalence between the hydrodynamic limit and the near horizon expansion explored in Bredberg *et al.* (2012). In order to obtain Navier-Stokes equations from Einstein's equations, we begin with a background Rindler spacetime written in ingoing Eddington-Finkelstein coordinates:

$$ds_0^2 = -rd\tau^2 + 2d\tau dr + dx_i dx^i. \tag{5.1}$$

Here i, j will be the spacelike fluid directions; for a fluid in $2+1$ dimensions, i, j run over $1, 2$ and the associated metric is four-dimensional. Constant r hypersurfaces in these coordinates are intrinsically flat and foliate the spacetime metric into hyperbolic slices.

We then choose one such slice, $r = r_c$, and perturb the spacetime there, generating extrinsic curvature for the $r = r_c$ slice as embedded in the full spacetime. We identify this extrinsic curvature κ_{ab} with the fluid stress tensor T_{ab}; here a, b run over the directions along the r_c slice (that is, a, b take values τ or i, j). The intrinsic metric of this slice γ_{ab} thus satisfies

$$\gamma_{ab} = -r_c d\tau^2 + dx^j dx_j, \qquad \gamma_{ab}\kappa - \kappa_{ab} \sim T^{NS}_{ab}. \tag{5.2}$$

For these perturbations, we impose regularity and infalling boundary conditions at the null horizon $r = 0$, thus generating the fluid-dual metric

$$\begin{aligned} ds^2 = &- r d\tau^2 + 2 d\tau dr + dx_i dx^i \\ &- 2\left(1 - \frac{r}{r_c}\right) v_i dx^i d\tau - 2\frac{v_i}{r_c} dx^i dr \\ &+ \left(1 - \frac{r}{r_c}\right)\left[(v^2 + 2P) d\tau^2 + \frac{v_i v_j}{r_c} dx^i dx^j\right] + \left(\frac{v^2}{r_c} + \frac{2P}{r_c}\right) d\tau dr \\ &- \frac{(r^2 - r_c^2)}{r_c} \partial^2 v_i dx^i d\tau + \mathcal{O}(\epsilon^3). \end{aligned} \tag{5.3}$$

The ϵ here refers to the order in the hydrodynamic or long wavelength expansion, explicitly

$$\partial_i \to \epsilon, \qquad \partial_\tau \to \epsilon^2, \qquad v \to \epsilon, \qquad P \to \epsilon^2. \tag{5.4}$$

The metric in (5.3) is arranged with background terms of order $\mathcal{O}(\epsilon^0)$ in the first line, $\mathcal{O}(\epsilon)$ terms in the second, and so on.

With these identifications, the $r = r_c$ constraint components of Einstein's equations, $G_{\tau\tau}$ and $G_{\tau i}$, become incompressibility and the Navier-Stokes equation:

$$\begin{aligned} G_{00} = 0 &\implies \partial_i v_i = 0, \\ G_{0i} = 0 &\implies \partial_\tau v_i - \eta \partial^2 v_i + \partial_i P + v^j \partial_j v_i = 0, \end{aligned} \tag{5.5}$$

where the shear viscosity η is identified[2] with r_c.

As in Bredberg *et al.* (2012), to relate the hydrodynamic limit to the near horizon limit, we introduce hatted coordinates and variables:

$$x_i = \frac{r_c \hat{x}_i}{\epsilon}, \qquad \tau = \frac{r_c \hat{\tau}}{\epsilon^2}, \qquad r = \hat{r} r_c, \qquad v_i = \epsilon \hat{v}_i \qquad P = \epsilon^2 \hat{P}. \tag{5.6}$$

Next, we rescale the metric and define a new perturbative parameter λ:

$$ds^2 \to d\hat{s}^2 = \frac{\epsilon^2}{r_c^2} ds^2 \qquad z^2 - t^2 = 4 r_c \to 4\lambda, \qquad \lambda \equiv \frac{\epsilon^2}{r_c}. \tag{5.7}$$

This new expansion parameter λ controls the near horizon expansion. The limit $\lambda \to 0$ sets the $r = r_c$ hypersurface to be null, just like the $r = 0$ Rindler horizon. In the near horizon expansion the metric thus becomes

$$\begin{aligned} d\hat{s}^2 = &- \frac{\hat{r}}{\lambda} d\hat{\tau}^2 \\ &+ \Big[2 d\hat{\tau} d\hat{r} + d\hat{x}_i d\hat{x}^i - 2(1-\hat{r}) \hat{v}_i d\hat{x}^i d\hat{\tau} + (1-\hat{r})(\hat{v}^2 + 2\hat{P}) d\hat{\tau}^2 \Big] \\ &+ \lambda \Big[(1-\hat{r}) \hat{v}_i \hat{v}_j d\hat{x}^i d\hat{x}^j - 2 \hat{v}_i d\hat{x}^i d\hat{r} + (\hat{v}^2 + 2\hat{P}) d\hat{\tau} d\hat{r} \\ &+ (\hat{r} - 1)[-(\hat{r}+1)\hat{\partial}^2 \hat{v}_i + (\hat{v}^2 + 2\hat{P}) 2 \hat{v}_i + 4 \hat{\partial}_i \hat{P}] d\hat{x} d\hat{\tau} \Big] + \mathcal{O}(\lambda^2). \end{aligned} \tag{5.8}$$

In this sense Bredberg *et al.* (2012) demonstrate that the near horizon expansion matches the long wavelength limit, consistent with the perspective that horizons behave as incompressible fluids.

As discussed further in appendix C, the replacements

$$x^i \to \epsilon x^i, \qquad \tau \to \epsilon^2 \tau, \qquad v \to \epsilon v, \qquad P \to \epsilon^2 P. \tag{5.9}$$

[2]Note that in the near horizon expansion $\eta \to 1$.

allow derivation of the incompressible Navier-Stokes equation starting from a solution of more complicated equations; essentially, any other terms become higher order terms in the ϵ expansion. Additionally, these replacements will bring a Navier-Stokes solution that is not initially in the long wavelength limit (5.4) into that limit. The near horizon expansion makes these replacements explicit, so it is valid for Navier-Stokes solutions that are not naturally in the hydrodynamic limit, such as vortices. Consequently, although we mostly use the hydrodynamic expansion ϵ below, we will return to the near horizon λ expansion when necessary.

5.3 Classical Double Copy

In the past few decades, significant steps have been made towards a deeper understanding of graviton scattering amplitudes and their relation to gauge scattering amplitudes. Most relevant for this article is the double copy prescription (see Bern *et al.* (2019a) and references within for a comprehensive review of the subject). Stated simply, the double copy obtains complicated graviton scattering amplitudes from simpler gauge theory amplitudes. The gauge theory amplitude $\mathcal{A}^{\rm YM}$ is written in a generalized gauge such that it takes the schematic form

$$\mathcal{A}^{\rm YM} \sim \sum_k \frac{n_k c_k}{\text{propagators}}, \tag{5.10}$$

where the sum is over all three-point vertex graphs, the n_k are the kinematic numerators associated with each graph, and the c_k are the color factors that satisfy a Jacobi identity of the form $c_i + c_j + c_k = 0$. The basic principle in obtaining the graviton amplitude relies on a particularly simple duality between color and kinematics, the BCJ duality first presented in Bern *et al.* (2008), being made manifest.

The double copy prescription then provides the corresponding graviton amplitude,

$$\mathcal{M}^{\rm grav} \sim \sum_k \frac{n_k n_k}{\text{propagators}}, \tag{5.11}$$

where the color factors c_k have been replaced with a second set of kinematic numerators n_k that are organized to also satisfy a Jacobi identity of the same form. There is also a 'zeroth copy' in the amplitudes story, where starting with (5.10), replacing the kinematic numerators n_i with a second set of color factors $\tilde{c}_i$ builds scalar amplitudes of the form

$$\mathcal{A}^{\text{scalar}} \sim \sum_k \frac{c_k \tilde{c}_k}{\text{propagators}}, \tag{5.12}$$

for bi-adjoint scalars $\phi^{aa'}$. As we will see below, a zeroth copy scalar can also be found in the classical double copy story; it will play a significant role for the potential flow fluid class.

When the double copy procedure is applied to pure (non-supersymmetric) Yang-Mills theory, the resulting theory on the gravity side is general relativity coupled to a two-form field and a dilaton. Although these amplitude relations are perturbative quantum statements, the authors of Monteiro *et al.* (2014) used these relations to inspire a double copy mapping between classical solutions in general relativity and classical solutions in the $U(1)$ sector of Yang-Mills.[3] This relation is referred to as the classical double copy.

5.3.1 Kerr-Schild Double Copy

The key connection between the classical gravity and gauge theory solutions first presented in Monteiro *et al.* (2014) is the use of Kerr-Schild coordinates, where

$$g_{\mu\nu} = \eta_{\mu\nu} + \phi k_\mu k_\nu. \tag{5.13}$$

Here, ϕ is a scalar function that plays the role of the zeroth copy, and satisfies the wave equation over the flat background, $\eta^{\mu\nu}\partial_\mu\partial_\nu\phi = 0$. The vector k_μ is null with

[3]Some nonabelian behavior is covered in e.g. Alfonsi *et al.* (2020); Bahjat-Abbas *et al.* (2020), but here we focus on only the abelian sector.

respect to both the full and background metrics,

$$g^{\mu\nu}k_\mu k_\nu = \eta^{\mu\nu}k_\mu k_\nu = 0. \tag{5.14}$$

This feature serves to truncate the inverse metric to $g^{\mu\nu} = \eta^{\mu\nu} - \phi k^\mu k^\nu$, with the further consequence that the null vector can be raised with either the background or full metric, $k^\mu = g^{\mu\nu}k_\nu = \eta^{\mu\nu}k_\nu$.

The classical double copy states that if $g_{\mu\nu}$ is a solution to the Einstein equations, then the gauge field given by

$$A^a_\mu = c^a \phi k_\mu \tag{5.15}$$

is a solution to Yang-Mills theory. Since the c^a are just constant color factors in these solutions, these solutions really live in a $U(1)$ sector of the gauge theory; that is, $A_\mu = \phi k_\mu$ will be a Maxwell solution. We refer to (5.15) as the single copy, in line with terminology in the amplitudes story.

The connection between the classical story and amplitudes story can be seen by replacing the color vector c^a in (5.15) with the null vector k_μ in (5.13) to obtain $h_{\mu\nu}$ from the gauge theory, akin to replacing $c_k \to n_k$. Moreover, the zeroth copy analogy can be seen by replacing $k_\mu \to c^{a'}$ in (5.15) to get $\phi^{aa'} = c^a c^{a'} \phi$, in the same spirit as replacing $n_i \to \tilde{c}_i$ to obtain (5.12) from (5.10). The mapping (5.15) has been extensively studied for various exact solutions living on flat space Monteiro *et al.* (2014); Adamo *et al.* (2018); Luna *et al.* (2015); Goldberger and Ridgway (2018); Carrillo González *et al.* (2019); Ridgway and Wise (2016); Luna *et al.* (2016); Goldberger and Ridgway (2017); Berman *et al.* (2019); Gurses and Tekin (2018); P. V. and Manu (2020); Ilderton (2018) and extended to solutions living on maximally-symmetric backgrounds Carrillo-González *et al.* (2018); Bahjat-Abbas *et al.* (2017).

Some classical solutions that have been shown to exhibit a reasonable double copy necessitate an extension to the ansatz (5.13); Luna *et al.* (2015, 2019); Lee (2018)

write the full metric in double Kerr-Schild form, where

$$g_{\mu\nu} = \eta_{\mu\nu} + \phi k_\mu k_\nu + \psi l_\mu l_\nu. \tag{5.16}$$

Here the vectors k and l are individually null as well as orthogonal (orthonullity);

$$k^2 = l^2 = k \cdot l = 0. \tag{5.17}$$

Again, the indices for both vectors can be raised and lowered with either the full metric $g_{\mu\nu}$ or the background metric $\eta_{\mu\nu}$. This form was necessary for the single copy study of the Taub-NUT solution Luna *et al.* (2015) as well as for the generic type D vacuum solutions in Luna *et al.* (2019), where the gauge field is given by

$$A^a_\mu = c^a\Big(\phi k_\mu + \psi l_\mu\Big). \tag{5.18}$$

5.3.2 Weyl Double Copy

In our work, we will utilize a different realization of the classical double copy, referred to as the Weyl double copy Luna *et al.* (2019). This prescription for the double copy relies on the spinor formulation of general relativity Penrose and Rindler (2011, 1988) in conjunction with the Petrov classification (see Stephani *et al.* (2003) chapters 3 and 4 for a review of both concepts) to build the map between the gravitational and gauge theories. This version of the double copy applies to four-dimensional spacetimes, although Monteiro *et al.* (2019) builds towards an extension to higher dimensions; for now we review the four-dimensional picture.

The Petrov classification labels metrics by the multiplicities of the principle null directions of their Weyl tensors. A principle null direction k^μ satisfies

$$k_\mu k^\mu = 0, \qquad k_{[\sigma} W_{\mu]\nu\rho[\sigma} k_{\lambda]} k^\nu k^\rho = 0, \tag{5.19}$$

where $W_{\mu\nu\lambda\gamma}$ is the Weyl tensor. All four-dimensional metrics will have four (not necessarily unique) solutions k^μ to these equations, but they can appear with different multiplicities. A spacetime is algebraically special if any two or more of these

principle null vectors coincide. If only two coincide, the spacetime is Petrov type II; if two pairs coincide, then it is type D. If all four principle null vectors coincide, then the spacetime is type N. The Weyl double copy will apply to type D and type N spacetimes, essentially factoring their principle null vector pairs.

Since a basic understanding of curved space spinor formalism is necessary to work with the Weyl double copy, we review the essentials in appendix A. We rewrite the usual Weyl tensor $W_{\mu\nu\lambda\gamma}$ in terms of the completely symmetric Weyl spinor C_{ABCD} using the formula

$$C_{ABCD} = \frac{1}{4} W_{\mu\nu\lambda\gamma} \sigma^{\mu\nu}_{AB} \sigma^{\lambda\gamma}_{CD}, \tag{5.20}$$

where $\sigma^{\mu\nu}_{AB}$ are defined in terms of the Pauli sigma matrices as in (A.7).

The form of the Weyl spinor C_{ABCD} is directly related to the Petrov classification of spacetimes, since the Weyl spinor can be decomposed as

$$C_{ABCD} = \alpha_{(A}\beta_B\gamma_C\delta_{D)}, \tag{5.21}$$

where the four principle spinors $\{\alpha_A, \beta_B, \gamma_C, \delta_D\}$ carry the information of the four principle null directions of the spacetime. The principle spinors can be related to the principle null vectors using the Pauli 4-vectors via (B.11).

Since the spinors composing C_{ABCD} are directly related to the principle null vectors, their multiplicity also depends on the Petrov type. If all four spinors are unique, the spacetime is algebraically general, of Petrov type I. Otherwise the spacetime is algebraically special. We focus on Petrov type D, where there are two unique principle spinors with multiplicity two, and Petrov type N, where there is one unique principle spinor. Their Weyl spinors can be written

$$C^{\mathrm{D}}_{ABCD} \sim \alpha_{(A}\alpha_B\beta_C\beta_{D)}, \qquad C^{\mathrm{N}}_{ABCD} \sim \alpha_A\alpha_B\alpha_C\alpha_D, \tag{5.22}$$

where here α (and β, for type D) are the principle null spinors.

On the gauge theory side, the spinor field strength f_{AB} is the key object, and can be obtained from the field strength tensor $F_{\mu\nu}$ directly using

$$f_{AB} = \frac{1}{2} F_{\mu\nu} \sigma^{\mu\nu}_{AB}. \tag{5.23}$$

In the same sense as the Weyl spinor, the f_{AB} corresponding to a type D spacetime can be written as $f^{\mathrm{D}}_{AB} \sim \alpha_{(A}\beta_{B)}$, whereas in the type N case we have $f^{\mathrm{N}}_{AB} \sim \alpha_A \alpha_B$. Thus we find

$$C_{ABCD} = \frac{1}{S} f_{(AB} f_{CD)}, \tag{5.24}$$

where S is a complex scalar field satisfying the wave equation in the flat background on which f_{AB} lives, and whose real part coincides with the Kerr-Schild scalar ϕ up to an overall constant. Therefore the scalar S plays the role of the zeroth copy in the Weyl double copy map.

We will use the decomposition of the Weyl spinor C_{ABCD} in terms of a spinor basis $\{o_A, \iota_B\}$:

$$C_{ABCD} = \Psi_0 \iota_A \iota_B \iota_C \iota_D - 4\Psi_1 o_{(A}\iota_B\iota_C\iota_{D)} + 6\Psi_2 o_{(A} o_B \iota_C \iota_{D)} - 4\Psi_3 o_{(A} o_B o_C \iota_{D)} + \Psi_4 o_A o_B o_C o_D. \tag{5.25}$$

Here, the $\Psi_I \in \mathbb{C},\ I = 0, 1, 2, 3, 4$ are called Weyl scalars, and are also related to the Petrov classification (see section 5.4). We will see that the Ψ_I, and the invariants built out of them, play a significant role in the Weyl double copy.

As Luna *et al.* (2019) shows, solutions built from this Weyl double copy picture match the expectations from the Kerr-Schild double copy as built in Monteiro *et al.* (2014). In addition to specific examples like the Kerr metric, Luna *et al.* (2019) also shows this matching for the most general type D vacuum solution as written in Plebanski-Demianski coordinates Plebanski and Demianski (1976) (see Griffiths and Podolsky (2006) and Podolsky *et al.* (2018) for an extended treatment).

We next look to analyze solutions to Navier-Stokes from the fluid gravity perspective that result in spacetimes that are candidates for the Weyl double copy. As we will now show, by constraining the velocity fields in the fluid metric (5.3) in one of two ways, we find that the resulting spacetime is either Petrov type N or type D, allowing for a double copy treatment via the Weyl method.

5.4 Fluid Solutions

The eigenbivectors of the Weyl tensor for the fluid metric reveal that it is algebraically special Bredberg *et al.* (2012); Lysov and Strominger (2011); specifically it is a type II spacetime according to the Petrov classification, with two coinciding principal null vectors. Below, we use the Newman-Penrose formalism to find which fluids correspond to metrics with even higher algebraic speciality. Additional details pertaining to the formalism and our choice of conventions can be found in Appendix B or in Stephani *et al.* (2003).

Briefly, the Newman-Penrose formalism relies on rewriting the metric in terms of a tetrad set l, n, m, $\bar{m}$, as in (B.1). The tetrad set is then used to compute the Weyl scalars, which then can be used to compute the invariants I, J, K, L, and N as in (5.27). While the Weyl scalars depend on the tetrad choice, the invariants do not and thus we will look at these invariants to classify our spacetimes.

We work in the hydrodynamic limit of the metric (5.3), where the first terms we do not write explicitly[4] arise at $\mathcal{O}(\epsilon^3)$. Thus we only know our Weyl scalars up to the

[4]Lysov and Strominger (2011) show that algebraically special spacetimes can be obtained to arbitrary order in the context of the fluid gravity duality in 5 or higher spacetime dimensions. Cai *et al.* (2013) also consider similar spacetimes in $d \geq 5$, however posit that additional constraints may be needed in Lysov and Strominger (2011) at higher orders to maintain algebraic specialty. Compere *et al.* (2011) construct a formulation that progresses to arbitrary order, however this construction deviates from algebraic specialty and in doing so relates the higher order pieces in the metric to

same order, and our algebraic classification of the spacetime is perturbative as well. In this limit, our tetrad choice (C.2) yields the following Weyl scalars up to $\mathcal{O}(\epsilon^3)$, which is where we would start to see contributions from neglected higher terms in the metric(5.3):

$$\begin{aligned}
\Psi_0 &= 0 + \mathcal{O}(\epsilon^3), \\
\Psi_1 &= 0 + \mathcal{O}(\epsilon^3), \\
\Psi_2 &= -i\frac{\epsilon^2}{4r_c}(\partial_x v_y - \partial_y v_x) + \mathcal{O}(\epsilon^3), \\
\Psi_3 &= 0 + \mathcal{O}(\epsilon^3), \\
\Psi_4 &= -\frac{\epsilon^2}{2r}(\partial_x v_x - \partial_y v_y + i(\partial_x v_y + \partial_y v_x)) + \mathcal{O}(\epsilon^3).
\end{aligned} \tag{5.26}$$

Ψ_2 is proportional to the vorticity of the fluid, while Ψ_4 is proportional to the derivative of $v_x + iv_y$ with respect to the complex coordinate $\bar{z} \equiv x - iy$.

In order to evaluate the algebraic speciality of our spacetimes, we compute the invariants $I,\ J,\ K,\ L$ and N, via the following relations:

$$\begin{aligned}
I &\equiv \Psi_0\Psi_4 - 4\Psi_1\Psi_3 + 3\Psi_2^2, \\
J &\equiv \begin{vmatrix} \Psi_4 & \Psi_3 & \Psi_2 \\ \Psi_3 & \Psi_2 & \Psi_1 \\ \Psi_2 & \Psi_1 & \Psi_0 \end{vmatrix}, \\
K &\equiv \Psi_1\Psi_4^2 - 3\Psi_4\Psi_3\Psi_2 + 2\Psi_3^3, \\
L &\equiv \Psi_2\Psi_4 - \Psi_3^2, \\
N &\equiv 12L^2 - \Psi_4^2 I.
\end{aligned} \tag{5.27}$$

corrections to the Navier-Stokes equations. Since our interest is primarily in making connection with the Weyl double copy picture, we restrict ourselves to the first few nontrivial orders of this metric. For more on convergence of the gradient expansion in a hydrodynamic and fluid gravity context, see Pinzani-Fokeeva and Taylor (2015); Grozdanov *et al.* (2019).

For a generic fluid-dual metric, we find

$$\begin{aligned} I &= 3\epsilon^4 \left[i \left(\frac{\partial_x v_y}{4r_c} - \frac{\partial_y v_x}{4r_c} \right) \right]^2 + \mathcal{O}(\epsilon^5), \\ J &= \epsilon^6 \left[i \left(\frac{\partial_x v_y}{4r_c} - \frac{\partial_y v_x}{4r_c} \right) \right]^3 + \mathcal{O}(\epsilon^7). \end{aligned} \tag{5.28}$$

These I and J satisfy $I^3 - 27J^2 = 0$, or more precisely,

$$\implies I^3 - 27J^2 = 0 + \mathcal{O}(\epsilon^{13}), \tag{5.29}$$

which implies that the general fluid metric is Petrov type II up to this order.

Next we look at the invariants K, L, and N:

$$\begin{aligned} K &= 0 + \mathcal{O}(\epsilon^7), \\ L &= \epsilon^4 \left[-\frac{\partial_x v_x}{2r} + \frac{\partial_y v_y}{2r} - i\frac{\partial_y v_x}{2r} - i\frac{\partial_x v_y}{2r} \right] \left[i\,\frac{\partial_y v_x}{4r_c} - i\,\frac{\partial_x v_y}{4r_c} \right] + \mathcal{O}(\epsilon^5), \\ N &= 9\epsilon^8 \left[-\frac{\partial_x v_x}{2r} + \frac{\partial_y v_y}{2r} - i\frac{\partial_y v_x}{2r} - i\frac{\partial_x v_y}{2r} \right]^2 \left[i\,\frac{\partial_y v_x}{4r_c} - i\,\frac{\partial_x v_y}{4r_c} \right]^2 + \mathcal{O}(\epsilon^9). \end{aligned} \tag{5.30}$$

Although K is in fact 0 through this order, that is not enough for further algebraic speciality (see Figure 9.1 in Stephani *et al.* (2003)). The nonzero invariants L and N are proportional to both the vorticity (from Ψ_2) and $\partial_{\bar{z}}(v_x + iv_y)$ (from Ψ_4).

Before we begin an analysis of which special fluids have dual metrics with higher algebraic speciality, we must mention briefly the perturbative nature of the metrics we use in this paper. While Lysov and Strominger (2011) constructed fluid-dual spacetimes by requiring algebraic speciality to hold at all orders, here we instead constrain ourselves only to the lowest orders necessary in order to establish the incompressible Navier-Stokes equations. Accordingly, we only establish the higher algebraic specialty of our spacetimes to lowest order.

To these orders discussed, the condition that the fluids spacetime is a type II metric, $I^3 - 27J^2 = 0$, is satisfied in either the near-horizon or the hydrodynamic

expansion:

$$I_\epsilon^3 - 27J_\epsilon^2 = 0 + \mathcal{O}(\epsilon^{13}), \qquad I_\lambda^3 - 27J_\lambda^2 = 0 + \mathcal{O}(\lambda). \tag{5.31}$$

Note that the highest non-error order available in the near-horizon λ expansion differs from the ϵ hydrodynamic expansions, but both spacetimes satisfy the type II constraint to at least one nontrivial order.

Specifically, in the near-horizon expansion, we find

$$\begin{aligned} I_\lambda &= -\frac{3}{16}(\partial_y v_x - \partial_x v_y)^2 + \mathcal{O}(\lambda), \\ J_\lambda &= -\frac{i}{64}(\partial_y v_x - \partial_x v_y)^3 + \mathcal{O}(\lambda), \end{aligned} \tag{5.32}$$

which matches (D.4) except for the expansion order. Since the order of terms differs between the two expansions, in the near-horizon expansion it turns out to be necessary to account for terms of order $\mathcal{O}(\lambda^2)$ in the metric (5.8), as was done in Bredberg *et al.* (2012). Accordingly we use the generic form of the tetrad (C.3) to perform computations in this expansion.

Since the fluid constraints required to produce higher algebraic speciality are the same at the lowest order of both expansions, we thus concentrate on only the ϵ hydrodynamic expansion for the remainder of this section. As we show below, constant vorticity fluids will correspond to type D spacetimes while potential flows correspond to type N metrics.

5.4.1 Petrov Type D Fluid Solutions

A Petrov type D spacetime satisfies the following conditions for the invariants:

$$I^3 - 27J^2 = 0; \qquad I, J \neq 0; \qquad K = N = 0. \tag{5.33}$$

Based on the forms of L and N in (5.30) and I and J in (D.4), these conditions imply

$$\partial_x v_y - \partial_y v_x \neq 0, \qquad -\partial_x v_x + \partial_y v_y - i\Big(\partial_y v_x + \partial_x v_y\Big) = 0. \tag{5.34}$$

These constraints imply that each component of the velocity satisfies Laplace's equation $\partial^2 v_i = 0$, where $i \in \{x, y\}$.

These conditions are solved by the fluid velocities

$$\begin{aligned} v_x(\tau, y) &= -\omega y + h_x(\tau), \\ v_y(\tau, x) &= \omega x + h_y(\tau), \end{aligned} \tag{5.35}$$

with pressures

$$P(\tau, x, y) = \frac{\omega^2}{2}\Big(x^2 + y^2\Big) + \Big(\omega h_y - \partial_\tau h_x\Big)x - \Big(\omega h_x + \partial_\tau h_y\Big)y + c(\tau). \tag{5.36}$$

In this paper, we will concentrate on the steady state solution centered at the origin; that is, we set $h_i(\tau) = c(\tau) = 0$. Turning these functions on would correspond to a vortex whose center follows the path $(x_0(\tau), y_0(\tau)) = (\int h_x d\tau, \int h_y d\tau)$ as time τ passes; a diffeomorphism returning to coordinates centered on the moving vortex would tune the effective time dependence back to zero.

Thus the fluid profile we study as representative of fluids dual to type D metrics satisfies

$$v_x(\tau, y) = -\omega y, \qquad v_y(\tau, x) = \omega x, \qquad P = \omega^2 \frac{(x^2 + y^2)}{2}, \tag{5.37}$$

consistent with vanishing pressure and velocity at the origin as would be expected for a fluid rotating with constant vorticity, centered at the origin.

5.4.2 Petrov Type N Fluid Solutions

To obtain a type N spacetime, the invariants must satisfy

$$I = 0, \quad J = 0, \quad K = 0, \quad L = 0, \quad N \neq 0. \tag{5.38}$$

For the general fluid metric, we already have $K = 0$ and the invariants I, J (D.4) and L (5.30) are each proportional to a positive power of the vorticity, so setting the fluid vorticity $\partial_x v_y - \partial_y v_x$ to zero leaves us with a type N dual metric.

The velocity and pressure profiles of vorticity-free fluids can be written in terms of a scalar potential ϕ:

$$v_i = \partial_i \phi, \qquad \partial_i P = -\partial_i \partial_\tau \phi - \partial^j \phi \partial_i \partial_j \phi. \tag{5.39}$$

For incompressible fluids, ϕ satisfies Laplace's equation $\partial^2 \phi = \partial_x^2 \phi + \partial_y^2 \phi = 0$, so vorticity-free incompressible fluids are referred to as potential flows.

These potential flows can be written cleanly in complex coordinates, i.e. using $z \equiv x + iy$. Since $\partial^2 \phi = 0$, we can rewrite a general solution for the potential ϕ using the sum of a holomorphic function f and an antiholomorphic function g:

$$\partial_z \partial_{\bar{z}} \phi = 0, \qquad \phi = f(z) + g(\bar{z}). \tag{5.40}$$

Imposing reality conditions so as to obtain real velocity and pressure fields requires that the antiholomorphic function $g(z)$ must be the complex conjugate of the function $f(z)$:

$$\phi = f(z) + \bar{f}(\bar{z}), \qquad \bar{f}(\bar{z}) \equiv (f(z))^*. \tag{5.41}$$

Returning to the dual fluid metric, the vorticity-free condition sets $\Psi_2 = 0$, leaving only Ψ_4 nonzero. We can express this nonzero Weyl scalar compactly as

$$\Psi_4 = -\frac{2}{r} \partial_{\bar{z}}^2 \phi = -\frac{2}{r} \partial_{\bar{z}}^2 \bar{f}(\bar{z}), \tag{5.42}$$

while the Weyl tensor becomes

$$C_{ABCD} = \Psi_4 o_A o_B o_C o_D. \tag{5.43}$$

Since the function $f(z)$ is holomorphic, we can write a general fluid solution as a Laurent series in z (and $\bar{z}$ for $\bar{f}$):

$$\phi = \sum_{n=-\infty}^{\infty} \alpha_{n+2} z^{n+2} + \text{c.c.}, \tag{5.44}$$

where α_n are in general complex valued coefficients and the holomorphic function $f(z) \equiv \sum_{n=-\infty}^{\infty} \alpha_{n+2} z^{n+2}$. Consequently the Weyl scalar Ψ_4 can also be written as a Laurent series.

It is instructive to look at the forms of the fluid potential and the Weyl scalars for a few specific fluid solutions here[5]. We begin by turning on only the $n = 0$ term in (5.44). For convenience we additionally choose $\alpha_2 = -\alpha/4$, with α real, obtaining the potential

$$\phi(z, \bar{z}) = -\frac{\alpha}{4}(z^2 + \bar{z}^2). \tag{5.45}$$

The corresponding fluid velocity and pressure profiles become

$$v_x = -\alpha x, \qquad v_y = \alpha y, \qquad P = P_0 - \alpha^2 \, \frac{x^2 + y^2}{2}. \tag{5.46}$$

This fluid profile is known as planar extensional flow; extensional flows have been well studied in the fluid-mechanics/materials science community, see e.g. Barnes *et al.* (1989). Our main interest in this fluid will be its simplicity in terms of the double copy prescription, as we will see below.

Using (5.42), for this fluid we find

$$\Psi_4 = \frac{\alpha}{r}. \tag{5.47}$$

Due to its simplicity and utility as a physical example, we begin with this fluid when we study the double copy prescription for the Type N fluid dual metrics in section 5.6.1.

Other potential flows can also be written compactly in terms of z and $\bar{z}$, using the form (5.44), as in Table 5.1. We will study the double copy of type N metrics dual to the generic potential flow fluid with potential (5.44) in section 5.6.2 below.

[5]Note as for the type D case, we neglect the time dependence that could be allowed in the α coefficients of the fluid potential and instead consider only steady state flows. As before, time dependence here will correspond to translating these steady state solutions.

Type of fluid solution	Fluid Potential $\phi(t,x,y)$	$\phi(z,\bar{z})$	Ψ_4
Source/Sink	$\alpha\ \ln(x^2+y^2)$	$\alpha \ln(z\bar{z})$	$2\ \alpha\, r^{-1}\bar{z}^{-2}$
Source to Sink (dipole)	$\frac{\alpha\delta x}{x^2+y^2}$	$\frac{\alpha\delta}{2}\frac{z+\bar{z}}{z\bar{z}}$	$2\, r^{-1}\alpha\delta\bar{z}^{-3}$
Line Vortex	$\alpha \arctan(y/x)$	$\frac{\alpha}{2i}\ln\left(\frac{z}{\bar{z}}\right)$	$i\alpha\, r^{-1}\bar{z}^{-2}$
Extensional flow	$-\frac{\alpha}{2}(x^2-y^2)$	$-\frac{\alpha}{4}(z^2+\bar{z}^2)$	$\frac{\alpha}{r}$

Table 5.1: Some examples of standard fluid solutions and the corresponding non-vanishing scalar Ψ_4 for type N solutions. For the dipole flow, δ refers to the distance between the source and the sink.

5.5 Type D Double Copy

5.5.1 Weyl Double Copy

Now that we've obtained velocity and pressure fields that correspond to either Petrov type D or type N, we look to build the Weyl double copy (5.24) corresponding to the particular fluid solutions. Accordingly, we use our results for the Weyl scalars (5.26) and the expansion of the Weyl spinor C_{ABCD}, given by (5.25). As we showed in section 5.4.1, the type D constraint leaves us with constant vorticity fluid solutions. The time-independent solution (5.35) and (5.36) takes the form

$$v_x = -\omega y, \qquad v_y = \omega x, \qquad P = \omega^2\frac{(x^2+y^2)}{2}. \tag{5.48}$$

From the expression for the Weyl scalars Ψ_I for arbitrary velocity fields (5.26), we find that the solution (5.48) leaves us with

$$\Psi_2 = -i\epsilon^2\frac{\omega}{2r_c} + \mathcal{O}(\epsilon^3), \tag{5.49}$$

while all other Ψ_I vanish to $\mathcal{O}(\epsilon^3)$. Consequently, the Weyl spinor is $C_{ABCD} = 6\Psi_2 o_{(A}o_B\iota_C\iota_{D)}$.

Using the Weyl double copy as defined in (5.24), we find the zeroth copy scalar and single copy gauge field are, to lowest order in ϵ,

$$S = \frac{i\omega r_c}{3} e^{2i\theta}, \qquad f_{AB} = e^{i\theta}\omega \begin{pmatrix} 1 & 0 \\ 0 & -1 \end{pmatrix}, \tag{5.50}$$

where θ is a constant (global) phase to be interpreted shortly. Since the double copy relation (5.24) and the vanishing of all $\Psi_{I\neq 2}$ force $f_{AB} \propto o_A \iota_B$, the matrix structure of f_{AB} here arises from the form of o_A and ι_B as in (B.11).

Next, we use the relation between the spacetime formalism and the spinor formalism as reviewed in appendix A to obtain the tensor form of the field strength $F^{\mu\nu}$ from the spinor f_{AB}. These relationships necessitate a vierbein for the background on which the gauge fields live. We choose to interpret the gauge fields as living on the Rindler background

$$ds^2_{(0)} = -r d\tau^2 + 2dr d\tau + dx^2 + dy^2, \tag{5.51}$$

where the scalar satisfies the wave equation, $\nabla^{(0)\mu}\nabla^{(0)}_\mu S = \Box^{(0)} S = 0$. The $\nabla^{(0)}_\mu$ are the covariant derivatives with respect to (5.51). From (B.10), we obtain the vierbeins

$$\begin{aligned} e^{(0),0}_\mu &= (-\sqrt{r}, \frac{1}{\sqrt{r}}, 0, 0), \\ e^{(0),1}_\mu &= (0, -\frac{1}{\sqrt{r}}, 0, 0), \\ e^{(0),2}_\mu &= (0, 0, 1, 0), \\ e^{(0),3}_\mu &= (0, 0, 0, 1). \end{aligned} \tag{5.52}$$

Using (A.13) to obtain $F^{\mu\nu}$ in terms of f_{AB}, the Pauli matrices, and the vierbeins, we find the only nonzero components are

$$F^{\tau r} = -\omega \cos\theta, \qquad F^{xy} = -\omega \sin\theta. \tag{5.53}$$

Recalling that the gauge field is in the $U(1)$ sector of Yang-Mills, the Maxwell equations

$$\nabla^{(0)}_{\nu} F^{\mu\nu} = 0, \qquad \nabla^{(0)}_{[\mu} F_{\rho\sigma]} = 0, \tag{5.54}$$

indeed show that the field strength (5.53) is a vacuum solution. This is to be expected, since the fluid solutions are obtained by demanding the Einstein equations are satisfied in vacuum, $G_{\mu\nu} = 0$, so we expect the single copy to follow suit. In the classical double copy, it is possible for the spacetime to have a singularity that maps to a gauge field source, as the point mass maps to a point charge in the Schwarzschild solution Monteiro *et al.* (2014) when parameters are chosen to turn off the dilaton Luna *et al.* (2020); Kim *et al.* (2020). Because Rindler space is free from singularities, no sources will be found on the gauge theory side, consistent with (5.54).

5.5.2 Effective Electric and Magnetic Fields

Interpreting the single copy gauge field strength (5.53) as a Maxwell solution allows us to discuss the electric and magnetic fields whose double copy generates the metric dual to a constant vorticity fluid.[6] These fields are defined covariantly by

$$E_\nu = F_{\nu\mu}\xi^\mu, \qquad B_\nu = \frac{1}{2}\varepsilon_{\mu\nu\rho\sigma}F^{\rho\sigma}\xi^\mu, \tag{5.55}$$

where ξ is the (timelike) Killing vector $\xi = \partial_\tau$. For the field strength under consideration, we find

$$E_\nu = \omega\cos\theta\delta^r_\nu, \qquad B_\nu = -\omega\sin\theta\delta^r_\nu. \tag{5.56}$$

We interpret these fields by choosing the global phase to be $\theta = \frac{3\pi}{2}$, which leaves us with a constant magnetic field pointing in the r direction, perpendicular to the $x-y$ plane. Under this choice of θ, the classical vector potential $\vec{A}$, which constructs

[6]Note that unlike references Ilderton (2018) and Andrzejewski and Prencel (2019), which discuss gauge and gravity solutions with vorticity, we are discussing metrics dual to fluids with vorticity.

the magnetic field by $\vec{B} = \nabla \times \vec{A}$, coincides with the velocity fields directly: $\vec{A} \propto \vec{v}$. Since the magnetic field is unchanged when the vector potential shifts by a constant, we see that the single copy gauge fields will similarly be unchanged when we shift the velocity by a constant.

We also compute the electromagnetic stress tensor

$$T^{\rho\sigma} = F^{\rho}{}_{\mu} F^{\sigma\mu} - \frac{1}{4} g^{\rho\sigma} F_{\mu\nu} F^{\mu\nu}, \tag{5.57}$$

finding the nonzero components

$$T^{\tau r} = -\frac{\omega^2}{2}, \quad T^{rr} = -\frac{r\omega^2}{2}, \quad T^{xy} = \frac{\omega^2}{2}. \tag{5.58}$$

The associated energy with respect to the Killing vector ξ is given by

$$T^{\mu\nu} \xi_\mu \xi_\nu = \omega^2 r/2, \tag{5.59}$$

while the spatial components of the Poynting vector, from $T^{\mu\nu}\xi_\mu$, become zero.

Physically, we can understand the fluid (5.48) as the solution inside of a slowly rotating cylinder with its axis along the r-direction and no-slip boundary conditions at the wall, where we have taken the radius of the cylinder to be large (with respect to all other scales in the problem). The corresponding single copy gauge field, $\vec{B} = \omega \hat{r}$, matches the uniform magnetic field along the axis of a solenoid with n turns per unit length whose current I is proportional to ω/n. The axis of the solenoid is aligned with the axis of the cylinder containing the fluid.[7] The double copy mapping therefore associates the vorticity of the fluid with the magnitude of the current sourcing the magnetic field. The field moreover has energy dependent on the radial location r, but has vanishing Poynting vector as expected for a pure magnetic field. In addition, we

[7]The velocity fields rotate counter-clockwise in the $x - y$ plane. After exchanging the vorticity parameter with a current parameter, the resulting magnetic field then points along positive $\hat{r}$, consistent with choosing $\theta = 3\pi/2$.

see from (5.50) that the zeroth copy S plays a passive role in that it trivially solves the wave equation. We thus find that all of the nontrivial information that is mapped through the double copy is contained in the field strengths f_{AB} or $F^{\mu\nu}$ for the type D spacetime.

5.5.3 Weyl Double Copy in the Near Horizon Expansion

The hydrodynamic limit can be related to a near horizon expansion of the metric by rescaling the metric as in (5.7) (Bredberg *et al.*, 2012). Since the full fluid solution (5.48) does not actually lie in the hydrodynamic regime[8], we repeat here the same analysis as in section 5.5.1, repeated in the near horizon expansion (5.8). We again find the same results.

Using the tetrad (C.3), we find the Weyl scalars for the near horizon metric (5.8) with the constant vorticity fluid (5.48). The only nonzero Weyl scalar is

$$\Psi_2 = \frac{i\omega}{2} + \mathcal{O}(\lambda). \tag{5.60}$$

All other Weyl scalars vanish at $\mathcal{O}(1)$, and have contributions from neglected pieces of the metric at $\mathcal{O}(\lambda)$ or higher. Following the method in section 5.5.1, we identify the zeroth copy scalar and single copy gauge field spinor:

$$S = \frac{1}{3}e^{i(\pi+2\theta)}, \qquad f_{AB} = \omega e^{i\theta}\begin{pmatrix} 1 & 0 \\ 0 & -1 \end{pmatrix}. \tag{5.61}$$

[8]The fluid solution (5.48) is only in the hydrodynamic regime (5.4) for x, $y \sim \epsilon^{-1}$ while the vorticity satisfies $\omega \sim \epsilon^2$. For either small x, y or large vorticity, the solution exits the hydrodynamic regime, although of course it still solves Navier-Stokes. Because of this technicality, the metric (5.3) is not trustable for small x, y. However, in the near-horizon expansion, because of the rescaling (5.7), the fluid solution does not need to be in the hydrodynamic regime, since this expansion is rewritten explicitly in terms of the hatted coordinates in (5.6) that are of $O(1)$. Here we explore an explicit realization of the near-horizon expansion, for completeness, as provided in equation (5.8).

As before, we obtain the appropriate flat space vierbien by setting the velocities and pressures to zero in the full tetrad and using eq. B.10; we find

$$e^{(0),a}_{\mu} = \begin{pmatrix} \frac{r+\lambda}{2\lambda} & \frac{r-\lambda}{2\lambda} & 0 & 0 \\ -1 & -1 & 0 & 0 \\ 0 & 0 & 1 & 0 \\ 0 & 0 & 0 & 1 \end{pmatrix}. \tag{5.62}$$

Using this flat space vierbien the gauge field strength tensor in the λ expansion becomes

$$F^{\tau r} = -\omega \cos\theta, \qquad F^{xy} = -\omega \sin\theta, \tag{5.63}$$

which should be thought of as living on a flat Rindler background. We then identify effective electric and magnetic fields, which are identical to the previous result (5.56) obtained in the hydrodynamic limit:

$$E_\nu = \omega \cos\theta \ \delta^r_\nu, \qquad B_\nu = -\omega \sin\theta \ \delta^r_\nu. \tag{5.64}$$

5.6 Type N Weyl Double Copy

In this section we will analyze the single copy gauge fields and zeroth copy scalar fields corresponding to the metrics dual to potential flow fluids. As we saw in section (5.4.2), these potential flows are the most general solution whose dual metrics satisfy the Petrov type N constraint. As potential flows, their velocity can be written as the gradient of a scalar potential, $v_i = \partial_i \phi$, where ϕ satisfies Laplace's equation in $\mathbb{R}^2$. For convenience, we defined $z = x + iy$ and its conjugate $\bar{z}$ so that we may write the Laplacian as $\partial^2 = \partial_z \partial_{\bar{z}}$, decomposing the scalar potential as $\phi(z, \bar{z}) = f(z) + \bar{f}(\bar{z})$. The resulting Weyl scalar, Ψ_4, is given by (5.42), and all others vanish. Therefore the Weyl double copy should satisfy

$$C_{ABCD} = -\frac{2}{r}\partial^2_{\bar{z}} \bar{f}(\bar{z}) o_A o_B o_C o_D = \frac{1}{S} f_{AB} f_{CD}. \tag{5.65}$$

5.6.1 Planar Extensional Flows

Let us start with the simple case of planar extensional flow, where $\phi(z, \bar{z}) = -\frac{\alpha}{4}(z^2 + \bar{z}^2)$ with α a real constant. The corresponding velocity fields are (5.46) $v_x = -\alpha x$ and $v_y = \alpha y$.

We can satisfy the double copy relation (5.65) by choosing

$$S = \frac{e^{2i\theta}}{\alpha}, \qquad f_{AB} = \frac{e^{i\theta}}{\sqrt{r}} \begin{pmatrix} 1 & 1 \\ 1 & 1 \end{pmatrix}, \tag{5.66}$$

where we again allow for a global phase θ. Here, since we have $\Psi_{I\neq 4} = 0$, we have $f_{AB} \propto o_A o_B$, therefore the matrix structure in (5.66) arises from (B.11). Although we could make another choice for S, this constant choice trivially satisfies $\Box^{(0)} S = 0$, and f_{AB} is the only choice which will satisfy the gauge field equations as we show below.

As for the type D case, we specify our background spacetime by using (B.10) to find the vierbeins corresponding to the tetrads used to compute Ψ_4, and then setting $v_i = P = 0$. The resulting vierbeins turn out to have the same form as (5.52). We then obtain the gauge field strength tensor via (A.13), finding

$$F^{rx} = -\sin\theta, \qquad F^{ry} = -\cos\theta, \qquad F^{\tau x} = -\frac{2\sin\theta}{r}. \tag{5.67}$$

As in the type D case, since this field strength has no nontrivial color factor dependence, we treat it as an effective Maxwell field; indeed it satisfies the vacuum Maxwell equations over the Rindler background (5.51) for arbitrary θ.

We obtain the electric and magnetic fields using the covariant expressions (5.55), yielding

$$E_\nu = (0, 0, \sin\theta, -\cos\theta) \tag{5.68}$$

and

$$B_\nu = (0, 0, \cos\theta, -\sin\theta). \tag{5.69}$$

Again, as in the type D case, we choose $\theta = 3\pi/2$ as a convenient parametrization; picking another θ will just result in a rotation in the x, y plane. Computing the electromagnetic stress tensor (5.57), we find

$$T^{\tau\tau} = \frac{4}{r^2}, \quad T^{\tau r} = \frac{2}{r}, \quad T^{rr} = 1. \tag{5.70}$$

The energy becomes

$$T^{\mu\nu}\xi_\mu\xi_\nu = 1, \tag{5.71}$$

while the spatial components of the Poynting vector become

$$S^i = -\delta^i_r. \tag{5.72}$$

We interpret this gauge field as the single copy field necessary to build up any fluid which has a potential component. Since any two-dimensional vector field can be decomposed, via the two-dimensional version of Helmholtz decomposition, we can write the velocity field as

$$v_i = \partial_i\phi + \epsilon_{ijk}\partial_j A_k, \tag{5.73}$$

where the vector fluid potential for the two-dimensional case satisfies $\vec{A} = |A|(\hat{x} \times \hat{y})$, and i, j, k run over the directions x and y as well as the direction $\hat{x} \times \hat{y}$. For the potential flows whose gravity duals are type N, we have only the first term; that is, $|A| = 0$. Most of the information in ϕ will be carried instead by the scalar S, so the field profile (5.67) is only building up the fluid-dual spacetime necessary to support a velocity field with a nonzero $\partial_i\phi$ term.

The nonzero Poynting vector (5.72) indicates the dissipative nature of these flows. The gravitational dual is carrying energy away from the $r = r_c$ hypersurface, towards the null horizon, satisfying the infalling Rindler boundary conditions that underlie the derivation of the fluid-dual metric (5.3). The same flow of energy towards the null horizon arises in the Poynting vector aligned in the $-\hat{r}$ direction.

5.6.2 General Potential Flows

As we will show, the analysis in section 5.6.1 will work very similarly for a potential flow $\phi = f(z) + \bar{f}(\bar{z})$ with generic holomorphic function $f(z)$.

Since $\Box^{(0)}$ on the Rindler background (5.51) will give zero when acting on any function which is a sum of holomorphic and antiholomorphic terms independent of τ and r, we can satisfy the type N Weyl double copy relation (5.65) for the metric dual to a generic potential flow with

$$S = -\frac{e^{2i\theta}}{2\partial_{\bar{z}}^2 \bar{f}(\bar{z})}, \qquad f_{AB} = \frac{e^{i\theta}}{\sqrt{r}} \begin{pmatrix} 1 & 1 \\ 1 & 1 \end{pmatrix}. \tag{5.74}$$

It is now the case that $\Box^{(0)} S = 0$ is nontrivially satisfied, and the resulting gauge field strength is unchanged from the analysis for the planar extensional flow. Thus for all potential flow fluids, such as those in Table 5.1, the Weyl double copy admits the same single copy gauge field as in the extensional flow, (5.67). The information for a potential flow on the fluid side resides entirely in the potential ϕ; similarly, under the double copy prescription, we find that the information from the potential resides entirely in the zeroth copy scalar field S, whereas the single copy gauge field is the same for all potential flows.

Since the single copy field profile is again (5.67), our interpretation of this field as building the fluid-dual spacetime for fluids with nonzero potential terms holds again. We do note that the fields (5.68) and (5.69) are constant; we expect that inclusion of higher order terms in the ϵ expansion could alter this result, since here we are really considering only a hydrodynamic expansion in small ϵ around the original $r = r_c$ cutoff surface.

5.7 Discussion

We have used the Weyl double copy prescription to find the single copy gauge fields and zeroth copy scalar fields arising from two classes of fluid-dual metrics. The first class, fluids with constant vorticity, maps to spacetime metrics with Petrov type D. The second class, potential flow fluids, maps to spacetime metrics with Petrov type N. For the type D spacetimes dual to fluids with constant vorticity, we find an (effectively abelian) dual gauge field with vanishing Poynting vector. For the type N spacetimes dual to potential flows, we find a gauge field whose Poynting vector points in towards the Rindler horizon, indicating that the dissipation in these fluids maps in the spacetime to energy flowing across the horizon due to the infalling boundary conditions there.

We also saw that the single and zeroth copy fields mapping to the two sets of fluid-dual metric classes store their information differently. In the type D case, the vector potential for the magnetic field corresponds to the fluid velocity profile, while the zeroth-copy scalar field is just a constant; only the single-copy gauge field is carrying nontrivial information about the fluid. For type N spacetimes, the story is in some sense opposite: the nontrivial components of the fluid are entirely due to the potential, which shows up only in the zeroth-copy scalar field. Here, the gauge field is fixed and appears to be the field necessary to build the fluid-dual spacetime for all potential flow fluids.

In fact, the two fluid classes we have studied fall into two simple classes under the Helmholtz decomposition, which rewrites the fluid vector field in terms of its rotational component and its irrotational or potential component, as in (5.73). The constant vorticity solutions which map to type D spacetimes have $\phi = 0$ while the potential flow solutions that map to type N spacetimes have $\vec{A} = 0$. Under the

double copy prescription, solutions with nonzero $\vec{A}$ map to a nontrivial gauge field whose behavior depends on the fluid velocity, but to a constant (trivial) zeroth copy scalar. Similarly, solutions with nonzero ϕ all map to the same gauge field (5.67), so instead the zeroth copy scalar carries the fluid information: it is proportional to the second derivative of the fluid potential as in (5.74). Consequently, we propose that any fluid-dual metric may be mapped to a single copy gauge field and zeroth copy scalar, each of which is a sum of the corresponding pieces from the rotational and irrotational components in the Helmholtz decomposition. We hope to explore this idea in future work.

We should note throughout that we work only to the lowest order in a perturbative expansion (mainly the hydrodynamic expansion). A more complete treatment may require understanding of the double copy prescription beyond a linear order; all double Kerr-Schild prescriptions are essentially linear due to the linearization of the equations of motion in those coordinates. The Weyl double copy itself is not linear in nature, but is unclear how it might relate to more advanced treatments that would go beyond a perturbative expansion as in Luna *et al.* (2017), such as the convolution prescription in Luna *et al.* (2020); Kim *et al.* (2020). Further development of this convolution prescription to include algebraically special spacetimes would be of interest.

The double-copy treatment in the fluid-gravity duality context may also be amenable to analysis using solution generating techniques. For example, the Ehler's transformations as implemented in Berkeley and Berman (2013) for fluids and further studied in Alawadhi *et al.* (2020); Huang *et al.* (2019) in the context of the double copy could allow access to a larger set of double-copy treatments for fluid-dual spacetimes. Indeed, such an analysis could shed light on the nature of single and zeroth copies for such spacetimes.

Since fluid-gravity duality itself can be understood from an AdS-CFT perspective (including the cutoff-prescription formulation, whose relationship to AdS-CFT was first understood in Brattan *et al.* (2011)), we hope the mapping here from fluid solutions to gravities and then through the double copy prescription to gauge theories (and scalars) can provide perspective both regarding the relationship of the double copy prescription to AdS-CFT duality, and also the understanding of fluid-gravity duality itself, including a deeper understanding of fluids as in Haehl *et al.* (2016).

Chapter 6

CONCLUSIONS

In this dissertation I have explored aspects of three sets of dualities, the gauge/gravity duality, color-kinematics duality or the double-copy paradigm and the fluid-gravity duality. The overarching theme has been the mapping of symmetries in classical and quantum field theories onto gravitational theories.

To summarize our results, first the Fermi-surface structure for gravitational theories with spatial modulation was examined. We considered the Einstein-Maxwell-Chern-Simons theory with a Dilaton and found that such gravitational models admit a rich phase space structure which depends upon the background geometry. We also observed Fermi shells in a subset of the cases that we considered.

The second set of dualities considered involved the application of the double-copy paradigm using the Weyl spinor to evaluate spin-1 representations of fluids spacetimes. We find that constant vorticity fluids and irrotational fluid velocity fields can be each distinctly identified with Petrov type-D and type-N spacetimes respectively. We also find that for type-D spacetimes, with a suitable gauge choice it is possible to identify the velocity fields with the gauge field itself. Finally one finds that the associated magnetic field is proportional to the vorticity of the fluid. For the irrotational potential flows we find that a large class of fluid solutions can be mapped on to the Weyl spinor. The coefficient of proportionality of the Weyl spinor (the Weyl scalar Ψ_4) can be identified as a Laurent series in $\bar{z} = x - iy$, where x and y are the

coordinates on the hypersurface upon which the fluid lives.

Below I briefly discuss potential future directions associated with the research presented in this thesis.

6.1 Spatially Modulated Phases and the Membrane Paradigm

A very natural extension of the work in chapter 3 involves the use of the membrane paradigm and its applications in the context of holographic condensed matter physics. For instance [Donos and Gauntlett (2015),Guo *et al.* (2018)]] solve Navier-Stokes equations for incompressible charged fluids on horizons to obtain DC thermoelectric conductivities. Spatially modulated phases can also be obtained in holography by obtaining a striped order on the horizons of black-holes in asymptotically AdS space-times with appropriate matter fields Donos and Gauntlett (2011).

Such approaches might provide additional tools to study Fermi surface structures for gravitational duals of spatially modulated phases. In general there are a large set of holographic models that could be revisited using such approaches.

6.2 The Single Copy of General Fluids.

In chapter 5 we constructed a single copy for the fluids metric. However we were able to do so when the fluid was either distinctly a potential flow i.e. irrotational or when it carried a constant vorticity. However this does not represent all possible types of velocities fluids can carry. It is an interesting question to consider whether it is possible to obtain a single copy for more general fluids that are described by type II spacetimes.

Asking such a question would incidently also provide clues towards the construction of a more general Weyl double-copy for type-II spacetimes. With regards to type-II spacetimes the Weyl spinor has the form,

$$C_{ABCD} = 6\Psi_2\, o_{(A}\iota_B o_C \iota_{D)} + \Psi_4 \iota_A \iota_B \iota_C \iota_D \stackrel{?}{=} \frac{1}{S} f^{(1)}_{(AB} f^{(2)}_{CD)}, \tag{6.1}$$

where we ask if it is possible to find spinors $f^{(i)}_{AB}$ whose associated tensors satisfy Maxwell's equations. The forms of the associated spinors f^{i}_{AB} based on the above would be,

$$f^{(1)}_{AB} = B\left(i\sqrt{6\Psi_2}\, o_{(A}\iota_{B)} + \sqrt{\Psi_4} o_A o_B\right) \qquad f^{(2)}_{AB} = \frac{S}{B}\left(-i\sqrt{6\Psi_2}\, o_{(A}\iota_{B)} + \sqrt{\Psi_4} o_A o_B\right), \tag{6.2}$$

where B is some undetermined function and S refers to the scalar function in the double-copy. The difficulty in the task is with the requirement that the spinors $f^{(i)}_{AB}$ be consistent with Maxwell's equations. To this end it is tantalizing to note that the Weyl scalars Ψ_2 and Ψ_4 can be expressed compactly in terms of a general fluid stream function χ and the complex coordinate $z \equiv x - iy$ as,

$$\Psi_2 = i\partial_z \partial_{\bar{z}} \chi \qquad \Psi_4 = 2i\partial_{\bar{z}} \partial_{\bar{z}} \chi \tag{6.3}$$

where the stream function χ gives the fluid velocities $v_i = \epsilon_{ij}\partial_j \chi$.

6.3 Concluding Remarks

The fluid-gravity program and more generally the membrane paradigm have been useful in providing insights on the behavior of black hole horizons. The double copy paradigm, on the other hand, in addition to providing useful insights has also been useful for the computation of gravitational waves associated with black-hole mergers. A union of the two concepts is thus a natural choice and will likely continue to be a program that yields significant physical insights.

The AdS/CM program has motivations that are very similar to the initial reasons that lead Ginzburg, Landau and others towards identifying a theory of phase transitions for superconductors — in that one follows the symmetries and try to write effective actions that capture the dynamics of these symmetries. Future work in this direction is likely to not only provide gravitational models for strongly interacting systems but more generally also give insights on the nature of gauge/gravity dualities and the constraints associated with their applicability for physical systems.

Adamo, T., E. Casali, L. Mason and S. Nekovar, "Scattering on plane waves and the double copy", Class. Quant. Grav. **35**, 1, 015004 (2018).

Aharony, O., O. Bergman, D. L. Jafferis and J. Maldacena, "N=6 superconformal Chern-Simons-matter theories, M2-branes and their gravity duals", JHEP **10**, 091 (2008).

Alawadhi, R., D. S. Berman, B. Spence and D. Peinador Veiga, "S-duality and the double copy", JHEP **03**, 059 (2020).

Alday, L. F., D. Gaiotto and Y. Tachikawa, "Liouville Correlation Functions from Four-dimensional Gauge Theories", Lett. Math. Phys. **91**, 167–197 (2010).

Alfonsi, L., C. D. White and S. Wikeley, "Topology and Wilson lines: global aspects of the double copy", (2020).

Alvarez-Gaume, L. and S. Hassan, "Introduction to S duality in N=2 supersymmetric gauge theories: A Pedagogical review of the work of Seiberg and Witten", Fortsch. Phys. **45**, 159–236 (1997).

Ammon, M., J. Erdmenger, V. Grass, P. Kerner and A. O'Bannon, "On Holographic p-wave Superfluids with Back-reaction", Phys. Lett. **B686**, 192–198 (2010a).

Ammon, M., J. Erdmenger, M. Kaminski and A. O'Bannon, "Fermionic Operator Mixing in Holographic p-wave Superfluids", JHEP **05**, 053 (2010b).

Anantua, R. J., S. A. Hartnoll, V. L. Martin and D. M. Ramirez, "The Pauli exclusion principle at strong coupling: Holographic matter and momentum space", JHEP **03**, 104 (2013).

Andrzejewski, K. and S. Prencel, "From polarized gravitational waves to analytically solvable electromagnetic beams", Phys. Rev. D **100**, 4, 045006 (2019).

Antonelli, A., A. Buonanno, J. Steinhoff, M. van de Meent and J. Vines, "Energetics of two-body Hamiltonians in post-Minkowskian gravity", Phys. Rev. D **99**, 10, 104004 (2019).

Bah, I., R. Dempsey and P. Weck, "Kerr-Schild Double Copy and Complex Worldlines", JHEP **20**, 180 (2020).

Bahjat-Abbas, N., A. Luna and C. D. White, "The Kerr-Schild double copy in curved spacetime", JHEP **12**, 004 (2017).

Bahjat-Abbas, N., R. Stark-Muchão and C. D. White, "Monopoles, shockwaves and the classical double copy", JHEP **04**, 102 (2020).

Barnes, H., K. John Fletcher Hutton, J. Hutton and K. Walters, *An Introduction to Rheology*, Rheology Series (Elsevier Science, 1989), URL `https://www.sciencedirect.com/bookseries/rheology-series/vol/3/suppl/C`.

Benini, F., C. P. Herzog, R. Rahman and A. Yarom, "Gauge gravity duality for d-wave superconductors: prospects and challenges", JHEP **11**, 137 (2010).

Benini, F., C. P. Herzog and A. Yarom, "Holographic Fermi arcs and a d-wave gap", Phys. Lett. **B701**, 626–629 (2011).

Berkeley, J. and D. S. Berman, "The Navier-Stokes equation and solution generating symmetries from holography", JHEP **04**, 092 (2013).

Berman, D. S., E. Chacón, A. Luna and C. D. White, "The self-dual classical double copy, and the Eguchi-Hanson instanton", JHEP **01**, 107 (2019).

Bern, Z., J. Carrasco and H. Johansson, "New Relations for Gauge-Theory Amplitudes", Phys. Rev. D **78**, 085011 (2008).

Bern, Z., J. J. Carrasco, M. Chiodaroli, H. Johansson and R. Roiban, "The Duality Between Color and Kinematics and its Applications", (2019a).

Bern, Z., C. Cheung, R. Roiban, C.-H. Shen, M. P. Solon and M. Zeng, "Black Hole Binary Dynamics from the Double Copy and Effective Theory", JHEP **10**, 206 (2019b).

Bern, Z., C. Cheung, R. Roiban, C.-H. Shen, M. P. Solon and M. Zeng, "Scattering Amplitudes and the Conservative Hamiltonian for Binary Systems at Third Post-Minkowskian Order", Phys. Rev. Lett. **122**, 20, 201603 (2019c).

Bhattacharyya, S., R. Loganayagam, S. Minwalla, S. Nampuri, S. P. Trivedi and S. R. Wadia, "Forced Fluid Dynamics from Gravity", JHEP **02**, 018 (2009a).

Bhattacharyya, S., S. Minwalla and S. R. Wadia, "The Incompressible Non-Relativistic Navier-Stokes Equation from Gravity", JHEP **08**, 059 (2009b).

Bianchi, M., D. Z. Freedman and K. Skenderis, "How to go with an RG flow", JHEP **08**, 041 (2001).

Bianchi, M., D. Z. Freedman and K. Skenderis, "Holographic renormalization", Nucl. Phys. B **631**, 159–194 (2002).

Bogomolny, E., "Stability of Classical Solutions", Sov. J. Nucl. Phys. **24**, 449 (1976).

Brattan, D., J. Camps, R. Loganayagam and M. Rangamani, "CFT dual of the AdS Dirichlet problem : Fluid/Gravity on cut-off surfaces", JHEP **12**, 090 (2011).

Bredberg, I., C. Keeler, V. Lysov and A. Strominger, "Wilsonian Approach to Fluid/Gravity Duality", JHEP **03**, 141 (2011).

Bredberg, I., C. Keeler, V. Lysov and A. Strominger, "From Navier-Stokes To Einstein", JHEP **07**, 146 (2012).

Bredberg, I. and A. Strominger, "Black Holes as Incompressible Fluids on the Sphere", JHEP **05**, 043 (2012).

Breitenlohner, P. and D. Z. Freedman, "Positive Energy in anti-De Sitter Backgrounds and Gauged Extended Supergravity", Phys. Lett. **115B**, 197–201 (1982a).

Breitenlohner, P. and D. Z. Freedman, "Stability in Gauged Extended Supergravity", Annals Phys. **144**, 249 (1982b).

Cai, R.-G., L. Li, Q. Yang and Y.-L. Zhang, "Petrov type I Condition and Dual Fluid Dynamics", JHEP **04**, 118 (2013).

Carrillo González, M., B. Melcher, K. Ratliff, S. Watson and C. D. White, "The classical double copy in three spacetime dimensions", (2019).

Carrillo-González, M., R. Penco and M. Trodden, "The classical double copy in maximally symmetric spacetimes", JHEP **04**, 028 (2018).

Chang, J., E. Blackburn, A. Holmes, N. B. Christensen, J. Larsen, J. Mesot, R. Liang, D. Bonn, W. Hardy, A. Watenphul *et al.*, "Direct observation of competition between superconductivity and charge density wave order in yba 2 cu 3 o 6.67", Nature Physics **8**, 12, 871 (2012).

Charmousis, C., B. Gouteraux, B. S. Kim, E. Kiritsis and R. Meyer, "Effective Holographic Theories for low-temperature condensed matter systems", JHEP **11**, 151 (2010).

Chen, J.-W., Y.-S. Liu and D. Maity, "$d + id$ Holographic Superconductors", JHEP **05**, 032 (2011).

Cheung, C., I. Z. Rothstein and M. P. Solon, "From Scattering Amplitudes to Classical Potentials in the Post-Minkowskian Expansion", Phys. Rev. Lett. **121**, 25, 251101 (2018).

Cocke, W. J., "Table for constructing the spin coefficients in general relativity", Phys. Rev. D **40**, 650–651, URL `https://link.aps.org/doi/10.1103/PhysRevD.40.650` (1989).

Compere, G., P. McFadden, K. Skenderis and M. Taylor, "The Holographic fluid dual to vacuum Einstein gravity", JHEP **07**, 050 (2011).

Compere, G., P. McFadden, K. Skenderis and M. Taylor, "The relativistic fluid dual to vacuum Einstein gravity", JHEP **03**, 076 (2012).

Cremonini, S., L. Li and J. Ren, "Holographic Fermions in Striped Phases", JHEP **12**, 080 (2018).

Cubrovic, M., J. Zaanen and K. Schalm, "String Theory, Quantum Phase Transitions and the Emergent Fermi-Liquid", Science **325**, 439–444 (2009).

Damascelli, A., Z. Hussain and Z.-X. Shen, "Angle-resolved photoemission studies of the cuprate superconductors", Reviews of Modern Physics **75**, 473–541 (2003).

Damour, T., "Black Hole Eddy Currents", Phys. Rev. **D18**, 3598–3604 (1978).

Damour, T., *Quelques proprietes mecaniques, electromagnet iques, thermodynamiques et quantiques des trous noir*, Ph.D. thesis, Paris U., VI-VII, URL `http://pagesperso.ihes.fr/~damour/Articles/` (1979).

Damour, T., "Surface Effects in Black-Hole Physics", in "Marcel Grossmann Meeting: General Relativity", p. 587 (1982).

Damour, T. and M. Lilley, "String theory, gravity and experiment", Les Houches **87**, 371–448 (2008).

De, S., S. Dey and B. R. Majhi, "Effective metric in fluid-gravity duality through parallel transport: a proposal", Phys. Rev. D **99**, 12, 124024 (2019).

de Boer, J., E. P. Verlinde and H. L. Verlinde, "On the holographic renormalization group", JHEP **08**, 003 (2000).

DeWolfe, O., S. S. Gubser and C. Rosen, "Fermi surfaces in N=4 Super-Yang-Mills theory", Phys. Rev. **D86**, 106002 (2012).

DeWolfe, O., O. Henriksson and C. Rosen, "Fermi surface behavior in the ABJM M2-brane theory", Phys. Rev. **D91**, 12, 126017 (2015).

Dey, S., S. De and B. Ranjan Majhi, "Gravity dual of Navier-Stokes equation of an uniformly rotating fluid through parallel transport", (2020).

Dong, X., S. Harrison, S. Kachru, G. Torroba and H. Wang, "Aspects of holography for theories with hyperscaling violation", Journal of High Energy Physics **2012**, 6, 41 (2012).

Donos, A. and J. P. Gauntlett, "Holographic striped phases", JHEP **08**, 140 (2011).

Donos, A. and J. P. Gauntlett, "Navier-Stokes Equations on Black Hole Horizons and DC Thermoelectric Conductivity", Phys. Rev. D **92**, 12, 121901 (2015).

Eling, C., I. Fouxon and Y. Oz, "The Incompressible Navier-Stokes Equations From Membrane Dynamics", Phys. Lett. B **680**, 496–499 (2009).

Eling, C. and Y. Oz, "Relativistic CFT Hydrodynamics from the Membrane Paradigm", JHEP **02**, 069 (2010).

Eling, C. and Y. Oz, "Holographic Vorticity in the Fluid/Gravity Correspondence", JHEP **11**, 079 (2013).

Faulkner, T., H. Liu and M. Rangamani, "Integrating out geometry: Holographic Wilsonian RG and the membrane paradigm", JHEP **08**, 051 (2011).

Figueroa-OFarrill, J., "Electromagnetic duality for children", URL `https://www.maths.ed.ac.uk/~jmf/Teaching/Lectures/EDC.pdf` (1998).

Fisher, D. S., "Scaling and critical slowing down in random-field ising systems", Phys. Rev. Lett. **56**, 416–419, URL `https://link.aps.org/doi/10.1103/PhysRevLett.56.416` (1986).

Fradkin, E. H., "Field Theories of Condensed Matter Physics", pp. 1–852 (2013).

Goldberger, W. D. and J. Li, "Strings, extended objects, and the classical double copy", JHEP **02**, 092 (2020).

Goldberger, W. D., S. G. Prabhu and J. O. Thompson, "Classical gluon and graviton radiation from the bi-adjoint scalar double copy", Phys. Rev. D **96**, 6, 065009 (2017).

Goldberger, W. D. and A. K. Ridgway, "Radiation and the classical double copy for color charges", Phys. Rev. **D95**, 12, 125010 (2017).

Goldberger, W. D. and A. K. Ridgway, "Bound states and the classical double copy", Phys. Rev. **D97**, 8, 085019 (2018).

Gonda, S., M. Kawasaki, S. Ohashi, Y. Kotaka, K. Kishio and H. Koinuma, "Superconducting gap observation by high-resolution photoelectron yield spectroscopy", Journal of Physics and Chemistry of Solids **56**, 12, 1877 – 1878, URL `http://www.sciencedirect.com/science/article/pii/0022369795000968`, proceedings of the Conference on Spectroscopies in Novel Superconductors (1995).

Gourgoulhon, E., "A Generalized Damour-Navier-Stokes equation applied to trapping horizons", Phys. Rev. D **72**, 104007 (2005).

Gourgoulhon, E. and J. L. Jaramillo, "A 3+1 perspective on null hypersurfaces and isolated horizons", Phys. Rept. **423**, 159–294 (2006).

Gourgoulhon, E. and J. L. Jaramillo, "New theoretical approaches to black holes", New Astron. Rev. **51**, 791–798 (2008).

Goutéraux, B., "Universal scaling properties of extremal cohesive holographic phases", JHEP **01**, 080 (2014).

Goutéraux, B. and V. L. Martin, "Spectral weight and spatially modulated instabilities in holographic superfluids", JHEP **05**, 005 (2017).

Griffiths, J. B. and J. Podolsky, "A New look at the Plebanski-Demianski family of solutions", Int. J. Mod. Phys. **D15**, 335–370 (2006).

Grozdanov, S. s., P. K. Kovtun, A. O. Starinets and P. Tadić, "Convergence of the Gradient Expansion in Hydrodynamics", Phys. Rev. Lett. **122**, 25, 251601 (2019).

Gubser, S., I. R. Klebanov and A. M. Polyakov, "Gauge theory correlators from noncritical string theory", Phys. Lett. B **428**, 105–114 (1998).

Gubser, S. S., Phys. Rev. **D78**, 065034 (2008).

Gubser, S. S. and S. S. Pufu, "The Gravity dual of a p-wave superconductor", JHEP **11**, 033 (2008).

Guo, X., P. Wang and H. Yang, "Membrane Paradigm and Holographic DC Conductivity for Nonlinear Electrodynamics", Phys. Rev. D **98**, 2, 026021 (2018).

Gurses, M. and B. Tekin, "Classical Double Copy: Kerr-Schild-Kundt metrics from Yang-Mills Theory", Phys. Rev. **D98**, 12, 126017 (2018).

Haehl, F. M., R. Loganayagam and M. Rangamani, "The Fluid Manifesto: Emergent symmetries, hydrodynamics, and black holes", JHEP **01**, 184 (2016).

Hartle, J. B., "Tidal Friction in Slowly Rotating Black Holes", Phys. Rev. **D8**, 1010–1024 (1973).

Hartle, J. B., "Tidal shapes and shifts on rotating black holes", Phys. Rev. **D9**, 2749–2759 (1974).

Hartnoll, S. A., C. P. Herzog and G. T. Horowitz, "Holographic Superconductors", JHEP **12**, 015 (2008).

Hartnoll, S. A., A. Lucas and S. Sachdev, "Holographic quantum matter", (2016).

Hartnoll, S. A. and E. Shaghoulian, "Spectral weight in holographic scaling geometries", JHEP **07**, 078 (2012).

Hawking, S. W. and J. B. Hartle, "Energy and angular momentum flow into a black hole", Commun. Math. Phys. **27**, 283–290 (1972).

Huang, Y.-T., U. Kol and D. O'Connell, "The Double Copy of Electric-Magnetic Duality", (2019).

Hubeny, V. E., S. Minwalla and M. Rangamani, "The fluid/gravity correspondence", in "Black holes in higher dimensions", pp. 348–383 (2012), [,817(2011)].

Huijse, L., S. Sachdev and B. Swingle, "Hidden Fermi surfaces in compressible states of gauge-gravity duality", Phys. Rev. **B85**, 035121 (2012).

Iizuka, N., S. Kachru, N. Kundu, P. Narayan, N. Sircar, S. P. Trivedi and H. Wang, "Extremal Horizons with Reduced Symmetry: Hyperscaling Violation, Stripes, and a Classification for the Homogeneous Case", JHEP **03**, 126 (2013).

Ilderton, A., "Screw-symmetric gravitational waves: a double copy of the vortex", Phys. Lett. B **782**, 22–27 (2018).

Iqbal, N. and H. Liu, "Universality of the hydrodynamic limit in AdS/CFT and the membrane paradigm", Phys. Rev. D **79**, 025023 (2009).

Iqbal, N., H. Liu and M. Mezei, "Lectures on holographic non-Fermi liquids and quantum phase transitions", in "Proceedings, Theoretical Advanced Study Institute in Elementary Particle Physics (TASI 2010). String Theory and Its Applications: From meV to the Planck Scale: Boulder, Colorado, USA, June 1-25, 2010", pp. 707–816 (2011).

Jimenez-Alba, A., K. Landsteiner, Y. Liu and Y.-W. Sun, "Anomalous magnetoconductivity and relaxation times in holography", JHEP **07**, 117 (2015).

Kälin, G. and R. A. Porto, "From Boundary Data to Bound States", JHEP **01**, 072 (2020).

Keeler, C., T. Manton and N. Monga, "From Navier-Stokes to Maxwell via Einstein", JHEP **08**, 147 (2020).

Kim, K., K. Lee, R. Monteiro, I. Nicholson and D. Peinador Veiga, "The Classical Double Copy of a Point Charge", JHEP **02**, 046 (2020).

Kosower, D. A., B. Maybee and D. O'Connell, "Amplitudes, Observables, and Classical Scattering", JHEP **02**, 137 (2019).

Kovtun, P., D. T. Son and A. O. Starinets, "Holography and hydrodynamics: Diffusion on stretched horizons", JHEP **10**, 064 (2003).

Kovtun, P., D. T. Son and A. O. Starinets, "Viscosity in strongly interacting quantum field theories from black hole physics", Phys. Rev. Lett. **94**, 111601 (2005).

Landsteiner, K. and Y. Liu, "The holographic Weyl semi-metal", Phys. Lett. B **753**, 453–457 (2016).

Lee, K., "Kerr-Schild Double Field Theory and Classical Double Copy", JHEP **10**, 027 (2018).

Lee, S.-S., "A Non-Fermi Liquid from a Charged Black Hole: A Critical Fermi Ball", Phys. Rev. **D79**, 086006 (2009).

Leigh, R. G., A. C. Petkou and P. Petropoulos, "Holographic Fluids with Vorticity and Analogue Gravity", JHEP **11**, 121 (2012a).

Leigh, R. G., A. C. Petkou and P. Petropoulos, "Holographic Three-Dimensional Fluids with Nontrivial Vorticity", Phys. Rev. D **85**, 086010 (2012b).

Liu, H., J. McGreevy and D. Vegh, "Non-Fermi liquids from holography", Phys. Rev. **D83**, 065029 (2011).

Luna, A., R. Monteiro, I. Nicholson, A. Ochirov, D. O'Connell, N. Westerberg and C. D. White, "Perturbative spacetimes from Yang-Mills theory", JHEP **04**, 069 (2017).

Luna, A., R. Monteiro, I. Nicholson and D. O'Connell, "Type D Spacetimes and the Weyl Double Copy", Class. Quant. Grav. **36**, 065003 (2019).

Luna, A., R. Monteiro, I. Nicholson, D. O'Connell and C. D. White, "The double copy: Bremsstrahlung and accelerating black holes", JHEP **06**, 023 (2016).

Luna, A., R. Monteiro, D. O'Connell and C. D. White, "The classical double copy for Taub–NUT spacetime", Phys. Lett. B **750**, 272–277 (2015).

Luna, A., S. Nagy and C. White, "The convolutional double copy: a case study with a point", (2020).

Luna, A., I. Nicholson, D. O'Connell and C. D. White, "Inelastic Black Hole Scattering from Charged Scalar Amplitudes", JHEP **03**, 044 (2018).

Lysov, V. and A. Strominger, "From Petrov-Einstein to Navier-Stokes", (2011).

Maldacena, J. M., "The Large N limit of superconformal field theories and supergravity", Int. J. Theor. Phys. **38**, 1113–1133, [Adv. Theor. Math. Phys.2,231(1998)] (1999).

Martin, V. L. and N. Monga, "Spectral weight in Chern-Simons theory with symmetry breaking", JHEP **10**, 116 (2019).

Monteiro, R., I. Nicholson and D. O'Connell, "Spinor-helicity and the algebraic classification of higher-dimensional spacetimes", Class. Quant. Grav. **36**, 065006 (2019).

Monteiro, R., D. O'Connell and C. D. White, "Black holes and the double copy", JHEP **12**, 056 (2014).

Montonen, C. and D. I. Olive, "Magnetic Monopoles as Gauge Particles?", Phys. Lett. B **72**, 117–120 (1977).

Nakamura, S., H. Ooguri and C.-S. Park, "Gravity Dual of Spatially Modulated Phase", Phys. Rev. **D81**, 044018 (2010).

Oz, Y. and M. Rabinovich, "The Penrose Inequality and the Fluid/Gravity Correspondence", JHEP **02**, 070 (2011).

P. V., A. and A. Manu, "Classical double copy from Color Kinematics duality: A proof in the soft limit", Phys. Rev. **D101**, 4, 046014 (2020).

Padmanabhan, T., "Thermodynamical Aspects of Gravity: New insights", Rept. Prog. Phys. **73**, 046901 (2010).

Parikh, M. and F. Wilczek, "An Action for black hole membranes", Phys. Rev. D **58**, 064011 (1998).

Penrose, R. and W. Rindler, *Spinors and Space-Time vol. 2: Spinor and Twistor Methods in Space-Time Geometry*, Cambridge Monographs on Mathematical Physics (Cambridge Univ. Press, Cambridge, UK, 1988).

Penrose, R. and W. Rindler, *Spinors and Space-Time*, Cambridge Monographs on Mathematical Physics (Cambridge Univ. Press, Cambridge, UK, 2011).

Pinzani-Fokeeva, N. and M. Taylor, "Towards a general fluid/gravity correspondence", Phys. Rev. D **91**, 4, 044001 (2015).

Plebanski, J. F. and M. Demianski, "Rotating, charged, and uniformly accelerating mass in general relativity", Annals Phys. **98**, 98–127 (1976).

Podolsky, J., O. Hruka and J. B. Griffiths, "Non-expanding PlebaskiDemiaski spacetimes", Class. Quant. Grav. **35**, 16, 165011 (2018).

Policastro, G., D. T. Son and A. O. Starinets, "The Shear viscosity of strongly coupled N=4 supersymmetric Yang-Mills plasma", Phys. Rev. Lett. **87**, 081601 (2001).

Policastro, G., D. T. Son and A. O. Starinets, "From AdS / CFT correspondence to hydrodynamics", JHEP **09**, 043 (2002a).

Policastro, G., D. T. Son and A. O. Starinets, "From AdS / CFT correspondence to hydrodynamics. 2. Sound waves", JHEP **12**, 054 (2002b).

Polyakov, A. M., "Particle Spectrum in the Quantum Field Theory", JETP Lett. **20**, 194–195 (1974).

Prasad, M. and C. M. Sommerfield, "An Exact Classical Solution for the 't Hooft Monopole and the Julia-Zee Dyon", Phys. Rev. Lett. **35**, 760–762 (1975).

Price, R. and K. Thorne, "Membrane Viewpoint on Black Holes: Properties and Evolution of the Stretched Horizon", Phys. Rev. D **33**, 915–941 (1986).

Rajaraman, R., *SOLITONS AND INSTANTONS. AN INTRODUCTION TO SOLITONS AND INSTANTONS IN QUANTUM FIELD THEORY* (1982).

Rangamani, M., "Gravity and Hydrodynamics: Lectures on the fluid-gravity correspondence", Class. Quant. Grav. **26**, 224003 (2009).

Ridgway, A. K. and M. B. Wise, "Static Spherically Symmetric Kerr-Schild Metrics and Implications for the Classical Double Copy", Phys. Rev. **D94**, 4, 044023 (2016).

Roberts, M. M. and S. A. Hartnoll, "Pseudogap and time reversal breaking in a holographic superconductor", JHEP **08**, 035 (2008).

Rozali, M., D. Smyth, E. Sorkin and J. B. Stang, "Holographic Stripes", Phys. Rev. Lett. **110**, 20, 201603 (2013a).

Rozali, M., D. Smyth, E. Sorkin and J. B. Stang, "Striped order in AdS/CFT correspondence", Phys. Rev. D **87**, 12, 126007 (2013b).

Seiberg, N., "Electric - magnetic duality in supersymmetric nonAbelian gauge theories", Nucl. Phys. B **435**, 129–146 (1995).

Shen, C.-H., "Gravitational Radiation from Color-Kinematics Duality", JHEP **11**, 162 (2018).

Shuryak, E., "Why does the quark gluon plasma at RHIC behave as a nearly ideal fluid?", Prog. Part. Nucl. Phys. **53**, 273–303 (2004).

Skenderis, K., "Lecture notes on holographic renormalization", Class. Quant. Grav. **19**, 5849–5876 (2002).

Son, D. T. and A. O. Starinets, "Viscosity, Black Holes, and Quantum Field Theory", Ann. Rev. Nucl. Part. Sci. **57**, 95–118 (2007).

Stephani, H., D. Kramer, M. A. H. MacCallum, C. Hoenselaers and E. Herlt, *Exact solutions of Einstein's field equations*, Cambridge Monographs on Mathematical Physics (Cambridge Univ. Press, Cambridge, 2003), URL `http://www.cambridge.org/uk/catalogue/catalogue.asp?isbn=0521461367`.

't Hooft, G., "Magnetic Monopoles in Unified Gauge Theories", Nucl. Phys. B **79**, 276–284 (1974).

Taylor, M., "TT deformations in general dimensions", (2018).

Teaney, D., "The Effects of viscosity on spectra, elliptic flow, and HBT radii", Phys. Rev. C **68**, 034913 (2003).

Thorne, K. S., R. Price and D. Macdonald, eds., *Black Holes: The Membrane Paradigm* (Yale Univ. Press, 1986).

Varma, C. M., P. B. Littlewood, S. Schmitt-Rink, E. Abrahams and A. E. Ruckenstein, "Phenomenology of the normal state of cu-o high-temperature superconductors", Phys. Rev. Lett. **63**, 1996–1999, URL `https://link.aps.org/doi/10.1103/PhysRevLett.63.1996` (1989).

Walker, M. and R. Penrose, "On quadratic first integrals of the geodesic equations for type [22] spacetimes", Commun. Math. Phys. **18**, 265–274 (1970).

Witten, E. and D. I. Olive, "Supersymmetry Algebras That Include Topological Charges", Phys. Lett. B **78**, 97–101 (1978).

APPENDIX A

SPINOR FORMALISM

In our notation, spacetime indices are given by $\{\mu,\nu,\gamma,...\}$, frame indices by $\{a,b,c,...\}$ and the spinor indices as $\{A,B,C,...\}$ with their conjugates $\{\dot{A},\dot{B},\dot{C},...\}$. The essential objects that translate between the spinor and tensor formalisms are the Pauli 4-vectors

$$\sigma^a_{A\dot{A}} = \frac{1}{\sqrt{2}}\big(1,\vec{\sigma}\big)_{A\dot{A}}, \qquad \vec{\sigma} = (\sigma_x,\sigma_y,\sigma_z). \tag{A.1}$$

The $\vec{\sigma}$ are the standard $SU(2)$ generators,

$$\sigma_x = \begin{pmatrix} 0 & 1 \\ 1 & 0 \end{pmatrix}, \qquad \sigma_y = \begin{pmatrix} 0 & -i \\ i & 0 \end{pmatrix}, \qquad \sigma_z = \begin{pmatrix} 1 & 0 \\ 0 & -1 \end{pmatrix}. \tag{A.2}$$

A spacetime vector is obtained from a frame vector by $V_\mu = e_\mu{}^a V_a$, where the $e_\mu{}^a$ are vierbeins that construct the full metric as $g_{\mu\nu} = e_\mu{}^a e_\nu{}^b \eta_{ab}$. Here, $\eta_{ab} = \eta^{ab} =$ diag(-1, 1, 1, 1). The frame indices are raised and lowered with the diagonal Minkowski space η_{ab}, while spinor indices are raised and lowered with a Levi-Civita symbol, which we define as

$$\varepsilon^{AB} = -\varepsilon_{AB} = \begin{pmatrix} 0 & 1 \\ -1 & 0 \end{pmatrix}. \tag{A.3}$$

A vector can be written in spinor indices or in frame indices using (A.1);

$$V_{A\dot{A}} = V_a \sigma^a_{A\dot{A}}, \qquad \Leftrightarrow \qquad V_a = \sigma_{aA\dot{A}} V^{A\dot{A}}, \tag{A.4}$$

where $\sigma_{aA\dot{A}} = \eta_{ab}\sigma^b_{A\dot{A}}$ and $V^{A\dot{A}} = \varepsilon^{AB} V_{B\dot{B}} \varepsilon^{\dot{B}\dot{A}}$. The (inverse) vierbein constructs the Pauli 4-vector in spacetime indices $\sigma^\mu_{A\dot{A}} = e^\mu{}_a \sigma^a_{A\dot{A}}$ which, with its inverse $\sigma^{A\dot{A}}_\mu = g_{\mu\nu}\varepsilon^{AB}\sigma^\nu_{B\dot{B}}\varepsilon^{\dot{B}\dot{A}}$, satisfies

$$\sigma^\mu_{A\dot{A}}\sigma^{A\dot{A}}_\nu = \delta^\mu_\nu, \qquad \sigma^\mu_{A\dot{A}}\sigma^{B\dot{B}}_\mu = \delta^B_A \delta^{\dot{B}}_{\dot{A}}. \tag{A.5}$$

Any tensor can be written as its spinor counterpart using the index doubling procedure. The Weyl tensor $W_{\mu\nu\lambda\gamma}$ becomes

$$W_{\mu\nu\lambda\gamma} \to \; W_{A\dot{A}B\dot{B}C\dot{C}D\dot{D}} = C_{ABCD}\varepsilon_{\dot{A}\dot{B}}\varepsilon_{\dot{C}\dot{D}} + \bar{C}_{\dot{A}\dot{B}\dot{C}\dot{D}}\varepsilon_{AB}\varepsilon_{CD}, \tag{A.6}$$

where the C_{ABCD} and $\bar{C}_{\dot{A}\dot{B}\dot{C}\dot{D}}$ are symmetric in their indices and related by complex conjugation. The object[1]

$$\sigma^{\mu\nu}_{AB} = \sigma^{[\mu}_{A\dot{C}}\bar{\sigma}^{\nu]\,\dot{C}C}\varepsilon_{CB}, \qquad \text{with} \qquad \bar{\sigma}^{\mu A\dot{A}} = e^\mu{}_a \bar{\sigma}^{a\dot{A}A}, \qquad \bar{\sigma}^{a\dot{A}A} = \frac{1}{\sqrt{2}}\big(1,-\vec{\sigma}\big)^{\dot{A}A} \tag{A.7}$$

serves to directly obtain the spinor form of a given tensor. For the Weyl spinor,

$$C_{ABCD} = \frac{1}{4} W_{\mu\nu\lambda\gamma}\sigma^{\mu\nu}_{AB}\sigma^{\lambda\gamma}_{CD}. \tag{A.8}$$

[1]Brackets denote antisymmetrization, and we use the convention $[A,B] = AB - BA$.

For the field strength tensor $F_{\mu\nu}$, we write

$$F_{\mu\nu} \rightarrow \ F_{A\dot{A}B\dot{B}} = f_{AB}\varepsilon_{\dot{A}\dot{B}} + \bar{f}_{\dot{A}\dot{B}}\varepsilon_{AB}, \tag{A.9}$$

where the spinor field strength can be computed as

$$f_{AB} = \frac{1}{2}F_{\mu\nu}\sigma^{(0)\mu\nu}_{AB}, \tag{A.10}$$

which is also symmetric in its spinor indices. In the above expression, the zero superscript is meant to remind that since $F_{\mu\nu}$ lives on flat space, the vierbein that's used to construct the $\sigma^{\mu}_{A\dot{A}}$ in (A.10) is that which constructs the flat space,

$$\sigma^{(0)\mu}_{A\dot{A}} = e^{(0)\mu}_{\ \ a}\sigma^{a}_{A\dot{A}}, \qquad e^{(0)a}_{\mu}e^{(0)b}_{\nu}\eta_{ab} = g^{(0)}_{\mu\nu}. \tag{A.11}$$

For example in section 5.5.1, $g^{(0)}_{\mu\nu}$ is Rindler space (5.51) and the $e^{(0)a}_{\mu}$ are (5.52). The vierbeins that are used to build $\sigma^{\mu\nu}_{AB}$ in (A.8) instead construct the full spacetime. For conciseness we will drop the 0-superscript in what follows.

To invert (A.10), it is tedious though straightforward to show

$$F^{\mu\nu} - \frac{i}{2}\frac{\varepsilon^{\mu\nu\alpha\beta}}{\sqrt{-g}}F_{\alpha\beta} = \sigma^{\mu A\dot{D}}f_{AB}\varepsilon^{BD}\bar{\sigma}^{\nu}_{\dot{D}D}, \tag{A.12}$$

where $g = \det g_{\mu\nu}$. $F^{\mu\nu}$ can be obtained directly by adding the complex conjugate of the right hand side in (A.12), yielding

$$F^{\mu\nu} = \frac{1}{2}\left[\sigma^{\mu A\dot{D}}f_{AB}\varepsilon^{BD}\bar{\sigma}^{\nu}_{\dot{D}D} + \sigma^{*\mu\dot{A}D}\bar{f}_{\dot{A}\dot{B}}\varepsilon^{\dot{B}\dot{D}}\bar{\sigma}^{*\nu}_{D\dot{D}}\right]. \tag{A.13}$$

For the second term in (A.13), the σ^* denotes standard complex conjugation, i.e.

$$\sigma^{*a}_{\dot{A}A} = \frac{1}{\sqrt{2}}\Big(1, \sigma_x, -\sigma_y, \sigma_z\Big)_{\dot{A}A}. \tag{A.14}$$

APPENDIX B

NEWMAN-PENROSE FORMALISM

We now briefly describe the Newman-Penrose (NP) formalism which we use to compute geometric quantities of interest such as the Weyl spinor. The NP formalism utilizes spinor language in order to simplify computations (Penrose and Rindler (2011),Penrose and Rindler (1988),Stephani *et al.* (2003)). There primarily are four sets of objects of interest for us in the NP formalism. Briefly, one rewrites the metric in terms of a tetrad set, this tetrad set then is used to compute spin coefficients[1],

$$g_{\mu\nu} = -l_{(\mu}n_{\nu)} + m_{(\mu}\overline{m}_{\nu)}. \tag{B.1}$$

Bilinears of the spin coefficients then give the set of Weyl scalars $\{\Psi_0, \Psi_1, \Psi_2, \Psi_3, \Psi_4, \}$,

$$\begin{aligned}
\Psi_0 &= D\sigma - \delta\kappa - (\rho + \bar{\rho} + 3\varepsilon + \bar{\varepsilon})\sigma + (\tau - \bar{\pi} + \bar{\alpha} + 3\beta)\kappa \\
\Psi_1 &= D\beta - \delta\varepsilon - (\alpha + \pi)\sigma - (\bar{\rho} - \bar{\varepsilon})\beta + (\mu + \gamma)\kappa + (\bar{\alpha} - \bar{\pi})\varepsilon \\
\Psi_2 &= D\mu - \delta\pi + (\varepsilon + \bar{\varepsilon} - \bar{\rho})\mu + (\bar{\alpha} - \beta - \bar{\pi})\pi + \nu\kappa - \sigma\lambda - R/12 \\
\Psi_3 &= \bar{\delta}\gamma - \Delta\alpha + (\rho + \varepsilon)\nu - (\tau + \beta)\lambda + (\bar{\gamma} - \bar{\mu})\alpha + (\bar{\beta} - \bar{\tau})\gamma \\
\Psi_4 &= \bar{\delta}\nu - \Delta\lambda - (\mu + \bar{\mu} + 3\gamma - \bar{\gamma})\lambda + (3\alpha + \bar{\beta} + \pi - \bar{\tau})\nu,
\end{aligned} \tag{B.2}$$

where the following are directional derivatives,

$$D = l^{\mu}\nabla_{\mu}, \qquad \Delta = n^{\mu}\nabla_{\mu}, \qquad \delta = m^{\mu}\nabla_{\mu}, \qquad \bar{\delta} = \bar{m}^{\mu}\nabla_{\mu}. \tag{B.3}$$

Finally in terms of these Weyl scalars one can rewrite the Weyl Spinor.

$$C_{ABCD} = \Psi_0\iota_A\iota_B\iota_C\iota_D - 4\Psi_1 o_{(A}\iota_B\iota_C\iota_{D)} + 6\Psi_2 o_{(A}o_B\iota_C\iota_{D)} - 4\Psi_3 o_{(A}o_B o_C\iota_{D)} + \Psi_4 o_A o_B o_C o_D \tag{B.4}$$

Finally in order to test the algebraic speciality of the spacetime we compute tetrad invariant combinations of the Weyl scalars; the equation below is equivalent to (5.27) in the main text as included here for completeness:

$$\begin{aligned}
I &\equiv \Psi_0\Psi_4 - 4\Psi_1\Psi_3 + 3\Psi_2^2, \\
J &\equiv \begin{vmatrix} \Psi_4 & \Psi_3 & \Psi_2 \\ \Psi_3 & \Psi_2 & \Psi_1 \\ \Psi_2 & \Psi_1 & \Psi_0 \end{vmatrix}, \\
K &\equiv \Psi_1\Psi_4^2 - 3\Psi_4\Psi_3\Psi_2 + 2\Psi_3^3, \\
L &\equiv \Psi_2\Psi_4 - \Psi_3^2, \\
N &\equiv 12L^2 - \Psi_4^2 I.
\end{aligned} \tag{B.5}$$

The spinors o_A, ι_A are related to the frame metric choice one makes. We will make explicit this connection now. The metric written in terms of vierbiens has the form,

$$g_{\mu\nu} = e_{\mu}{}^{a}e_{\nu}{}^{b}\eta_{ab} \quad \text{where} \quad \eta_{ab} = \text{diag}\{-1, 1, 1, 1\}. \tag{B.6}$$

[1]We utilize the method outlined in Cocke (1989) to obtain spin-coefficients, this approach comes with the computational benefit of replacing certain covariant derivatives with partial derivatives)

The frame metric η_{ab} can itself be written as outer products of a tetrad set, this will allow us to make identifications between the vierbiens and the tetrad set.

$$\begin{aligned} \eta_{ab} &= -\hat{l}_{(a}\hat{n}_{b)} + \hat{m}_{(a}\hat{\overline{m}}_{b)} \\ \implies g_{\mu\nu} &= e_{\mu}{}^{a} e_{\nu}{}^{b}(-\hat{l}_{(a}\hat{n}_{b)} + \hat{m}_{(a}\hat{\overline{m}}_{b)}) \\ \implies g_{\mu\nu} &= -l_{(\mu}n_{\nu)} + m_{(\mu}\overline{m}_{\nu)} \end{aligned} \tag{B.7}$$

Where in the last step we have made the identifications,

$$e_{\mu}{}^{a}\hat{l}_{a} = l_{\mu} \quad e_{\mu}{}^{a}\hat{n}_{a} = n_{\mu} \quad e_{\mu}{}^{a}\hat{m}_{a} = m_{\mu} \quad e_{\mu}{}^{a}\hat{\overline{m}}_{a} = \overline{m}_{\mu} \tag{B.8}$$

Now the tetrad set that reproduces the Minkowski frame metric is,

$$\begin{aligned} \hat{l}_{a} &= \frac{1}{\sqrt{2}}\{1,-1,0,0\} \\ \hat{n}_{a} &= \frac{1}{\sqrt{2}}\{1,1,0,0\} \\ \hat{m}_{a} &= \frac{1}{\sqrt{2}}\{0,0,i,1\} \\ \hat{\overline{m}}_{a} &= \frac{1}{\sqrt{2}}\{0,0,-i,1\} \end{aligned} \tag{B.9}$$

The expression B.8 can be inverted to go from tetrads to vierbiens via the following,

$$\begin{aligned} e_{\mu}{}^{0} &= \frac{1}{\sqrt{2}}(l_{\mu} + n_{\mu}) \qquad & e_{\mu}{}^{1} &= \frac{1}{\sqrt{2}}(l_{\mu} - n_{\mu}) \\ e_{\mu}{}^{2} &= \frac{i}{\sqrt{2}}(\bar{m}_{\mu} - m_{\mu}) \qquad & e_{\mu}{}^{3} &= \frac{1}{\sqrt{2}}(m_{\mu} + \bar{m}_{\mu}) \end{aligned} \tag{B.10}$$

In order to obtain the spinors we write these four vectors in an SL(2,C) representation by contracting them with relevant σ matrices. Note in our conventions we have $\sigma^{a}_{A\dot{A}} = \{\mathbb{I}, \vec{\sigma}\}$, while the curved space equivalents can be obtained by contracting these with vierbiens (i.e. $\sigma^{\mu}_{A\dot{A}} = e^{\mu}{}_{a}\,\sigma^{a}_{A\dot{A}}$). For eg., for $\{o_A, \iota_A\}$ we have,

$$\begin{aligned} o_A o_{\dot{A}} \equiv \hat{l}_{a}\,\sigma^{a}_{A\dot{A}} &= \frac{1}{2}\begin{pmatrix} 1 & 1 \\ 1 & 1 \end{pmatrix} \\ \implies o_A &= \frac{1}{\sqrt{2}}\{1,1\} \\ \iota_A \iota_{\dot{A}} \equiv \hat{n}_{a}\,\sigma^{a}_{A\dot{A}} &= \frac{1}{2}\begin{pmatrix} 1 & -1 \\ -1 & 1 \end{pmatrix} \\ \implies \iota_A &= \frac{1}{\sqrt{2}}\{1,-1\} \end{aligned} \tag{B.11}$$

Further noting that one can transform from SL(2,C) left to right by complex conjugation we use the convention,

$$(o_A)^{*} \equiv o_{\dot{A}} \tag{B.12}$$

This further verifies that the two remaining contractions will hold the following relations correctly,

$$\begin{aligned} \hat{m}_a \, \sigma^a_{A\dot{A}} &= \frac{1}{2} \begin{pmatrix} 1 & 1 \\ -1 & -1 \end{pmatrix} = \iota_A o_{\dot{A}} \\ \hat{\overline{m}}_a \, \sigma^a_{A\dot{A}} &= \frac{1}{2} \begin{pmatrix} 1 & -1 \\ 1 & -1 \end{pmatrix} = o_A \iota_{\dot{A}} \end{aligned} \tag{B.13}$$

APPENDIX C

TETRADS IN THE HYDRODYNAMIC AND THE NEAR HORIZON EXPANSIONS

In the hydrodynamic limit as discussed in section 2 in the body of the paper, the velocities and the pressure must satisfy the scaling (5.4), where i runs over x and y, the spacelike coordinates on the cutoff surface $r = r_c$. We can make this scaling of derivatives explicit by making the following identifications to simplify keeping track of the ϵ orders:

$$v_i \to v_{i,\epsilon} \equiv v_i(\epsilon^2\tau, \epsilon x_i), \qquad P \to P_\epsilon \equiv P(\epsilon^2\tau, \epsilon x_i). \tag{C.1}$$

With these identifications having been established we can now write out the tetrad set we use for the computation in the hydrodynamic expansion:

$$\begin{aligned}
l_\mu &= \left\{-\frac{\sqrt{r}}{\sqrt{2}}, 0, 0, 0\right\} \\
&\quad + \epsilon^2 \left\{-\frac{\sqrt{r}\left(4r_c P_\epsilon + (3r - 2r_c)\left(v_{x,\epsilon}^2 + v_{y,\epsilon}^2\right)\right)}{4\sqrt{2}r_c^2}, \frac{\sqrt{r}\left(v_{x,\epsilon}^2 + v_{y,\epsilon}^2\right)}{2\sqrt{2}r_c^2}, 0, 0\right\} + \mathcal{O}(\epsilon^3); \\
n_\mu &= \left\{-\sqrt{\frac{r}{2}}, \sqrt{\frac{2}{r}}, 0, 0\right\} + \epsilon^2 \left\{-\frac{(r - 2r_c)\left(4r_c P_\epsilon + r\left(v_{x,\epsilon}^2 + v_{y,\epsilon}^2\right)\right)}{4r_c^2\sqrt{2r}}, 0, 0, 0\right\} + \mathcal{O}(\epsilon^3); \\
m_\mu &= \left\{0, 0, -\frac{i}{\sqrt{2}}, \frac{1}{\sqrt{2}}\right\} + \epsilon^2 \left\{0, 0, \frac{i(r - r_c)v_{x,\epsilon}^2}{2\sqrt{2}r_c^2}, \frac{i(r - r_c)v_{y,\epsilon}\left(2v_{x,\epsilon} + iv_{y,\epsilon}\right)}{2\sqrt{2}r_c^2}\right\} + \mathcal{O}(\epsilon^3); \\
\bar{m}_\mu &= m_\mu^*.
\end{aligned} \tag{C.2}$$

The mathematical equivalence between the hydrodynamic expansion and the near horizon expansion involves a rescaling of the metric as was shown in Bredberg *et al.* (2012). In computations we present in the near horizon expansion, we utilize the expansion parameter $\lambda \equiv \frac{\epsilon^2}{r_c}$. Because the λ expansion has reorganized the series, we write below the tetrad set used for the near horizon computation, in particular for the type D or rotational velocity and pressure profiles in (5.48). Note that in this expansion, the coordinates we work with are rescaled to be really $\hat{x}$ and $\hat{y}$; for clarity in the expressions below we have dropped the hats.

The near horizon tetrad we use for the fluid metric dual to (5.48) is

$$
\begin{aligned}
l_\mu &= \left\{\frac{1}{\sqrt{2}},0,0,0\right\}+\lambda\left\{\frac{3r\omega^2\left(x^2+y^2\right)}{4\sqrt{2}},0,0,0\right\}+\lambda^2\left\{0,-\frac{\omega^2\left(x^2+y^2\right)}{2\sqrt{2}},0,0\right\}\\
&\quad+\lambda^3\left\{\frac{9r\left(r^2-4\right)\omega^6\left(x^2+y^2\right)^3}{64\sqrt{2}},-\frac{r\omega^4\left(x^2+y^2\right)^2}{2\sqrt{2}},0,0\right\}+\mathcal{O}(\lambda^4);\\
n_\mu &= \lambda^{-1}\left\{\frac{r}{\sqrt{2}},0,0,0\right\}+\left\{-\frac{((r-2)r+2)\omega^2\left(x^2+y^2\right)}{2\sqrt{2}},-\sqrt{2},-\frac{ry\omega}{\sqrt{2}},\frac{rx\omega}{\sqrt{2}}\right\}\\
&\quad+\lambda\left\{\frac{3r\omega^4\left(x^2+y^2\right)^2}{4\sqrt{2}},\frac{r\omega^2\left(x^2+y^2\right)}{\sqrt{2}},-\frac{(r-1)\left(4q_x+(r-2)y\omega^3\left(x^2+y^2\right)\right)}{2\sqrt{2}},\right.\\
&\qquad\left.\frac{(r-1)\left((r-2)x\omega^3\left(x^2+y^2\right)-4q_y\right)}{2\sqrt{2}}\right\}\\
&\quad+\lambda^2\left\{0,\frac{\omega\left(2(r-2)yg^{(2)}_{rx}-2(r-2)xg^{(2)}_{ry}+3(r-1)\omega^3\left(x^2+y^2\right)^2\right)}{2\sqrt{2}},\right.\\
&\qquad\frac{\omega\left(4(r-2)yg^{(2)}_{xx}+(r-1)\omega\left(x^2+y^2\right)\left(12rq_x+(r-1)y\omega^3\left(4(r+1)x^2+(5r+2)y^2\right)\right)\right)}{8\sqrt{2}},\\
&\qquad\left.-\frac{\omega\left(4(r-2)xg^{(2)}_{yy}+(r-1)\omega\left(x^2+y^2\right)\left((r-1)x\omega^3\left((5r+2)x^2+6ry^2\right)-12rq_y\right)\right)}{8\sqrt{2}}\right\}\\
&\qquad+\mathcal{O}(\lambda^3);\\
m_\mu &= \left\{-\frac{(r-2)\omega(x-iy)}{2\sqrt{2}},0,\frac{i}{\sqrt{2}},\frac{1}{\sqrt{2}}\right\}\\
&\quad+\lambda\left\{\frac{3r^2\omega^3(x-iy)\left(x^2+y^2\right)}{8\sqrt{2}},\frac{\omega(x-iy)}{\sqrt{2}},\frac{(r-1)y\omega^2(x-iy)}{2\sqrt{2}},\right.\\
&\qquad\left.-\frac{(r-1)x\omega^2(x-iy)}{2\sqrt{2}}\right\}\\
&\quad+\lambda^2\left\{0,\frac{4ig^{(2)}_{rx}+4g^{(2)}_{ry}+(r-2)\omega^3(x-iy)^2(x+iy)}{4\sqrt{2}},\right.\\
&\qquad\left.\frac{4ig^{(2)}_{xx}+(r-1)^2y\omega^4\left(2x^3-ix^2y+2xy^2-iy^3\right)}{8\sqrt{2}},\frac{4g^{(2)}_{yy}-(r-1)^2x^2\omega^4\left(x^2+y^2\right)}{8\sqrt{2}}\right\}\\
&\qquad+\mathcal{O}(\lambda^3);\\
\bar{m}_\mu &= m^*_\mu.
\end{aligned}
\tag{C.3}
$$

In the above expressions, the functions q_i and $g^{(2)}_{ij}$ refer to higher order terms necessary in the λ expansion to ensure that Einstein's equations are appropriately satisfied, as in Bredberg *et al.* (2012). These functions do not appear in the lowest order Petrov invariants. Note that this tetrad has been chosen to ensure that Ψ_2 is the only nonzero Ψ_I; the invariants (B.5) do not change under tetrad rotations, but the explicit form

of the C_{ABCD} in terms of ι and o does change. For simplicity, we thus choose a tetrad which preserves (5.49).

APPENDIX D

PERTURBATIVE CONSIDERATIONS TOWARDS ALGEBRAIC SPECIALTY

In this section we quantify the consequences of having the fluids metric accurate at the most upto and including $O(\epsilon^2)$ in the hydrodynamic expansion and similarly to only having an explicit form for the metric in the near horizon expansion till $O(\lambda)$. We will provide a detailed discussion of the ϵ expansion here.

Based on the accuracies of the tetrad eq. (C.2)[1], we have the following non vanishing orders for the spin-coefficients.

	ϵ^0	ϵ^1	ϵ^2	ϵ^3	ϵ^4	ϵ^5
κ				✓		✓
σ			✓		✓	
ρ			✓		✓	
τ		✓		✓		✓
ν				✓		✓
μ			✓		✓	
λ			✓		✓	
π		✓		✓		
ε	✓		✓		✓	
β		✓		✓		✓
γ	✓		✓		✓	
α		✓		✓		✓

Table D.1: Nonzero ϵ-Orders For Spin Coefficients.

We've colored the higher order ϵ in red because *we do not trust the validity of the calculation past* $O(\epsilon^2)$.

We next want to use the NP-equations to compute the Weyl scalars Ψ_i's:

$$\begin{aligned}
\Psi_0 &= D\sigma - \delta\kappa - (\rho + \bar{\rho} + 3\varepsilon + \bar{\varepsilon})\sigma + (\tau - \bar{\pi} + \bar{\alpha} + 3\beta)\kappa \\
\Psi_1 &= D\beta - \delta\varepsilon - (\alpha + \pi)\sigma - (\bar{\rho} - \bar{\varepsilon})\beta + (\mu + \gamma)\kappa + (\bar{\alpha} - \bar{\pi})\varepsilon \\
\Psi_2 &= D\mu - \delta\pi + (\varepsilon + \bar{\varepsilon} - \bar{\rho})\mu + (\bar{\alpha} - \beta - \bar{\pi})\pi + \nu\kappa - \sigma\lambda - R/12 \\
\Psi_3 &= \bar{\delta}\gamma - \Delta\alpha + (\rho + \varepsilon)\nu - (\tau + \beta)\lambda + (\bar{\gamma} - \bar{\mu})\alpha + (\bar{\beta} - \bar{\tau})\gamma \\
\Psi_4 &= \bar{\delta}\nu - \Delta\lambda - (\mu + \bar{\mu} + 3\gamma - \bar{\gamma})\lambda + (3\alpha + \bar{\beta} + \pi - \bar{\tau})\nu
\end{aligned} \tag{D.1}$$

R is the Ricci scalar[2]. Even though we have the spin coefficients confidently to $O(\epsilon^2)$, it's important to look carefully at the ϵ-order we can keep for the Weyl scalars.

[1]Note that in these computations for the spin-coefficients we have interchanged $l \leftrightarrow n$. This follows from the chronology of our computations, a significant part of the computation was obtaining suitable a tetrad set. The results however are presented for the correct tetrad and involve simply interchanging $\Psi_0 \leftrightarrow \Psi_4$ and $\Psi_1 \leftrightarrow \Psi_3$

[2]We know the first nonzero order for R is at $O(\epsilon^4)$ from the Einstein equations.

	Lowest contribution of tetrad error to scalars	ϵ^k;k=
Ψ_0	$(3\epsilon+\bar{\epsilon})\sigma$	3
Ψ_1	$\gamma\kappa$; $\epsilon(\bar{\alpha}-\bar{\pi})$	3
Ψ_2	$(\epsilon+\bar{\epsilon})\mu$	3
Ψ_3	$\epsilon\nu$; $(\beta-\bar{\tau})\gamma$	3
Ψ_4	$(3\gamma-\bar{\gamma})\lambda$	3

Given that Ψ_4 is 0 with this choice of tetrads we will need to interchange Ψ_0 and Ψ_4 and Ψ_1 and Ψ_3, in order to follow the classification scheme provided in Stephani *et al.* (2003). Explicitly then we find that the Weyl scalars have the form,

A quick inspection of the terms above in D.1 reveals that the Weyl scalars are sensible only upto and excluding $O(\epsilon^3)$, stated equivalently the first ϵ order when an error to the scalars shows up is $O(\epsilon^3)$. Using these we can quantify the errors in our Weyl scalars,

	ϵ^0	ϵ^1	ϵ^2	ϵ^3	ϵ^4	ϵ^5
Ψ_0					✓	
Ψ_1				✓		✓
Ψ_2			✓		✓	
Ψ_3				✓		✓
Ψ_4			✓		✓	

Table D.2: Nonzero ϵ-Orders For Weyl Scalars.

As stated in chapter 5 this provides us with the following Weyl scalars,

$$\begin{aligned}
\Psi_0 &= 0 + O(\epsilon^3) \\
\Psi_1 &= 0 + O(\epsilon^3) \\
\Psi_2 &= \frac{-i\epsilon^2}{4r_c}(\partial_x v_y - \partial_y v_x) + O(\epsilon^3) \\
\Psi_3 &= 0 + O(\epsilon^3) \\
\Psi_4 &= -\frac{\epsilon^2}{2r}(\partial_x v_x - \partial_y v_y + i(\partial_x v_y + \partial_y v_x)) + O(\epsilon^3)
\end{aligned} \tag{D.2}$$

By trusting terms only to and including $O(\epsilon^2)$ for the Weyl scalars, we can deduce the following:

$$\begin{aligned}
I \sim O(\epsilon^4) &\implies I^3 \sim O(\epsilon^{12}) \\
J \sim O(\epsilon^6) &\implies J^2 \sim O(\epsilon^{12}) \\
K &\sim O(\epsilon^6) \\
L \sim O(\epsilon^4) &\implies L^2 \sim O(\epsilon^8) \\
N &\sim O(\epsilon^8)
\end{aligned} \tag{D.3}$$

Further, given that the Ricci scalar shows up at order ϵ^4 onwards, the contribution of the Ricci scalar to the invariants will only show up at O(ϵ^8) for I and O(ϵ^{12}) for J. The invariants I and J are of the form,

$$
\begin{aligned}
I &= 3\left[\epsilon^2\, i\,\left(\frac{\partial_x v_y}{4r_c} - \frac{\partial_y v_x}{4r_c}\right)\right]^2 + O(\epsilon^5) \\
J &= \left[\epsilon^2\, i\,\left(\frac{\partial_x v_y}{4r_c} - \frac{\partial_y v_x}{4r_c}\right)\right]^3 + O(\epsilon^7) \\
\implies & I^3 - 27J^2 = 0 + O(\epsilon^{13})
\end{aligned}
\tag{D.4}
$$

Similar computations can be performed for the near-horizon λ expansion. The above process allows us to quantify the extent to which we know that our space-time is algebraically special. That is not to say that it won't maintain algebraic specialty beyond this order, however our metric would need additional pieces in order for such conditions to be accurately met.

APPENDIX E

PERMISSIONS

The results presented in this document constitute work published by the author in the *Journal Of High Energy Physics* titled "Spectral weight in Chern-Simons theory with symmetry breaking" by V.L Martin and the author and "From Navier-Stokes to Maxwell, via Einstein" by C. Keeler and T. Manton and the author. The author has permission from all co-authors to include the material in this document. Note that the *Journal Of High Energy Physics* has alphabetized authorship by last name, the work presented here has significant or dominant contributions from the author.